AN1722
APPLICATION NOTE

Design and Realization of a CCFL Application Using TSM108, STN790A, or STS3DPFS30, and STSA1805

1. ABSTRACT

This technical document shows how to use the integrated circuit TSM108, the PNP power bipolar transistor STN790A, or the P channel power MOSFET STS3DPFS30, the NPN power bipolar transistor STSA1805 and the diode 1N5821 in order to design and realize a CCFL application. Such work allows STMicroelectronics' customers to choose an alternative design and STMicroelectronics itself to supply all devices concerning the power transistor part and also the control and driver part for these applications (KIT approach).
In the application block diagram below, the several STMicroelectronics' power devices are inserted in the related block.

Figure 1: Block diagram of the application

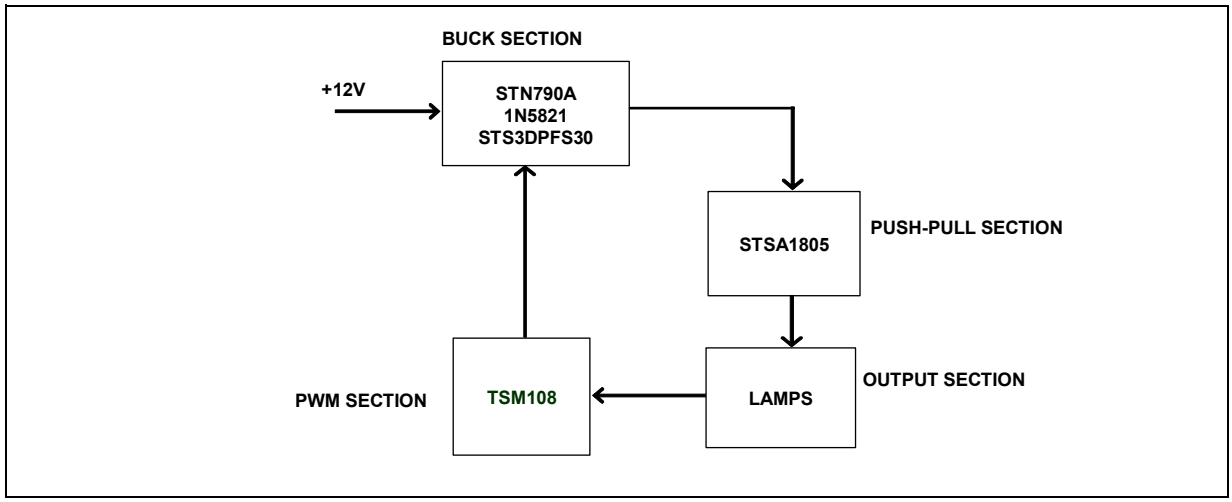

2. TSM108 DESCRIPTION

TSM108 is a PNP power bipolar or P channel power MOSFET controller. TSM108 includes a PWM generator (AMP3 in fig. 2), voltage and current control loops (AMP1 and AMP2 respectively in fig. 2) and it also includes safety functions that lock the PNP power bipolar or P channel power MOSFET in off state. The TSM108 can sustain 60V on V_{cc} and the I_{sink} (base or gate drive sink current to switch on the device) and I_{source} (base or gate drive source current to switch off the device) are respectively 15 mA (min value) and 30 mA (max value).

Rev. 2

Figure 2: TSM108 schematic circuit

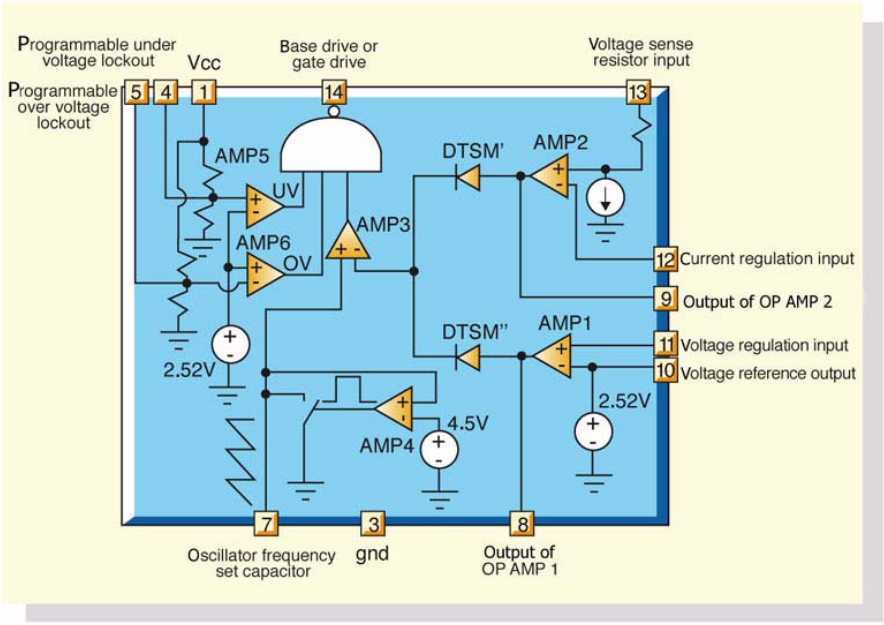

As exposed above, the safety functions UV and OV can switch off the power transistor (PNP power bipolar or P channel power MOSFET) when the V_{cc} is under a definite min voltage or when the V_{cc} overcomes a definite max voltage. In fact, in these cases the output signal of the AMP 5, or the AMP 6, is low and the NAND output is high. Considering the UV function, fig. 3 shows the circuit part concerning it.

Figure 3: UV schematic circuit detail

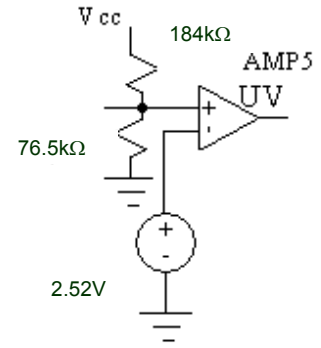

The V_+ voltage (the one in the non-inverting pin of the AMP5) is:

$$V_+ = \frac{76.5}{184 + 76.5} V_{cc} \qquad \textbf{(1.1)}$$

and considering:

$$V_- = 2.52V \qquad \textbf{(1.2)}$$

the minimum V_{cc} under which the application will switch off is:

$$V_{cc} = \frac{2.52}{76.5}(184 + 76.5) \approx 8.5V \qquad \textbf{(1.3)}$$

Considering the OV function, fig. 4 shows the circuit part concerning it.

Figure 4: OV schematic circuit detail

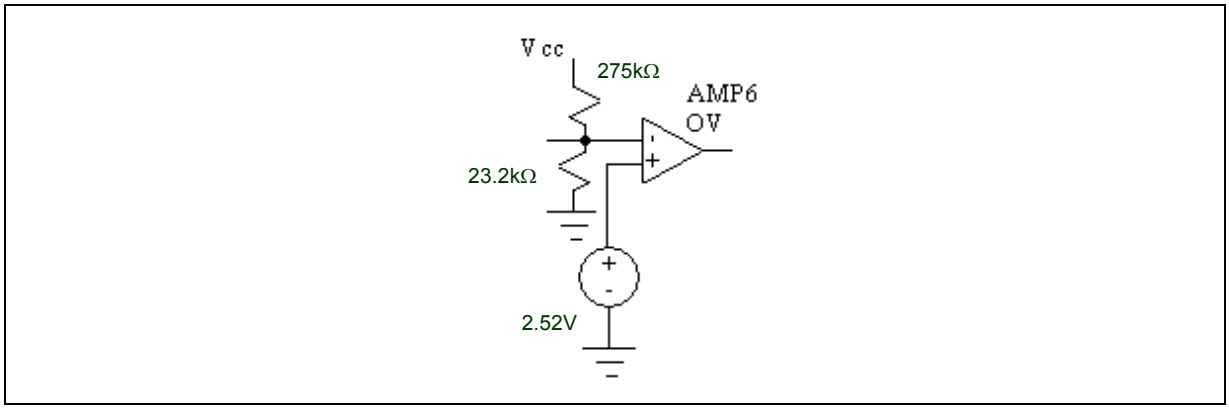

The V_- voltage (the voltage in the inverting pin of the AMP6) is:

$$V_- = \frac{23.2}{275 + 23.2} V_{cc} \qquad \textbf{(1.4)}$$

and considering:

$$V_+ = 2.52V \qquad \textbf{(1.5)}$$

the maximum V_{cc} over which the board will switch off is:

$$V_{cc} = \frac{2.52}{23.2}(275 + 23.2) \approx 32.4V \qquad \textbf{(1.6)}$$

In order to adjust the UV and OV voltages it is necessary to insert suitable resistances as showed later in this paper.

It is important to highlight that, normally, the max δ (duty cycle) of the base drive, or gate drive, is around 95 %.

3. STN790A DESCRIPTION

The STMicroelectronics' power bipolar transistor device STN790A is housed in the SOT-223 package. Such device is manufactured in PNP planar technology using a 'Base Island' layout that involves a very high gain performance and a very low saturation voltage.

The main characteristics of the STN790A device are:

1) $V_{eco} \geq 30V$

2) $V_{ecs} \geq 40V$

3) $V_{beo} \geq 5V$

4) I_c = -3 A (continuous current)

5) I_b = 1 A (continuous current)

6) $V_{ec(sat)}$ = 1.2 mV (typ) @ I_b = -20 mA @ Ic = -2 A (typical conditions)

7) H_{fe} = 100 (min) @ I_c = -2.5 A @ V_{ec} = 3V (typical conditions)

4. 1N5821 DESCRIPTION

The STMicroelectronics' SCHOTTKY diode is integrated in the package DO-201AD and has very small conduction losses, negligible switching losses and extremely fast switching.

The main characteristics of the 1N5821 device are:

1) $V_{RRM} \geq 30V$

2) I_F = 3A

5. STS3DPFS30 DESCRIPTION

The STS3DPFS30 device is mounted inside a P channel power MOSFET, using the STripFET layout that allows a lower Rds(on) and a SCHOTTKY diode. It is housed in the SO-8 package.

The main characteristics of the STS3DPFS30L device are:

1) $V_{sd} \geq 30V$

2) $V_{sg} \geq 20V$

3) $R_{ds(on)\_max}$ = 0.09 Ohm @ I_d = 1.5 A @ V_{sg}=10V

4) I_F = 3A (integrated diode);

5) V_{F_max} = 0.51 V (integrated diode)

6) V_{RRM} = 30V (integrated diode)

6. STSA1805 DESCRIPTION

The STMicroelectronics' power bipolar transistor device STSA1805 is housed in the TO-92 package. Such device is manufactured in NPN planar technology using a 'Base Island' layout that involves a very high gain performance and a very low saturation voltage.

The main characteristics of the STSA1805 device are:

1) $V_{ceo} \geq 60V$

2) $V_{ces} \geq 150V$

3) $V_{ebo} \geq 7V$

4) I_c = 5A (continuous current)

5) I_b = 1A (continuuous current)

6) $V_{ce(sat)}$ = 140 mV (typ) @ I_b = 50 mA @ I_c = 2A (typical conditions)

7) H_{fe} = 270 (typ) @ Ic = 2A @ V_{ce} = 1V (typical conditions)

7. APPLICATION INTRODUCTION

The CCFL applications (Cold Cathode Fluorescent Lamp) are generally used for the monitor back lighting which is often used to illuminate the signs.

The part of the circuit driving the CCFL lamps is composed of a DC-AC converter. The CCFL applications use special compact fluorescent lamps. The lamps number can be 1, 2, 4, or 6 and the output power can be in the range of 2-24W. The DC-AC converters transform the low DC in input voltage in necessary high AC output voltage for the fluorescent tubes. The CCFL are usually powered with a 12 V_{dc} voltage.

Today, two topologies are available for driving the above-mentioned special tubes: the 'ROYER' and the FULL BRIDGE solutions.

The 'ROYER' solution uses a Push-Pull current fed converter where the current source is due to an inductor and where it is possible to regulate the lamps brightness. Such a regulation is carried out by means of the inductor current controls, through a PNP power bipolar or P channel power MOSFET transistors (STN790A or STS3DPFS30 respectively), working in PWM mode, and a free wheeling diode. The diode, the transistor and the inductor make a BUCK converter stage before of the PUSH-PULL converter stage. The PUSH-PULL converter uses two NPN power bipolar transistors (STSA1805). The other solution, the FULL BRIDGE topology, uses four power MOSFET transistors, two pair of complementary power MOSFET transistors, driven by a suitable IC.

The design described in this paper uses the 'ROYER' topology, thus, only such topology will be studied.

In the graph below a schematic circuit of a CCFL application, using two paralleled 6W lamps and only one transformer, is shown (this is one of the several possible output stage configurations).

Figure 5: 'ROYER' converter schematic circuit

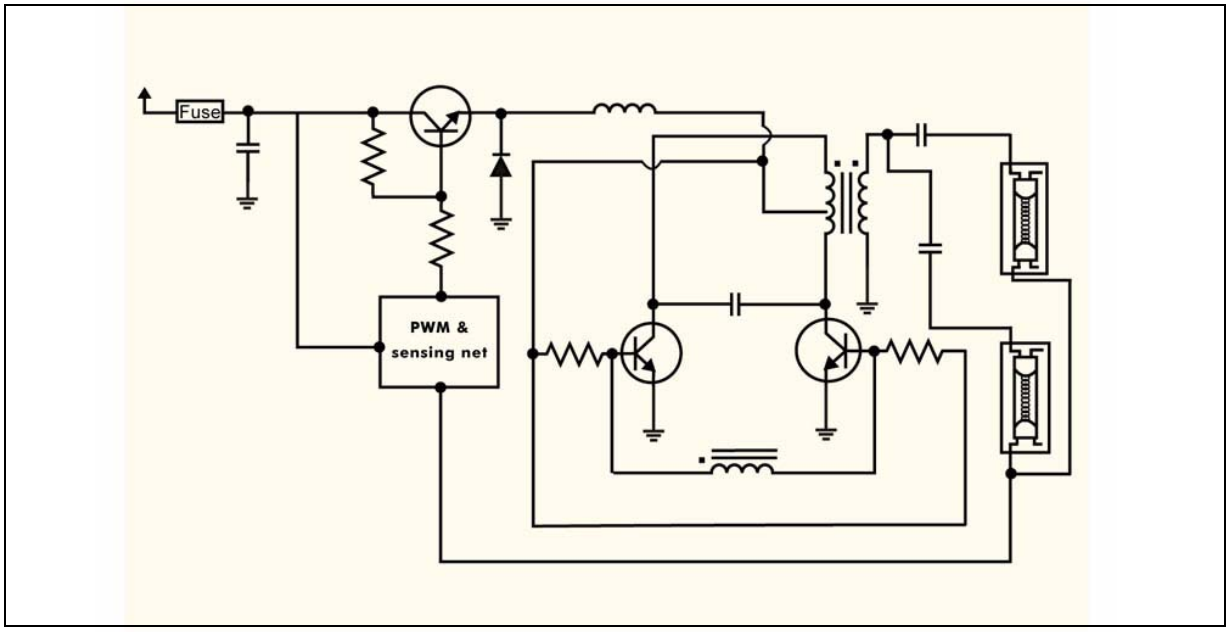

8. FLUORESCENT TUBES CHARACTERISTICS

Fluorescent lamps are generally made with tubes filled with a gas mixture at low pressure. The inner sides of the tubes are covered with fluorescent elements. During the start-up, before the tube lights on, the lamp has a very high resistance. Usually, in the common fluorescent lamps, the electrodes voltage increases up to around 500V and starts to warm up and emit ions, but in the CCFL tubes the voltage between the lamp electrodes reaches up to 1300V. Fig. 6 shows CCFL lamp characteristics before the striking.

Figure 6: Lamp voltage before striking

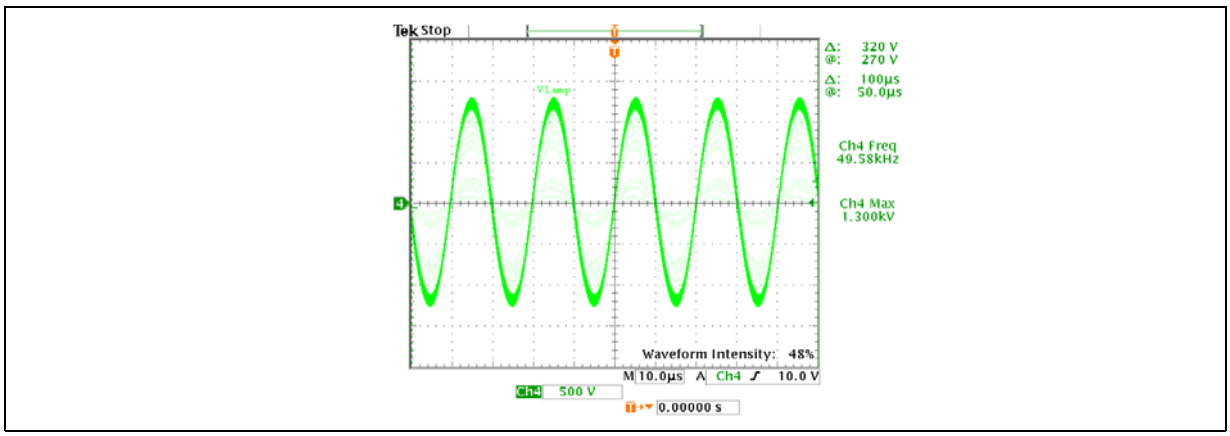

When the fluorescent lamp lights on, the gas mixture inside is fully ionized, and an arc across the two electrodes occurs. In this new condition, the lamp resistance drops to 60 KOhm and the voltage across the lamps drops to about 800V (Fig. 7 and Fig. 8 show the lamp characteristics and the V-I characteristic respectively after the striking).

Figure 7: Voltage and current Lamp after striking

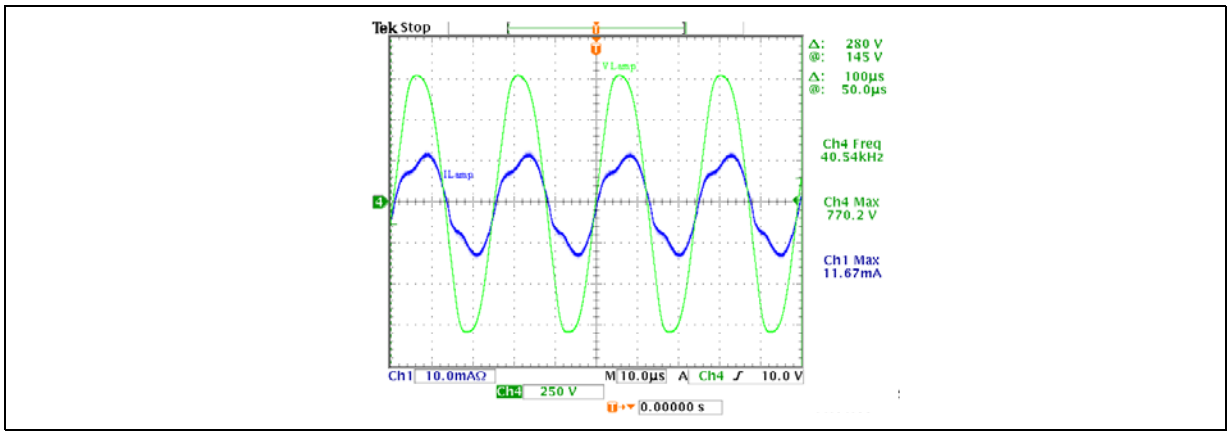

Figure 8: V-I Characteristic after striking

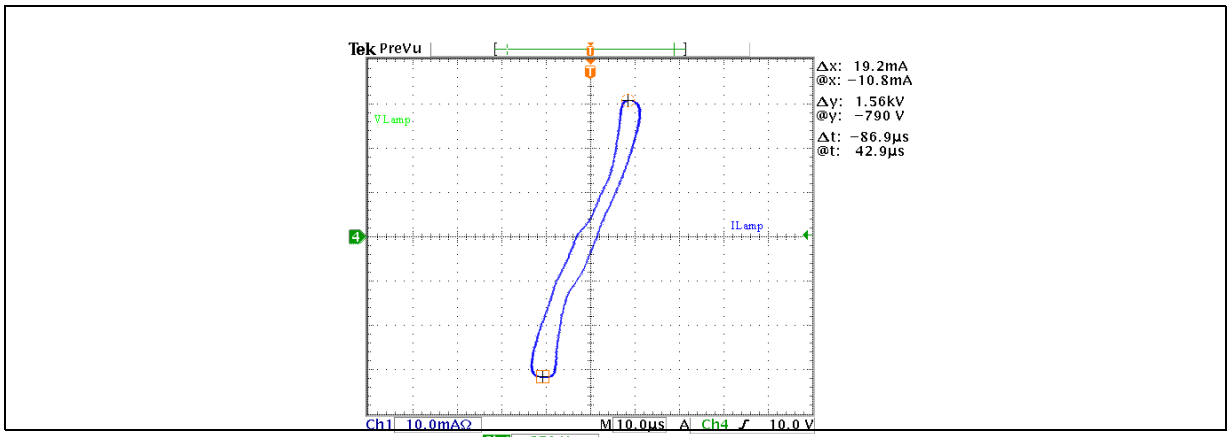

After the striking, the gas mixture emits radiations able to excite the fluorescent elements inside the tube producing the light in the visible spectrum. In this example, after the striking, the maximum electrodes voltage falls from 1300V down to 770V with a peak current of 12 mA. In the common fluorescent lamp

the voltage between the tube terminals drops from about 500V, before the striking, to about 220V after the striking.
Usually, after the striking, in order to increase the light efficiency, the tube works with a frequency around 25-50KHz, in fact, in this frequency range, the light output can increase up to 15 % for the same input energy.
Generally, the common fluorescent lamps can be considered only as a resistive load. In the CCFL lamps, instead, even if the tubes show a resistive behavior, a small but evident capacitive behavior is observed as it is shown in fig.7. In fig. 7 it is evident that the V-I Characteristic is linear until the established voltage value is reached (in this case about 500V). After reaching this voltage value, the characteristic starts to become flat because no ion can emit other radiations.

9. TRANSFORMER DESCRIPTION

The transformer named T_1 shown in fig. 5 has three windings. The primary winding terminals are connected to the collectors of the Q_2 and Q_3 NPN power bipolar transistors. The same primary winding has a central terminal where the inductor L_1 output is connected. The secondary winding terminals are connected to the loads.
The third winding terminals are connected to the base of the transistors Q_2 and Q_3 so that the first is on while the second is off and vice versa. During the Q_2 on state the current flows through the device and the related half primary winding, instead, when Q_3 is on the current passes through this second device and the other half primary winding. Usually the LT primary inductance of the transformer T_1 is much lower compared to the inductance L_1. The resonance frequency of the PUSH-PULL converter is also due to the LT inductance. In the design, N_2 (number of secondary turns) and $N_1/2$ (number of half primary turns) ratio is around 80-90 while, $N_1/2$ and N_3 (number of third turns) ratio, is around 4-5. In fact, considering a 12 V_{dc} input voltage, the $v_{1/2max}$ voltage (the max voltage between the terminal of the central point of the primary winding and the reference when the PNP power bipolar or the P channel power MOSFET transistors are always on) is:

$$v_{1/2\max} = \frac{\pi}{2} \cdot V_{dc} \qquad \textbf{(9.1)}$$

as then demonstrated around 19V, the v_{2max} (the max voltage between the secondary terminals of the transformer) is:

$$v_{2\max} = \frac{\pi}{2} \cdot V_{dc} \frac{N_2}{(N_1/2)} \qquad \textbf{(9.2)}$$

around 1500-1700V and the v_{3max} (the max voltage between the terminals of the third transformer winding) is:

$$v_{3\max} = \frac{\pi}{2} \cdot V_{dc} \frac{(N_3)}{N_1/2} \qquad \textbf{(9.3)}$$

As exposed above, the $N_1/2$ value and not N_1 is highlighted. In order to understand the reason of it, it is

necessary to consider the graph below.

Figure 9: Detail of the transformer T_1

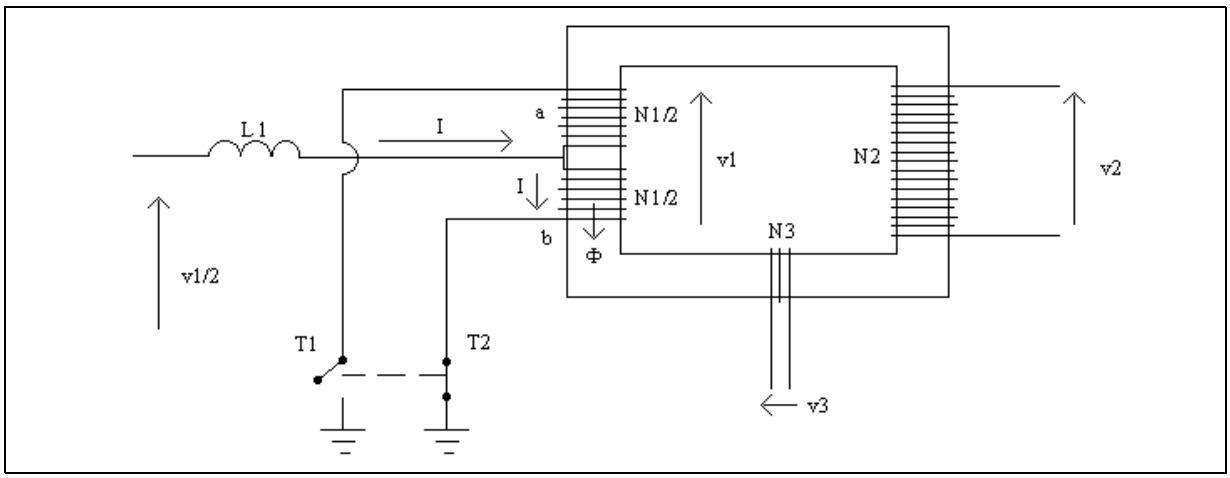

As already exposed, when the Q_2 transistor is on, the other is off and vice versa. Now, considering fig. 9 where the T_2 switch is on, the I current passes through the 'b' half primary winding of the transformer T_1 and generates a magnetic force (Hopkinson law):

$$\frac{N_1}{2} \cdot I = \Re \cdot \Phi \quad \textbf{(9.4)}$$

where Φ is the magnetic flux and $\Re$ is the magnetic reluctance of the T_1 core, thus Φ is:

$$\Phi = \frac{\frac{N_1}{2} \cdot I}{\Re} \quad \textbf{(9.5)}$$

The magnetic reluctance $\Re$ is:

$$\Re = \frac{l}{\mu \cdot A} \quad \textbf{(9.6)}$$

where μ is the core permeability, A is the core section and l is the core length. When T_2 switches off and T_1 switches on, the current flows through the other half primary winding 'a' of the transformer T_1 and the flux Φ inverts its direction. Such a flux flows in the magnetic core T_1 creating a link respectively with the windings N_2 and N_3, and also with the other half of the primary windings $N_1/2$, and generating the voltages v_2 and v_3 (magnetic law-Lenz law):

$$v_2 = -N_2 \frac{\Delta\Phi}{\Delta t}; v_3 = -N_3 \frac{\Delta\Phi}{\Delta t}; v_{1/2} = -\frac{N_1}{2} \frac{\Delta\Phi}{\Delta t} \quad \textbf{(9.7)}$$

thus:

$$\frac{v_2}{v_{1/2}} = \frac{N_2}{N_1/2}, \frac{v_3}{v_{1/2}} = \frac{N_3}{N_1/2}, \frac{v_1}{v_{1/2}} = 2 \quad \textbf{(9.8)}$$

Furthermore, the current i_2 (the current flowing through the secondary winding of T_1) is:

$$i_2 = I\frac{N_1/2}{N_2} \quad \textbf{(9.9)}$$

in fact, the apparent input power is:

$$A_{in} = V_{1/2}I \quad \textbf{(9.10)}$$

while the apparent output power is:

$$A_{out} = V_2 i_2 \quad \textbf{(9.11)}$$

and considering an ideal transformer:

$$V_2 i_2 = V_{1/2}I \quad \textbf{(9.12)}$$

and thus:

$$\frac{i_2}{I} = \frac{V_{1/2}}{V_2} = \frac{N_1/2}{N_2} = \frac{1}{k} \quad \textbf{(9.13)}$$

10. THE 'ROYER' CONVERTER TOPOLOGY

As previously exposed, the topology solution for CCFL applications used in this paper is the 'ROYER' topology. This topology solution has a current feed PUSH-PULL switching converter stage and also an inductor that together with a PNP power bipolar, or P channel power MOSFET transistor and a free wheeling diode, makes a BUCK converter stage before the PUSH-PULL stage. The PNP power bipolar, or the P channel power MOSFET transistor fixes the output power and thus the lamps brightness. All this is performed through a PWM signal able to drive either the PNP bipolar transistor or P channel MOSFET depending on the kind of device used. In order to implement the PWM of the transistor it is necessary to make an output current sensing (the lamps current) and to compare such a signal to the reference voltage in the AMP1 (see fig. 10 and fig.11 for the schematic circuit designed in this paper using the PNP power bipolar transistor STN790 and the power MOSFET transistor STS3DPFS30 respecticvely). The reference is fixed to 2.52V by the TSM108 internal voltage generator.

Figure 10: CCFL schematic circuit using the PNP power bipolar transistor

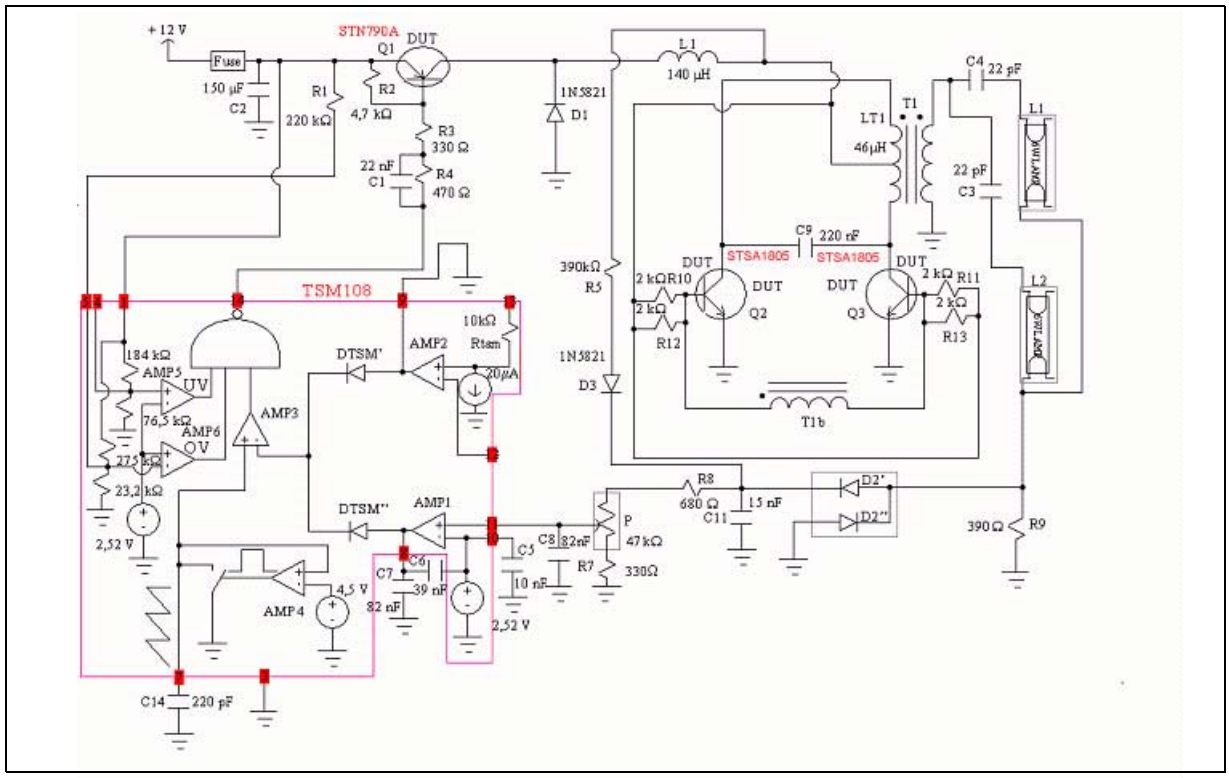

Figure 11: CCFL schematic circuit using the P channel power MOSFET transistor

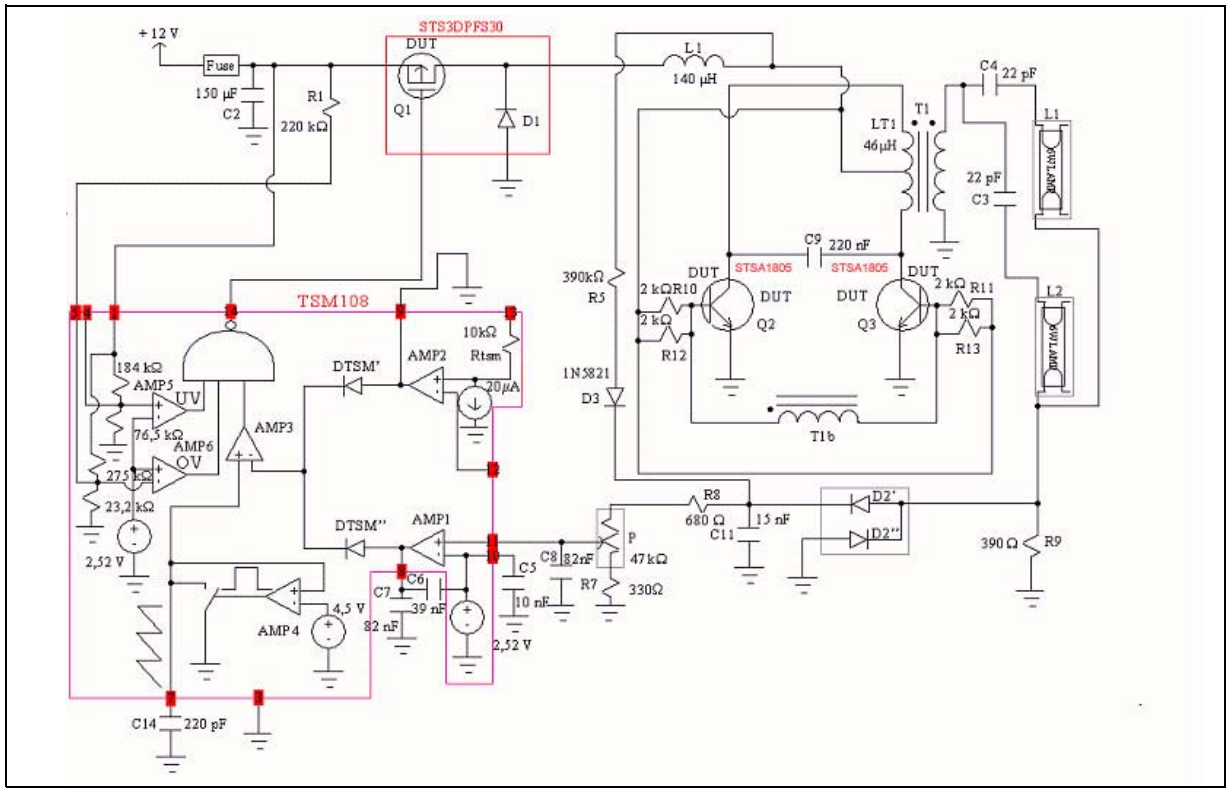

Such a sensing net fixes also the right output power during the voltage net fluctuations.

The component values for capacitors, resistors, and inductors are selected based on the load power, the operation frequency of the lamp before and after the striking (the operation lamp frequency must be in the range of 25-50Khz), and the current ripple. The PNP power bipolar, or the P channel power MOSFET operation frequency is fixed by means of the 220 pF capacitor C_{14} (around 90KHz).

Before the lamps strike the operation frequency is due to the resonance between the capacitor C_9 and the primary transformer windings inductance LT of the T_1 transformer (see fig. 12):

$$f = \frac{1}{2 \cdot \pi \sqrt{LTC_9}} \qquad \textbf{(10.1)}$$

Figure 12: Resonant schematic circuit before lamps striking

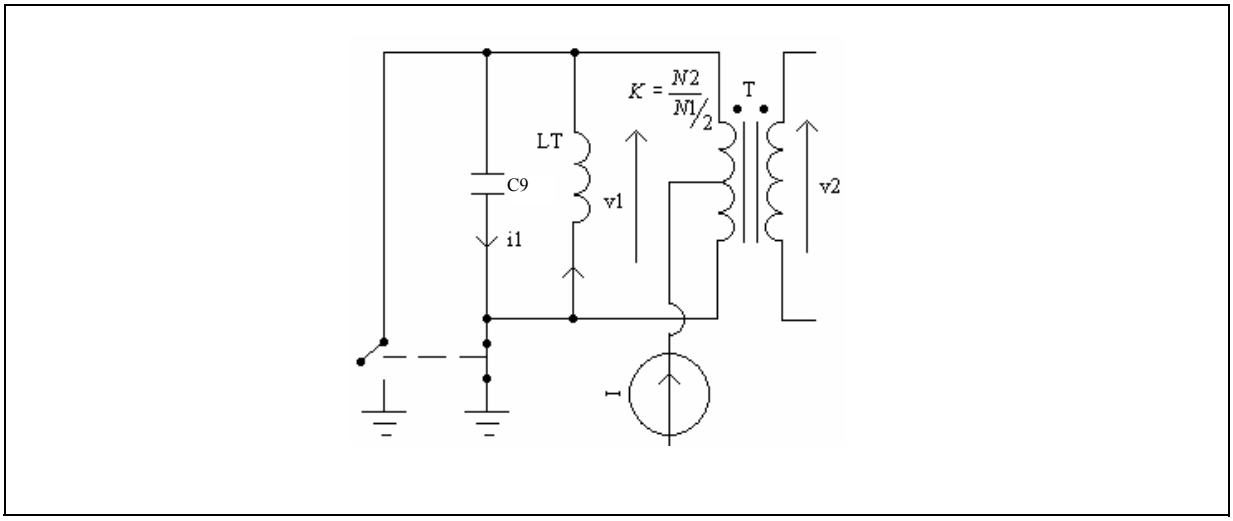

When the lamps are connected, the transformer circuit, considering the ideal transformer, can be represented as in the following graph.

Figure 13: Resonant circuit of the transformer after lamps striking

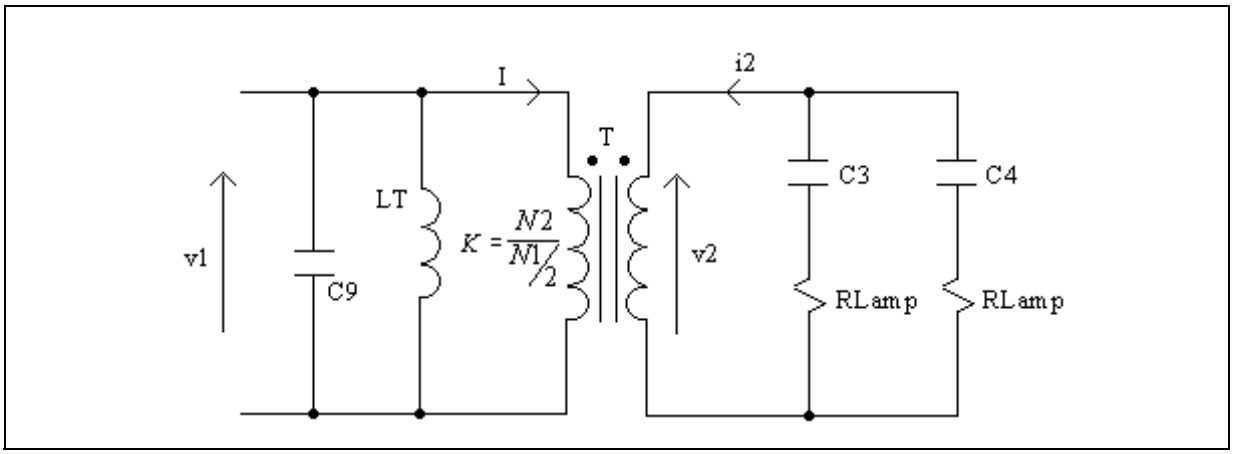

In this condition, the apparent input power is:

$$A_{in} = v_1 I \qquad \textbf{(10.2)}$$

Now it is possible to consider a new equivalent transformer circuit as shown in the graph below and where the apparent power is the same as before.

Figure 14: Equivalent resonant circuit of the transformer after lamps striking

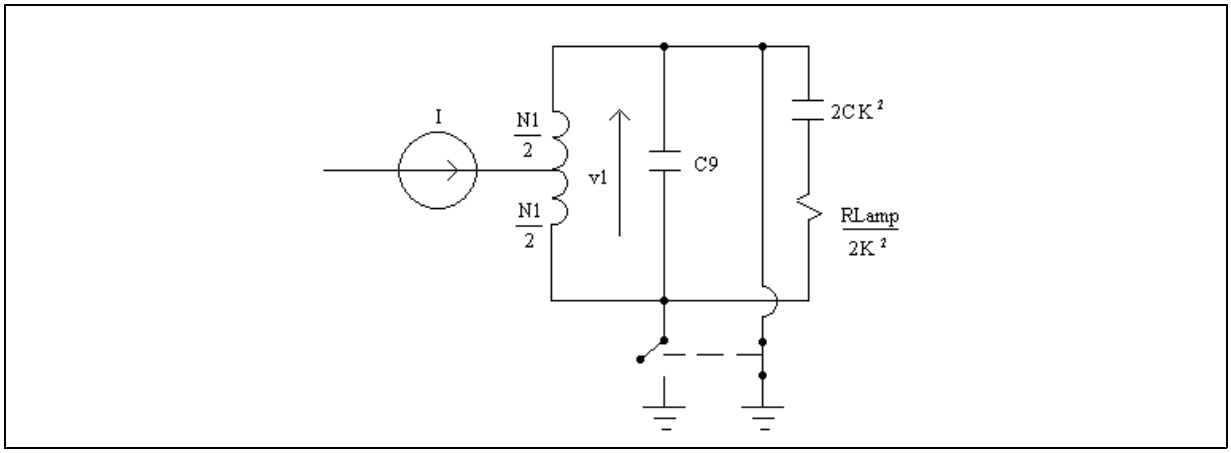

In this equivalent transformer circuit the output impedance is transferred from the secondary winding to the primary winding of the transformer T_1. In fact, considering that C_3 and C_4 have the same value (C3=C4=C) and that R_{lamp} is the same for both lamps, considering also that the C_3-R_{lamp} net and the C_4-R_{lamp} net are in parallel configuration, the output impedance can be written as:

$$\frac{R_{Lamp}}{2} - j\frac{1}{2\cdot\omega\cdot C} \qquad \textbf{(10.3)}$$

but:

$$V_1 I = V_2 i_2 = i_2^{\,2}\left(\frac{R_{Lamp}}{2} - j\frac{1}{2\cdot\omega\cdot C}\right) \qquad \textbf{(10.4)}$$

thus:

$$\frac{V_1 I}{i_2^{\,2}} = \left(\frac{R_{Lamp}}{2} - j\frac{1}{2\cdot\omega\cdot C}\right) = \frac{V_1}{i_2}\frac{I}{i_2} = \frac{V_1}{I}\frac{N_2^{\,2}}{(N_1/2)^2} = \frac{V_1}{I}k^2 \qquad \textbf{(10.5)}$$

and thus:

$$\frac{V_1}{I} = z_{eq1} = \frac{1}{k^2}\left(\frac{R_{Lamp}}{2} - j\frac{1}{2\cdot\omega\cdot C}\right) \qquad \textbf{(10.6)}$$

where:

$$\frac{R_{Lamp}}{2k^2} \qquad \textbf{(10.7)}$$

is the primary equivalent resistance, while:

$$2Ck^2 \qquad \textbf{(10.8)}$$

is the primary equivalent capacitance.

Now, the equivalent primary admittance (Yeq_1) is:

$$Y_{eq1} = \frac{-j}{\omega \cdot LT} + j\omega \cdot C_9 + \frac{k^2 j2\omega C}{(1 + j\omega C R_{Lamp})} \qquad \textbf{(10.9)}$$

where:

$$\frac{k^2 j2\omega \cdot C}{(1 + jCR_{Lamp}\omega)} \qquad \textbf{(10.10)}$$

is the admittance of the series net:

$$\frac{R_{Lamp}}{2k^2} - 2Ck^2 \qquad \textbf{(10.11)}$$

Considering the impedance of the

$$\frac{R_{Lamp}}{k^2}$$

negligible compared to Ck^2 , deriving the Yeq_1 with respect to the pulsation ω and equaling to zero, it is possible to find the frequency that maximizes the Y_{eq1} and, thus, minimizes the Z_{eq1} impedance (such frequency is the resonance frequency of the application during the lamps on state):

$$\omega^2 \cong \frac{1}{LT(C_9 + 2k^2 C)} \qquad \textbf{(10.12)}$$

and thus:

$$f \cong \frac{1}{2 \cdot \pi \sqrt{LT(C_9 + 2k^2 C)}} \qquad \textbf{(10.13)}$$

When the board is powered, the resistances R_{10} and R_{11} (see fig. 15) enable the power bipolar devices Q_2 and Q_3 and the lamps turn on. After the start-up, during the Q_2 on state, the current flowing through the inductance L_1, through the half primary winding of the transformer T_1 and through the transistor Q_2, increases with an angular coefficient given by:

$$\mathrm{tg}\alpha = \frac{v_{L1} * \Delta t}{L_1} \qquad \textbf{(10.14)}$$

After a first instant, the current curve becomes flat and its average value depends on the impedance Z_{eq1} and on the output power. However, when the PNP power bipolar, or P channel power MOSFET is on, after the lamps start-up, the current oscillates around the average value because the ripple on it depends only on the inductance L_1. In PWM mode, instead, it depends also, linearly, on the duty cycle of the transistor.

Figure 15 shows the 'ROYER' converter schematic circuit during the start-up considering the current I graph through the inductor.

Figure 15: 'ROYER' converter schematic circuit with inductor current theoretical behavior at star- up

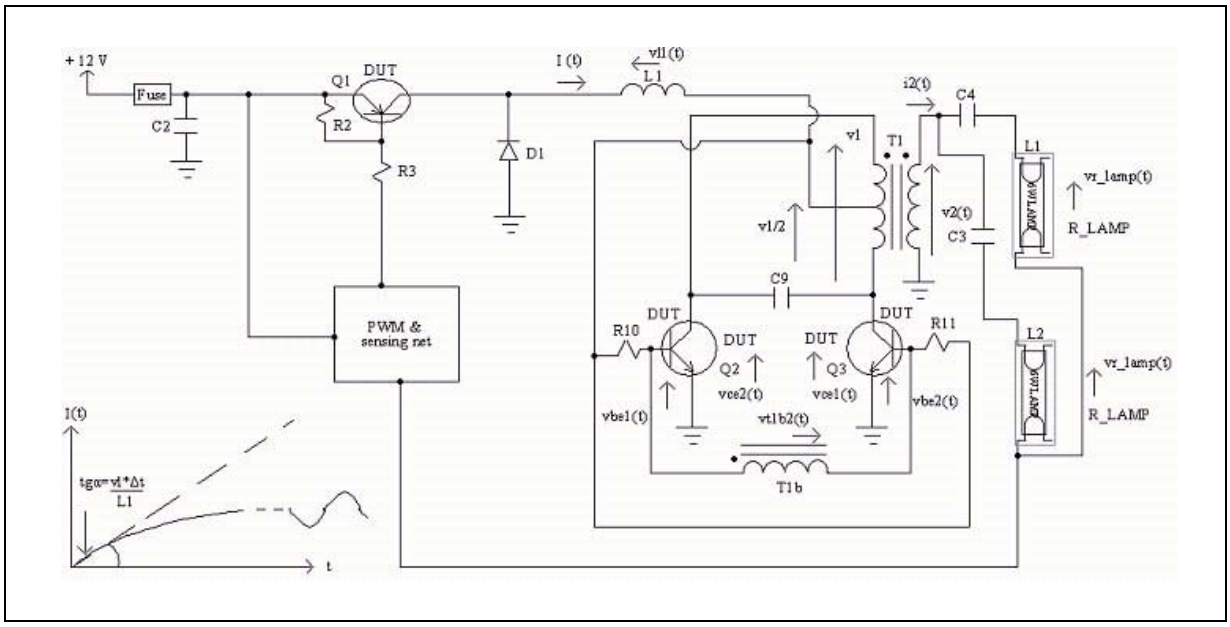

After the striking, the primary current 'I' generates the current i_2 into the secondary winding of the transformer T_1. At the beginning, the current i_2 can be written as:

$$i_2 = \frac{V_2}{R_{Lamp}/2} \qquad \textbf{(10.15)}$$

because the capacitors C_3 and C_4 are discharged. Immediately after, these capacitors get charged and the current i_2 drops to zero, while vc_3 and vc_4 reach the maximum voltage. At this time, the current i_2 inverts its direction and the capacitors C_3 and C_4 start discharging until the charge inside them becomes zero and the current i_2 reaches its maximum negative value. Furthermore, when the current i_2 inverts the direction also the voltage v_{t1b2} reverts the polarities so that Q_2 switches off, Q_3 switches on, and the current 'I' starts flowing into the other half winding of the transformer T_1 (see fig. 16).

Figure 16: 'ROYER' converter schematic circuit with theoretical behavior of v_1, v_2, and i_2

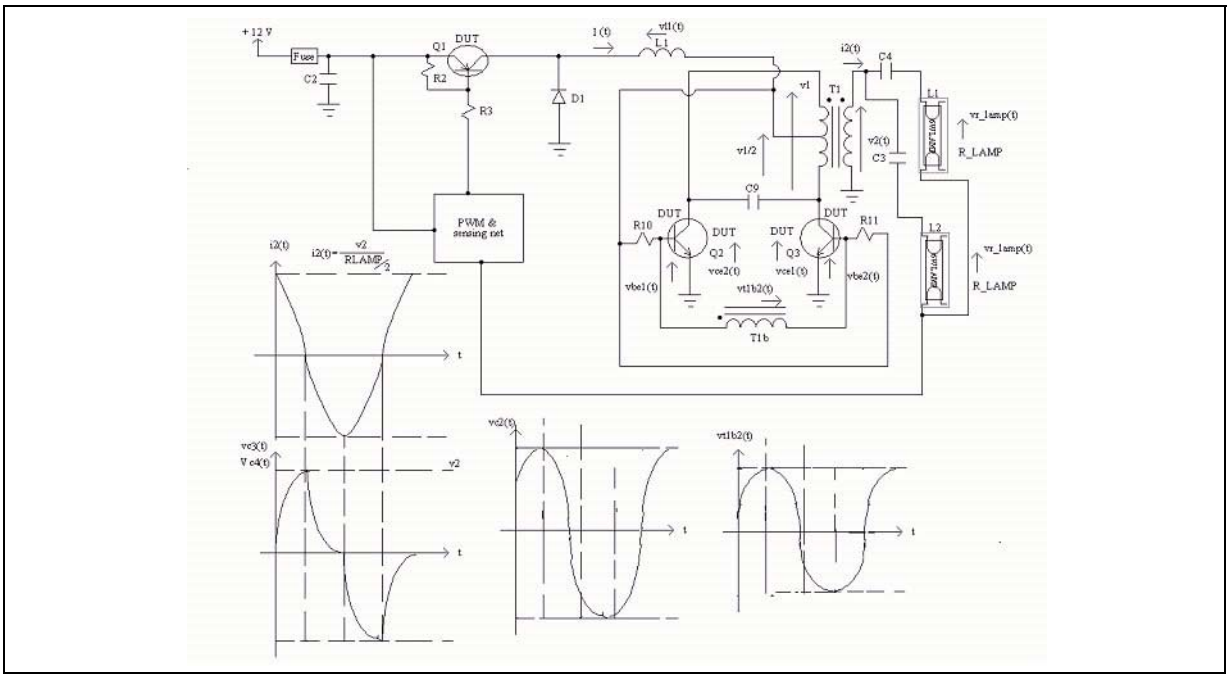

The main output electrical parameters v_2 (t), $I_{Lamp}(t)$, $V_{Lamp}(t)$, $v_{c3}(t)$ and $v_{c4}(t)$ (these last two are the voltages across the capacitors C_3 and C_4) are shown in the following graph under a vectorial representation.

Figure 17: Vectorial representation of v_2, i_2, v_{lamp}, v_{c3} and v_{c4}

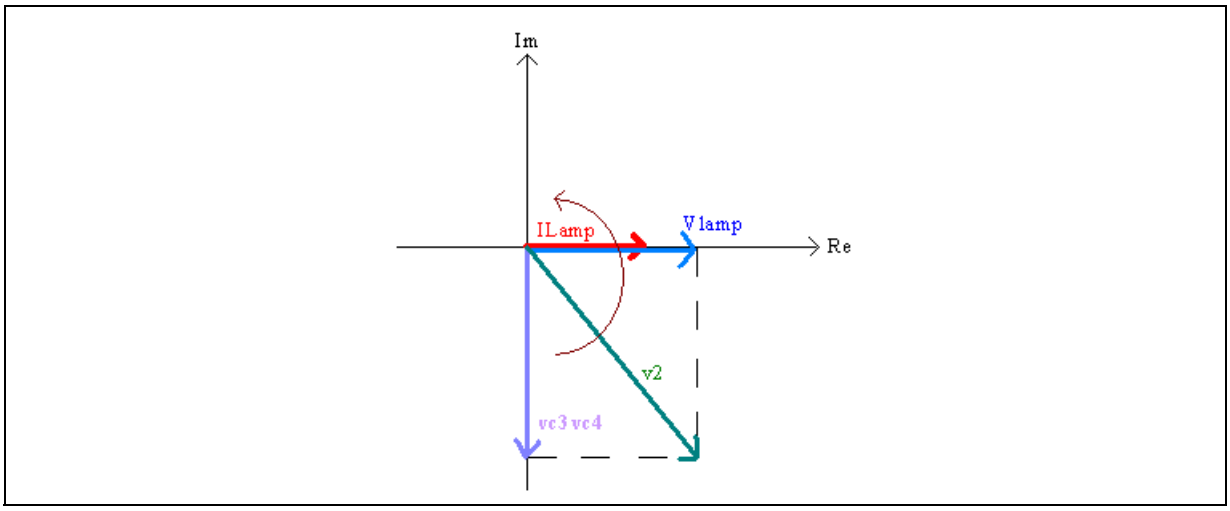

In fact, assuming that, the lamps have only resistive behavior, the I_{Lamp} currents flowing through them and the V_{lamp} (the voltage across them) can be written as:

$$V_{Lamp} = I_{Lamp} * R_{Lamp} \quad \textbf{(10.16)}$$

The graph also assumes that the vectors V_{Lamp} and I_{Lamp} are on the real axis at the time taken into consideration. The I_{Lamp} currents flow also through the capacitors C_3 and C_4 and, thus, the voltages v_{c3}

and v_{c4} can be represented as -90 ° phase shifted vectors compared to the I_{Lamp} vectors. The voltage v_2 is the vectorial sum between the V_{Lamp} and v_{c3}, or v_{c4}. Before the striking, the resistance lamps R_{lamp} are very high compared to reactance of C_3 and C_4, the currents I_{Lamp} are low and the voltages V_{lamp} are very much comparable to the voltage v_2 across the secondary winding of the transformer T_1. After the striking, R_{lamp} drops to about 60 KOhm and the reactance C_3-C_4 becomes higher compared to the first one, thus making the voltages v_{c3} and v_{c4} comparable to v_2. However, in order to keep the lamps on, after the striking, the max V_{lamp} must be about 700V across the tubes.

The voltage v_{l1} (voltage across the inductor L_1) is the difference between the V_{dc} and the $v_{1/2}$ voltages considering the PNP power bipolar in on-state, or the P channel power MOSFET transistor (see fig. 18).

Figure 18: 'ROYER' converter schematic circuit with the theoretical behavior of v_1, $v_{1/2}$, v_{L1}, and V_{dc}

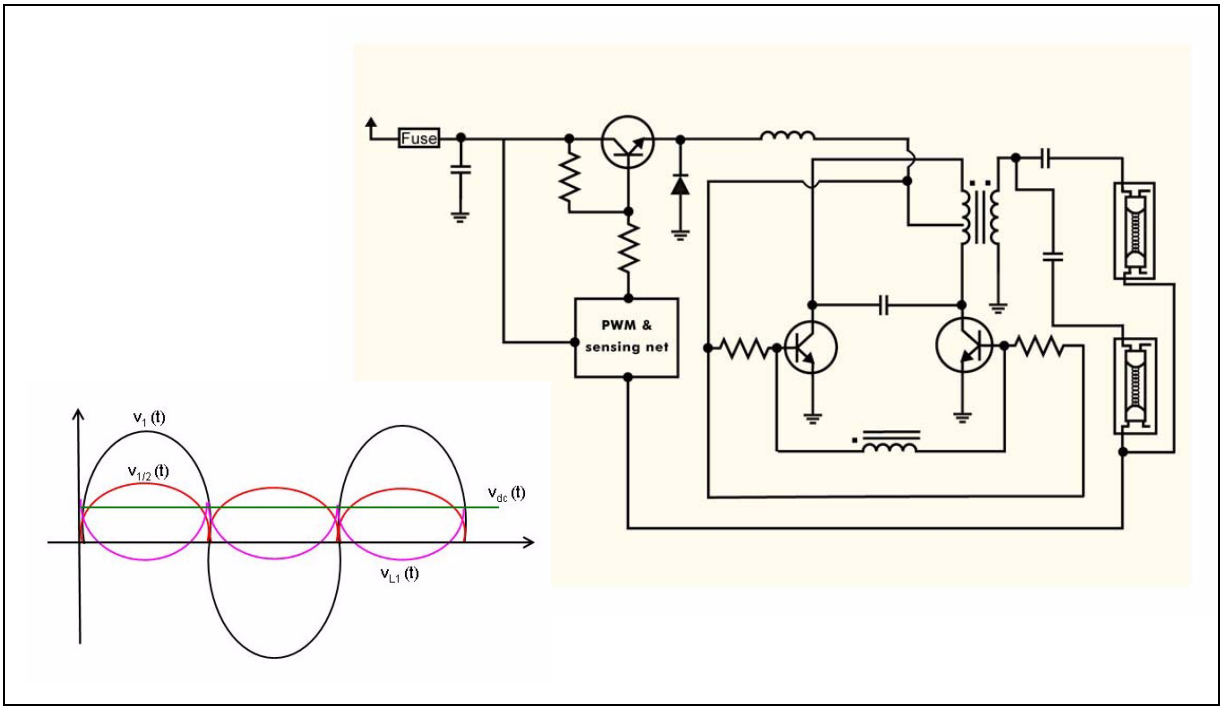

During the off state of the transistor Q_1, the diode D_1 turns on and the voltage v_{L1} becomes:

$$V_{L1} = -V_{1/2} \qquad \textbf{(10.17)}$$

Figure 19: v_1, $v_{1/2}$,v_{L1}, and V_{dc} theoretical behavior when the P channel power MOSFET switches off and the diode D1 freewheels

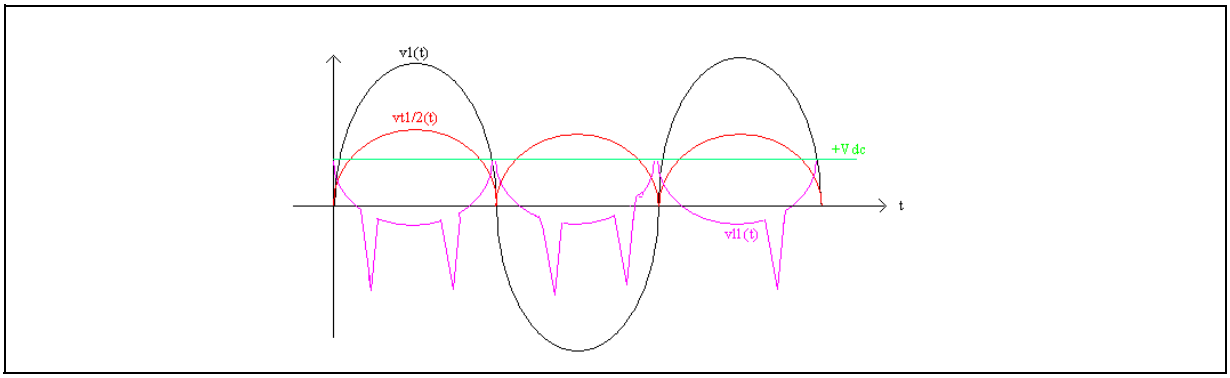

In fact, supposing Q1 always in on state, focusing the attention only on one half-period of the periodic voltage $v_{1/2}$, as showed in fig. 20, the area A_2 must be equal to the area A_1 because the half-sine wave voltage $v_{1/2}$ and the voltage V_{dc} must have the same average value.

Figure 20: $v_{1/2}$ half-sine wave and Vdc graphs

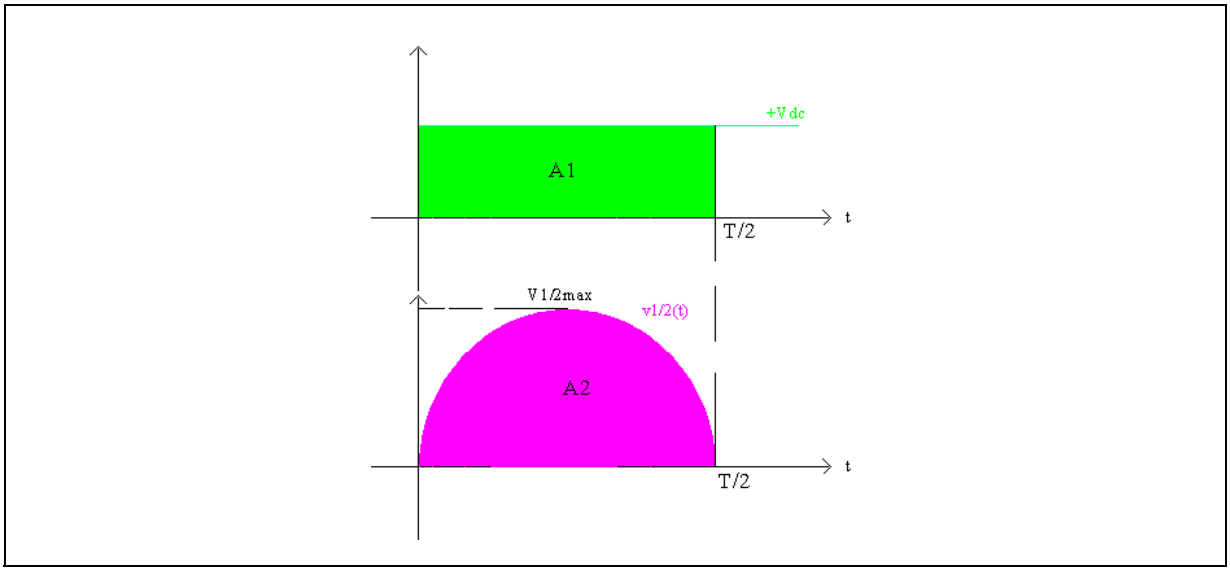

So writing A_1 as:

$$A_1 = V_{dc}\frac{T}{2} \qquad \textbf{(10.18)}$$

and considering A_2:

$$A_2 = \int_0^{\frac{T}{2}} V_{1/2\,max}\,\mathrm{sen}\left(\frac{2\pi}{T}t\right)dt = \qquad \textbf{(10.19)}$$

$$= \frac{T}{2\pi} V_{1max} [-\cos(\frac{2\pi}{T})t]_0^{\frac{T}{2}} = \frac{T}{\pi} V_{1/2max} \quad \textbf{(10.19)}$$

$$A_1 = A_2 \quad \textbf{(10.20)}$$

$$V_{dc} \frac{T}{2} = \frac{T}{\pi} V_{1max} \Rightarrow V_{1/2max} = \frac{\pi}{2} V_{dc} \quad \textbf{(10.21)}$$

and finally, the max voltage v_1 is:

$$v_{1max} = \pi \cdot V_{dc} \quad \textbf{(10.22)}$$

During the half-period T/2, Q_1 can switch off and, in this short time, any voltage is supplied to the board. Fig.21 shows a possible example.

Figure 21: $v_{1/2}$ half-sine wave and V_{dc} graphs when $\delta \neq$ 100%

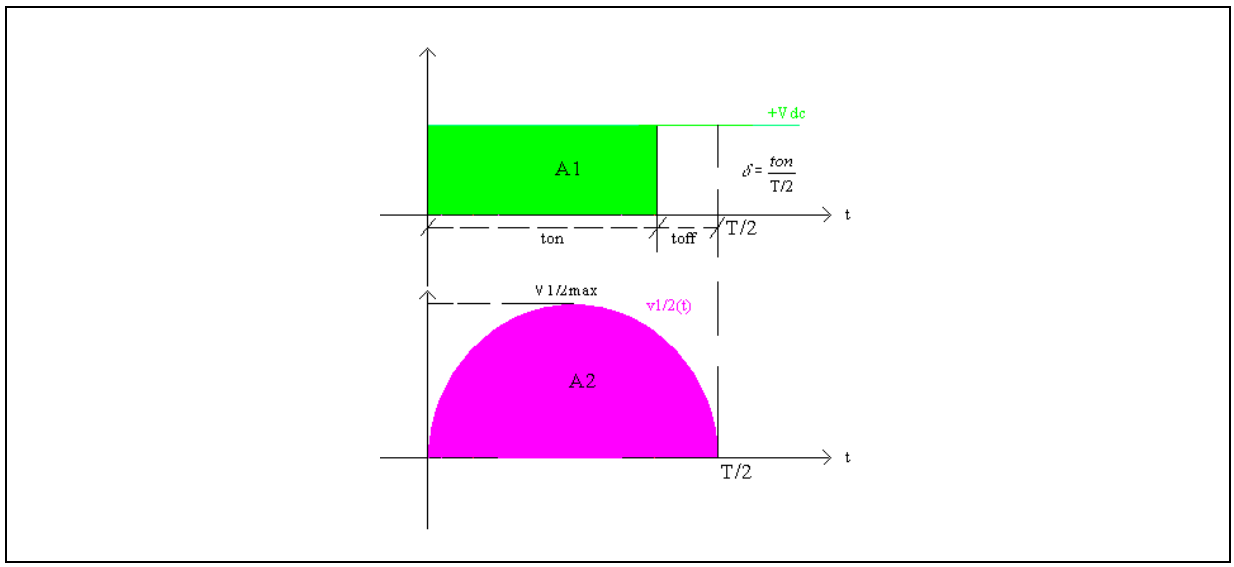

In this condition, the voltages $v_{1/2max}$ and v_{1max} become:

$$V_{1/2max} = \delta \frac{\pi}{2} V_{dc} \quad \textbf{(10.23)}$$

$$V_{1max} = \delta \cdot \pi \cdot V_{dc} \quad \textbf{(10.24)}$$

where δ is the duty cycle of Q_1.

Now focusing the attention only on one half-period of the voltage v_{L1} and considering Q_1 always in on state (see fig. 22).

Figure 22: : v_{l1} theoretical behavior detail

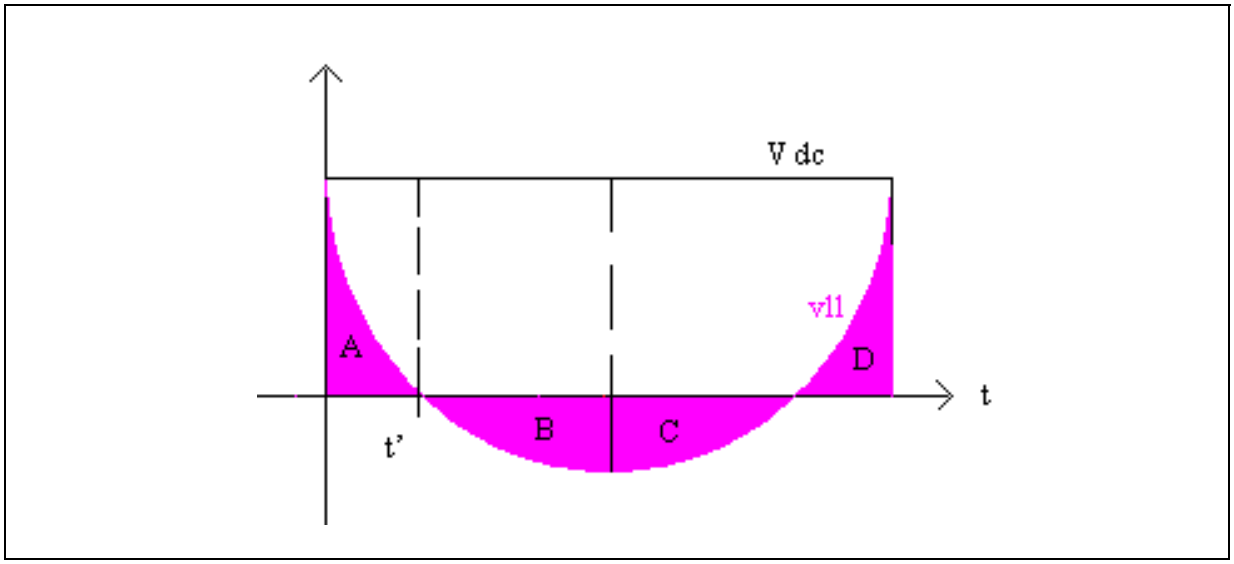

As previously exposed, after the lamps striking, the current 'I' fluctuates around an average value, thus it can be written:

$$I_{max} - I_{avg} = I_{avg} - I_{min} = \Delta I \qquad \textbf{(10.25)}$$

where I_{avg} is the average value current 'I' that involves:

$$v_{avg} = 0 \qquad \textbf{(10.26)}$$

where v_{avg} is the average voltage value across L_1.

The voltage v_{avg} is:

$$v_{avg} = \frac{(A + D - B - C)}{T} \qquad \textbf{(10.27)}$$

where now T is the period of the voltage v_{L1}, and thus:

$$A + D = B + C \qquad \textbf{(10.28)}$$

and:

$$A = B \qquad \textbf{(10.29)}$$

because:

$$C = B,\ D = A \qquad \textbf{(10.30)}$$

The voltage v_{L1} is:

$$v_{L1} = V_{dc} - \frac{\pi}{2} V_{dc} \cdot sen(\frac{2 \cdot \pi}{T} t) \qquad \textbf{(10.31)}$$

and t' is the time when v_{L1} is zero:

$$0 = V_{dc} - \frac{\pi}{2} V_{dc} \cdot sen(\frac{2 \cdot \pi}{T} t') \qquad \textbf{(10.32)}$$

Solving the equation t' becomes:

$$t' = \frac{T}{2 \cdot \pi} arcsen(\frac{2}{\pi}) \qquad \textbf{(10.33)}$$

During the design of the application, the max current ripple of 'I' is fixed. Usually, the $\Delta I_{max\%}$ is about 20-40% of the average value of 'I', where:

$$\Delta I_{max\,\%} = \frac{\Delta I_{max}}{I_{avg}} \qquad \textbf{(10.34)}$$

and thus:

$$\Delta I_{max\,\%} \cdot I_{avg} = \Delta I_{max} \qquad \textbf{(10.35)}$$

Considering the Lenz law:

$$v_{avg} = L1_{min} \frac{\Delta I_{max}}{\Delta t} \qquad \textbf{(10.36)}$$

it is possible to find L_{min} (L_1 minimum value) as:

$$L_{1min} = \frac{\Delta t}{\Delta I_{max}} v_{avg} \qquad \textbf{(10.37)}$$

During the time interval 0-t' the current 'I' increases of

$$\frac{\Delta I_{max}}{2}$$

and the v_{avg} is:

$$v_{avg} = \frac{1}{t'} \int_0^{t'} v_{L1} \cdot dt = \frac{1}{t'} \int_0^{t'} [V_{dc} - \frac{\pi}{2} V_{dc} \cdot sen(\frac{2 \cdot \pi}{T} t)] dt \qquad \textbf{(10.38)}$$

and thus:

$$v_{avg} = \frac{1}{t'} \{V_{dc} \cdot t' - \frac{T}{4} V_{dc} [1 - \cos(\frac{2 \cdot \pi}{T} t')]\} \qquad \textbf{(10.39)}$$

Finally, $L1_{min}$ can be calculated as:

$$L1_{min} = \frac{2}{\Delta I_{max}} \{V_{dc} \cdot t' - \frac{T}{4} V_{dc} [1 - \cos(\frac{2 \cdot \pi}{T} t')]\} \qquad \textbf{(10.40)}$$

When PWM is used, the current ripple depends also on frequency and duty cycle of Q_1. Such ripple is lower compared to the case where Q_1 is permanently in an on-state, therefore this is the worst condition with regard to the ripple.

The attention will be now focused on the PNP power bipolar transistor, or P channel power MOSFET, on Q_1 and the diode D_1. During the Q_1 on-state, the diode D_1 is disabled, 'I' flows through the same device, while during the Q_1 off-state 'I' freewheels into D_1 (see fig. 23).

Figure 23: Q_1 and D_1 theoretical behavior

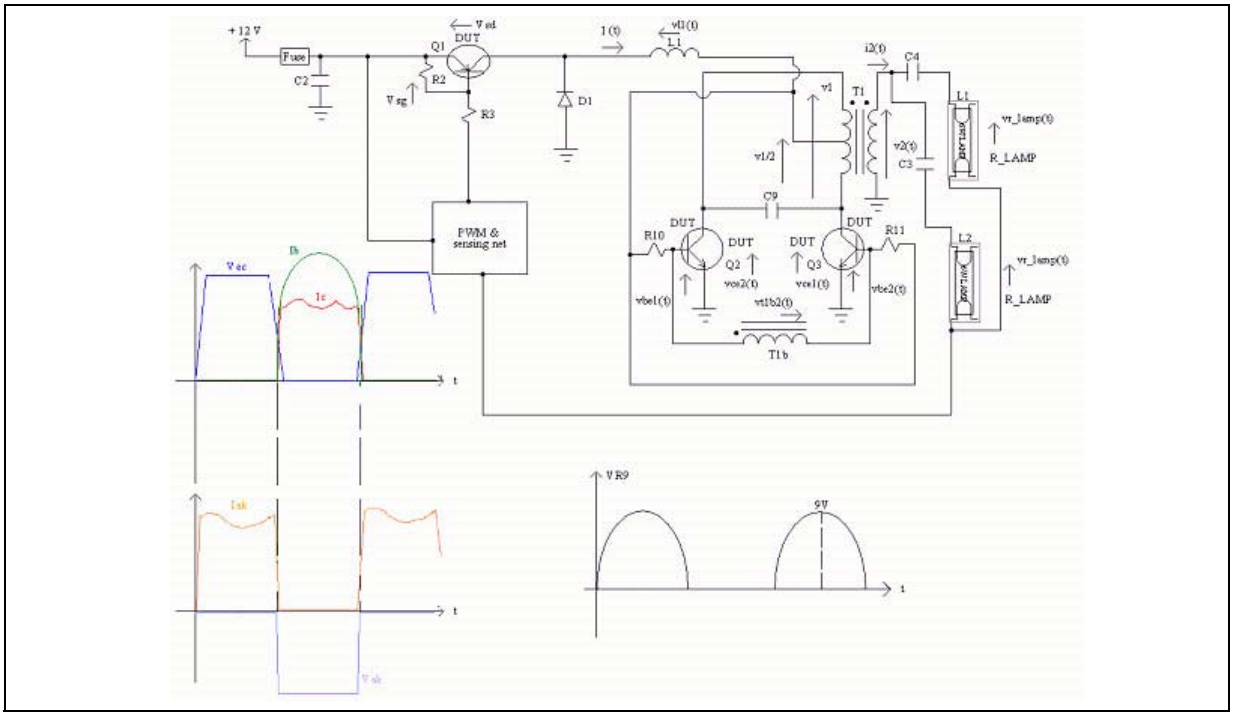

With regard to Q_2 or Q_3, when the first is on, the current flows through the device, while the second is off and vice versa (see fig. 24).

Figure 24: Q_2 and Q_3 voltages and currents theoretically calculated

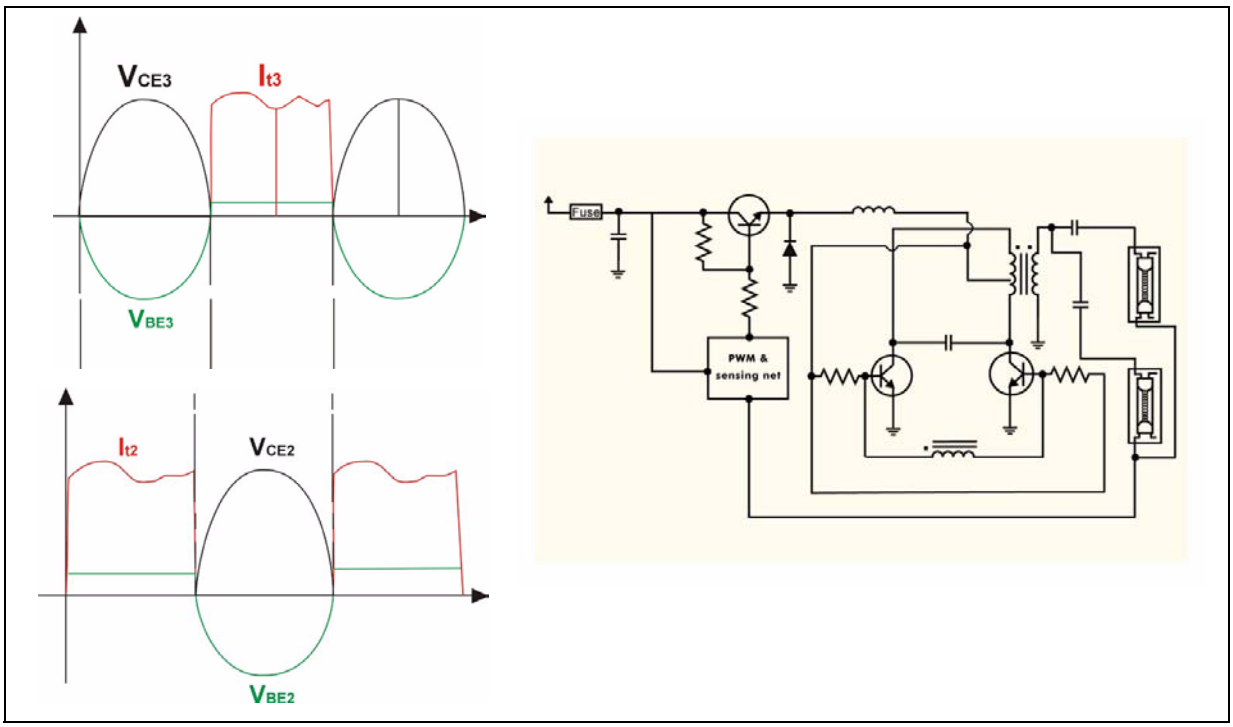

11. SENSING NET AND PWM NET WITH TSM108

The following picture highlights the sensing net considering the CCFL design used in this paper.

Figure 25: Sensing circuitry detail

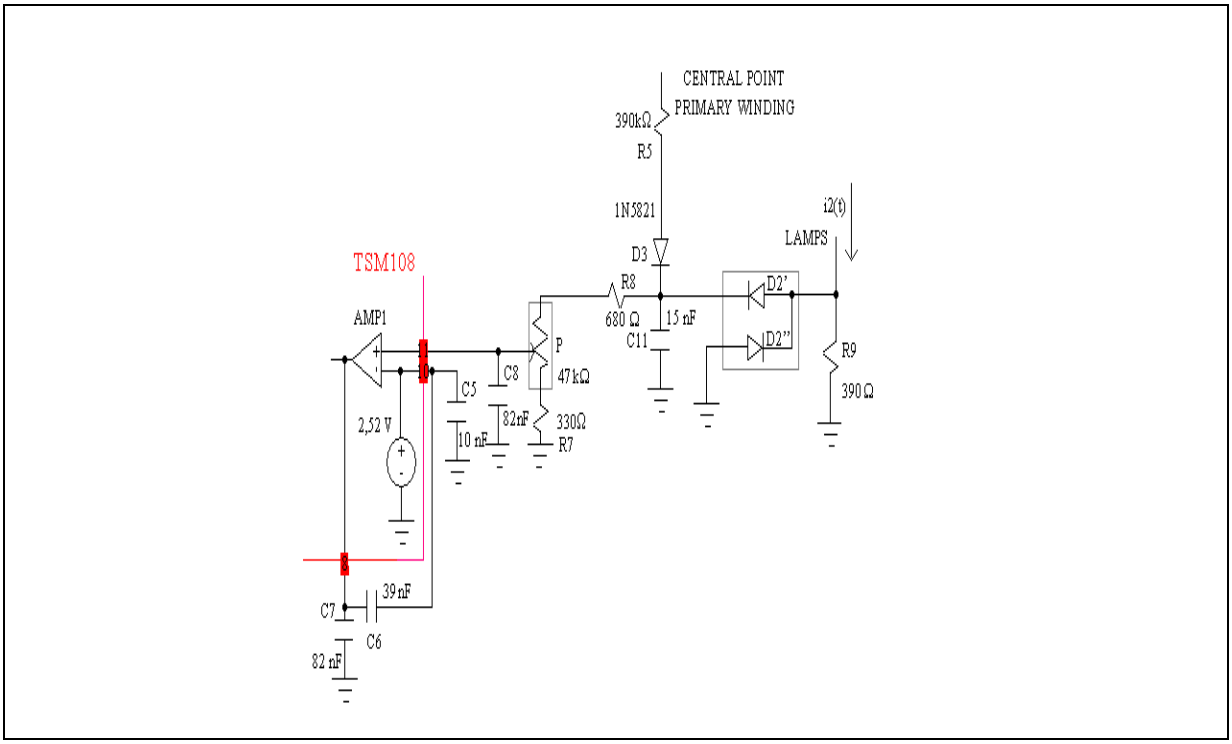

During the i_2 positive half-sine-wave the current, mainly, passes through the resistance R_9. The voltage across R_9 enables the diode $D_{2'}$ and the net C_{11}-R_8-P-R_7-C_8. When Q_1 is in on-state the max output power on the lamps reaches about 16W, thus, the i_{2eff} (RMS current) is:

$$i_{2eff} = \sqrt{\frac{P_{out}}{R_{Lamp}}} = \sqrt{\frac{16}{60000}} \cong 16mA \qquad \textbf{(11.1)}$$

While its maximum value i_{2max} is:

$$i_{2\max} = 16\sqrt{2} \cong 23mA \qquad \textbf{(11.2)}$$

The maximum voltage across R9, V_{R9} is:

$$V_{R9\max} = R_9 \cdot i_{2\max} = 390 \cdot 23 \cdot 10^{-3} \cong 9V \qquad \textbf{(11.3)}$$

The maximum voltage V_{R9} is important because if it overcomes 9V it can make the TSM108 instable.

Figure 26: V_{R9} theoretical behavior

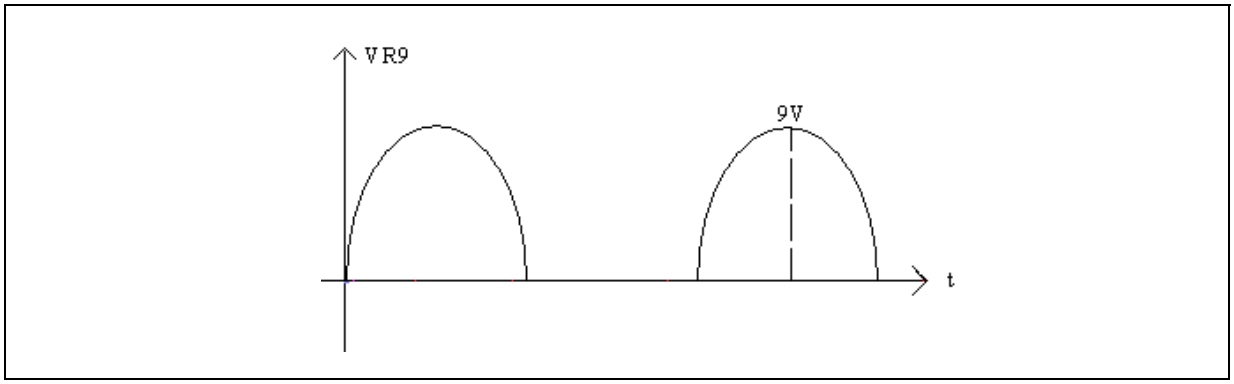

During the i_2 negative half-sine-wave, the diode $D_{2"}$ carries the current bypassing the resistance R_9 and increasing the application efficiency. During the i_2 positive half-sine-wave, the capacitor C_{11} gets charged, keeps constant the voltage across it and discharges on the R_8-P-R_7 net during the i_2 negative half-wave.

The inverting input of the AMP1 is fixed at 2.52V and it tries to keep the non-inverting input at the same voltage. When the output power increases, the current i_2 increases as well and the voltage in the non-inverting input overcomes the 2.52V but, immediately after, the AMP1 output and TSM108 regulate the duty cycle of Q_1 limiting the output power and in turn reducing the non-inverting input voltage to 2.52V.

Regulating the trimmer P, the lamps brightness can be regulated. In fact, increasing the trimmer P resistance the lamps brightness can be decreased because the non-inverting input overcomes 2.52V and TSM108 decreases the Q_1 duty cycle and vice versa. In the following figure the AMP1 characteristics are shown.

Figure 27: TSM108 AMP1measured waveforms

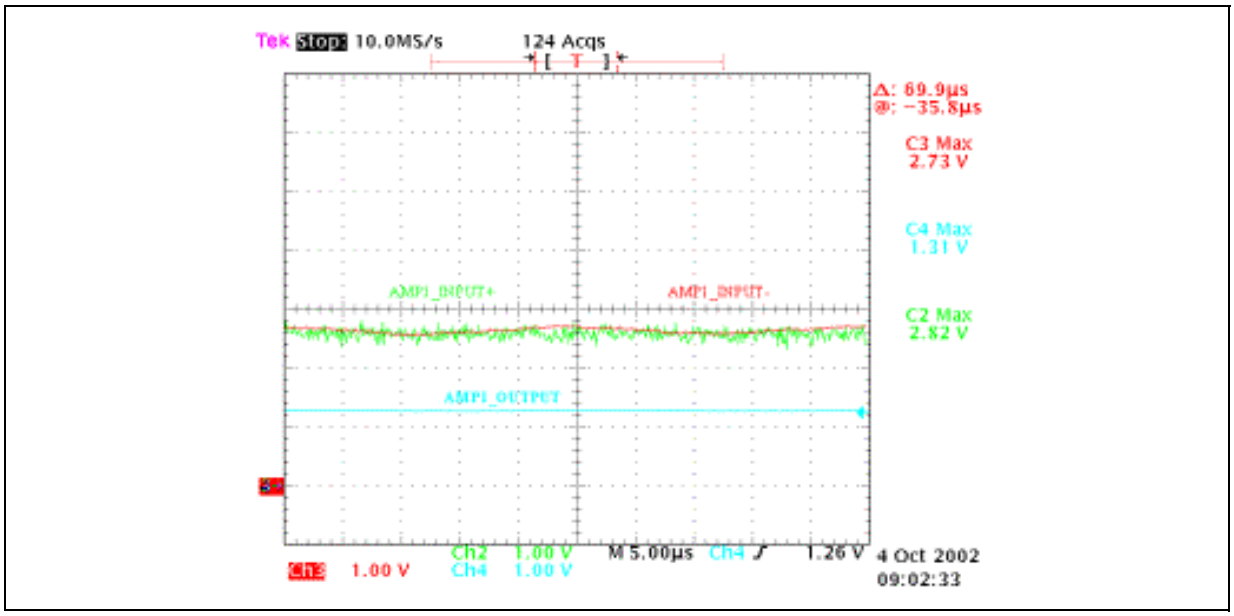

The capacitor C_8 keeps the voltage in the non-inverting input of the AMP1 constant, thus avoiding

situations of instability. The resistor R_5 regulates the minimum output power on the lamps. It is connected to the central point of the primary winding of T_1 on one side, and, on the other side, to the diode D_3 whose cathode goes to the capacitor C_{11}. The diode D_3 avoids a current flowing from C_{11}-R_8-P-R_7-C_8 net to the T_1 transformer. Without this net, the minimum output power would never reach a value under the 40% of the nominal lamps power. C_7 is the compensation capacitor of the AMP1 output, while the C_5 is the voltage reference bias capacitor. The capacitor C_6 allows the flickering of the lamps to be avoided. The following picture shows the driving circuitry of Q_1.

Figure 28: Q_1 driver circuitry

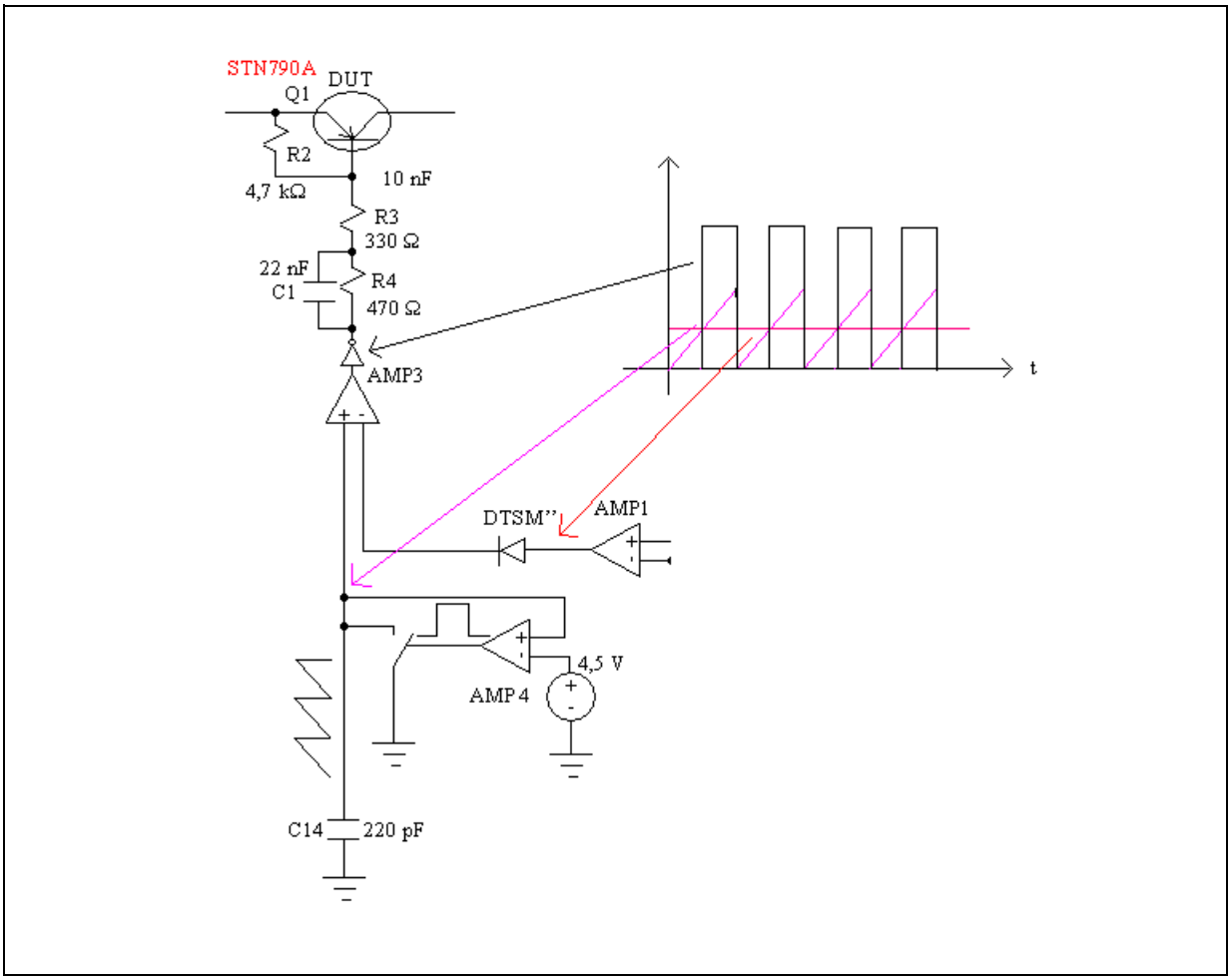

The AMP1 output is the AMP3 inverting input and is compared to the saw tooth signal generated from AMP4. The frequency of the saw tooth signal is established by the capacitor C_{14}. In this design the 220pF capacitor generates a saw tooth signal with about 90KHz switching frequency. Usually the Q_1 switching frequency must be at least twice the lamps frequency. It can reach up to about 250 KHz using a P channel power MOSFET. When the AMP1 output is higher compared to the saw tooth signal, the AMP3 output is low and Q_1 switches on and vice versa. The following picture shows the AMP3 characteristics.

Figure 29: TSM108 AMP3 measured waveforms

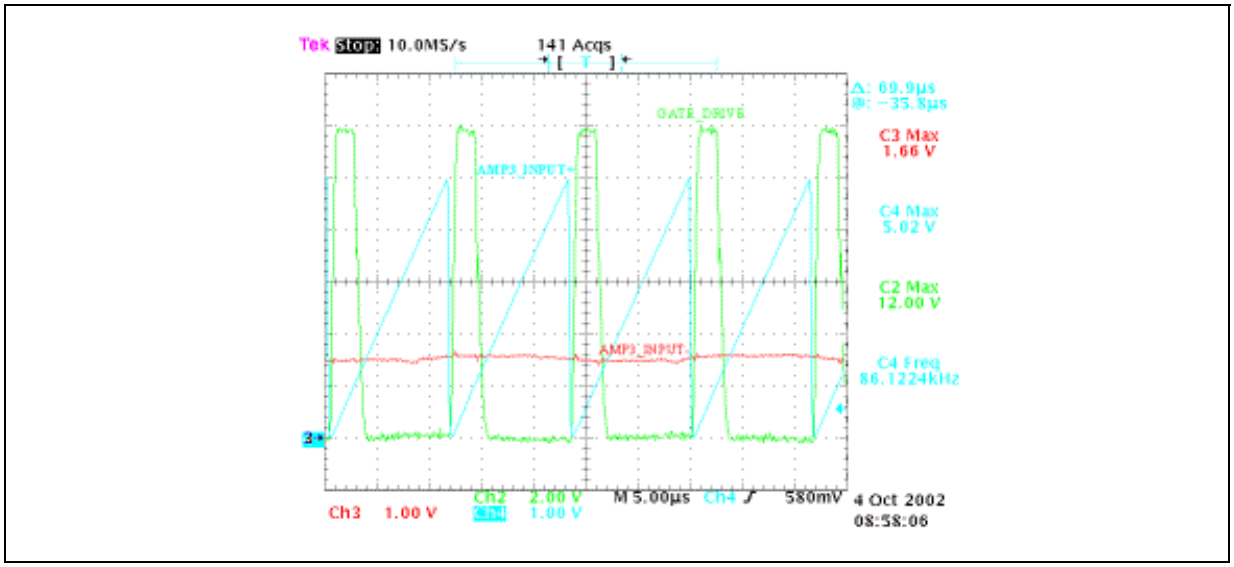

It is important to highlight that such design allows the regulation of the output power on the lamps in the 2-16W range.

As considered in section 1, the TSM108 has the Q_1 lock functions UV (under voltage lockout) and OV (over voltage lockout). Without any external components, as previously said, the input voltage range accepted by the TSM108 is between 8.5V and 32.4V. In this application, being such voltage 12V, the chosen voltage range is 8.5-15.5V. While the minimum input voltage value corrisponds to the standard UV of the TSM108, being the maximum chosen input voltage lower than the standard OV, it is necessary to introduce an external a 220KOhm resistor R1 between +12V and the pin 5 of the TSM108, in order to decrease such value (see fig. 30).

Figure 30: OV modified circuit

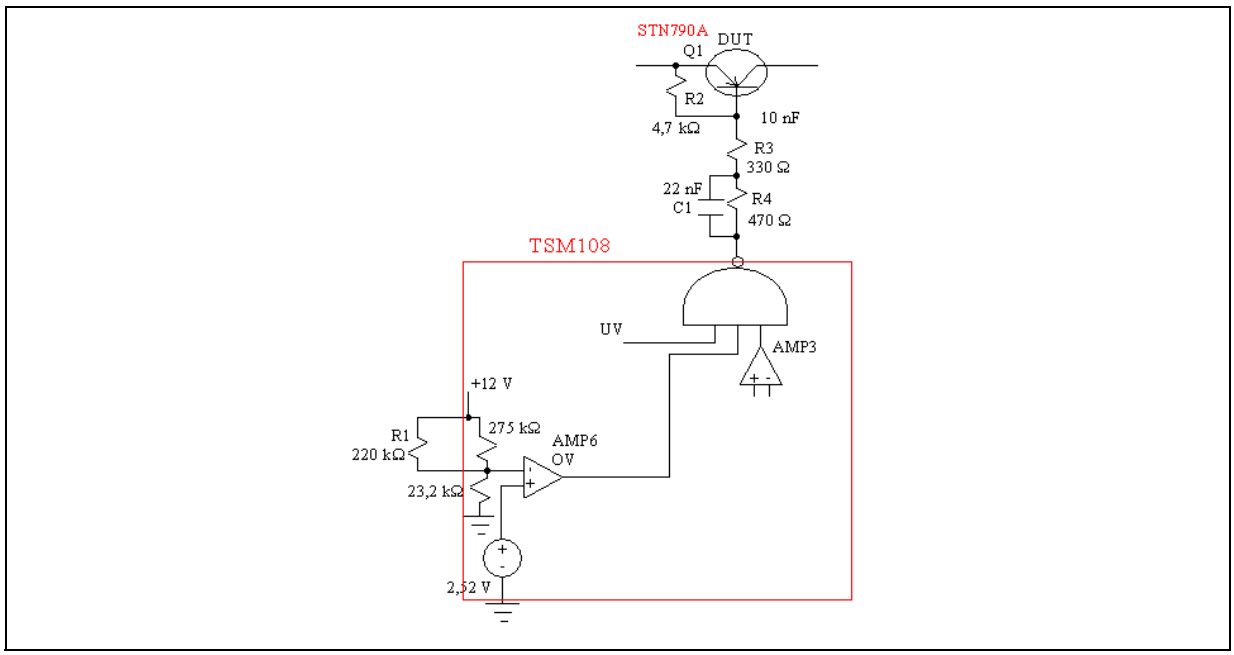

Considering the equation 2.6, the OV voltage is:

$$Vcc = \frac{2.52}{23.2}(275//220+23.2) = \frac{2.52}{23.2}[(\frac{275*220}{275+220})+23.2] = 15.8V \quad \textbf{(11.1)}$$

12. DESIGN OF THE CCFL APPLICATION USING TSM108 AND THE STMicroelectronics' POWER TRANSISTORS

In Table 1 all the components of the design, taken as an example, are listed. Figures 31 and 32 show the schematic circuits of the application using the STN790A power bipolar and STS3DPFS30 respectively and the TSM108.

Table 1: Components list

COMPONENT	NAME	VALUE
RESISTANCE	R1	220 kOhm
RESISTANCE	R2	4,7 kOhm
RESISTANCE	R3	330 Ohm
RESISTANCE	R4	470 kOhm
RESISTANCE	R5	390 kOhm
RESISTANCE	R7	330 Ohm
RESISTANCE	R8	680 Ohm
RESISTANCE	R9	390 Ohm
RESISTANCE	R10	2 kOhm
RESISTANCE	R11	2 kOhm
RESISTANCE	R12	2 kOhm
RESISTANCE	R13	2 kOhm
CAPACITOR	C1	22 nF
CAPACITOR	C2	150 uF
CAPACITOR	C3	22 pF
CAPACITOR	C4	22 pF
CAPACITOR	C5	10 nF
CAPACITOR	C6	39 nF
CAPACITOR	C7	82 nF
CAPACITOR	C8	82 nF
CAPACITOR	C9	220 nF
CAPACITOR	C11	15 nF
CAPACITOR	C13	10 nF
CAPACITOR	C14	220 pF
STS3DFPS30-POWER MOSFET	Q1	
STN790A-PNP POWER BIPOLAR	Q1	
STSA1805-NPN POWER BIPOLAR	Q2	
STSA1805-NPN POWER BIPOLAR	Q3	
TSM108-IC		
1N5821-DIODE	D1	
1N5821-DIODE	D3	
6 W LAMP	I1	
6 W LAMP	I2	
INDUCTOR	L1	140 uH
TRIMMER	P	47 kOhM
FUSE		2 A

Figure 31: CCFL schematic circuit using the PNP power bipolar transistor

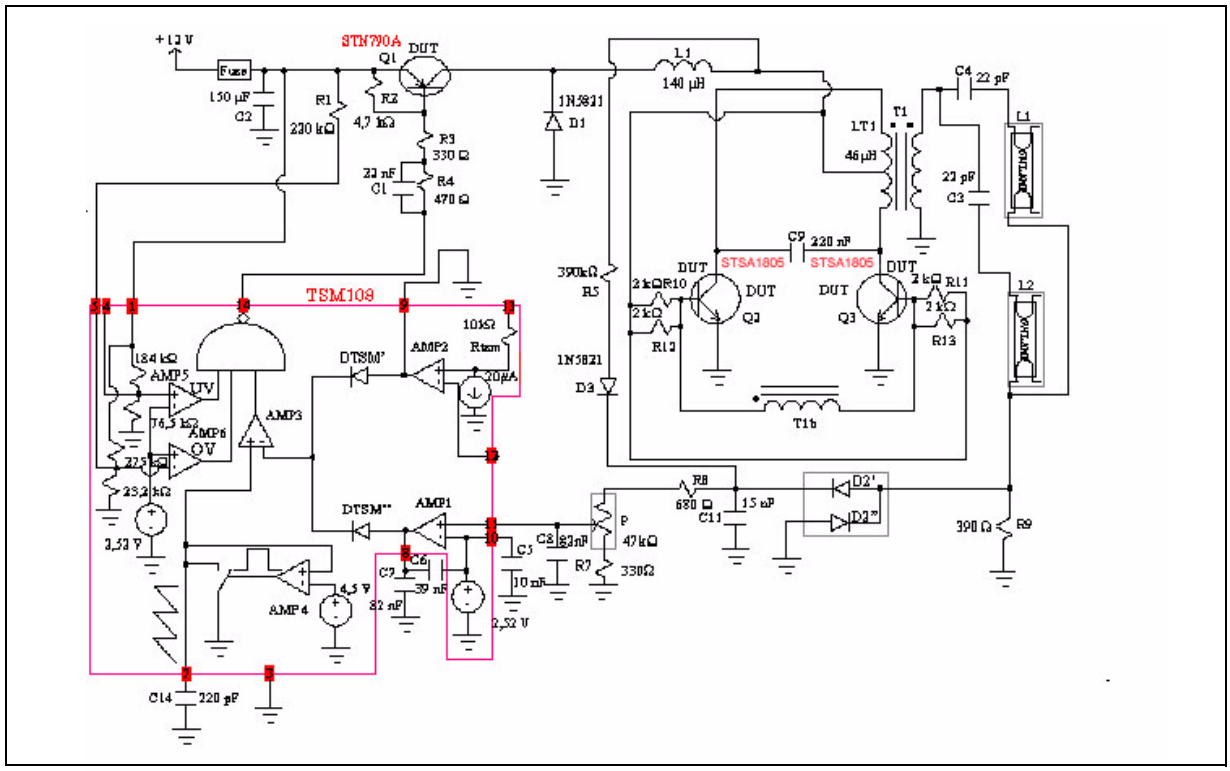

Figure 32: CCFL schematic circuit using the P channel power MOSFET transistor

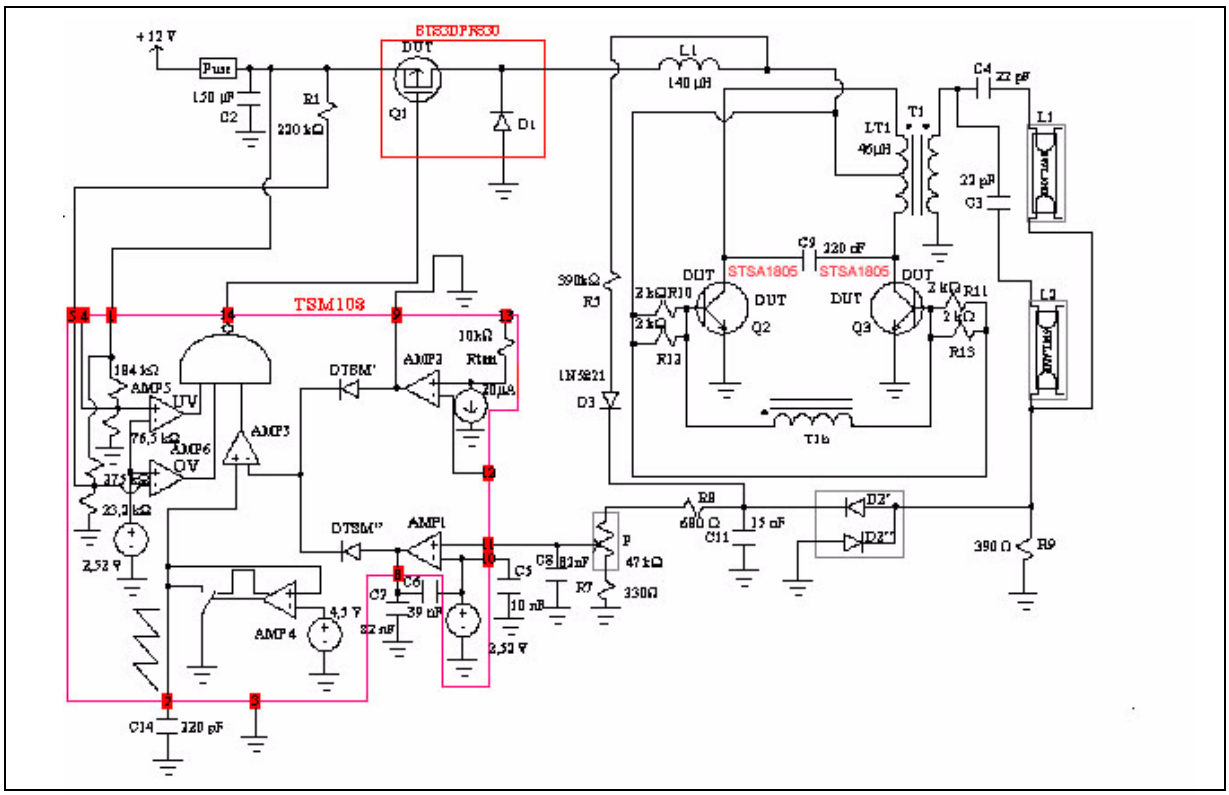

The following graphs show the voltage characteristics of the transformer while no lamps are connected to the converter.

Figure 33: v_2 measured waveforms before striking

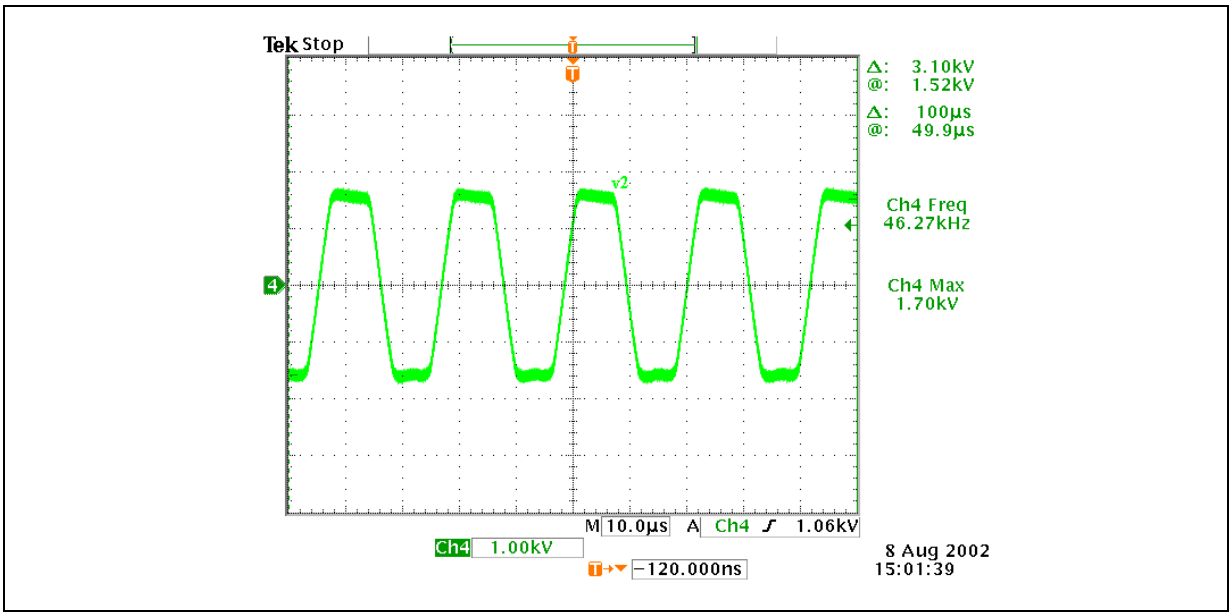

Figure 34: v_1 measured waveforms before striking

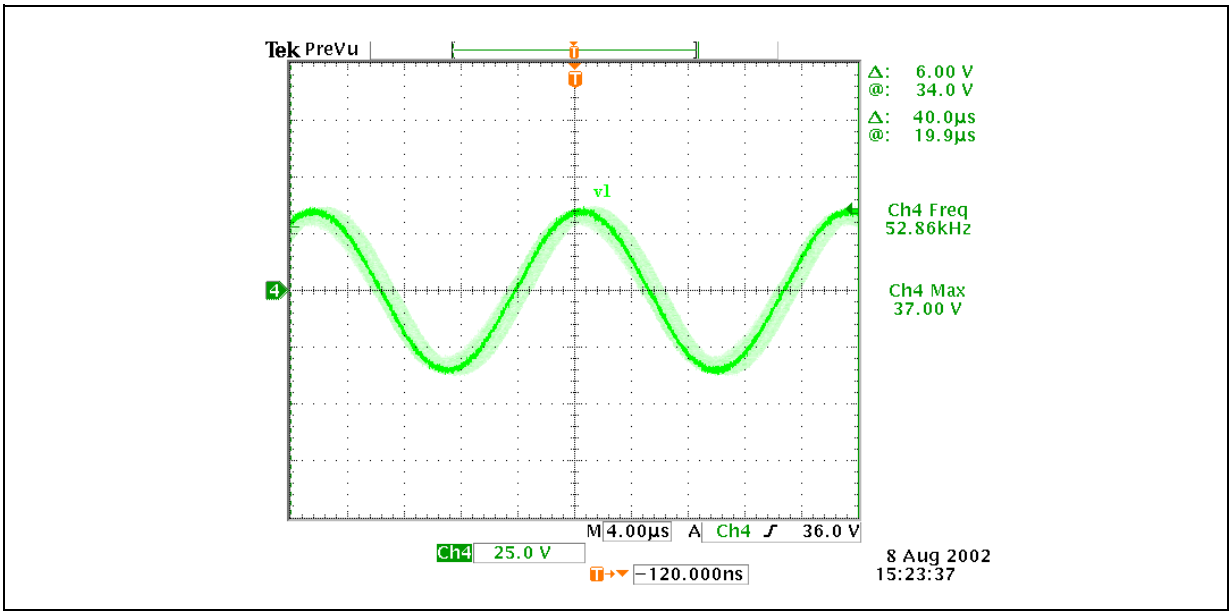

Figure 35: V3 measured waveforms before striking

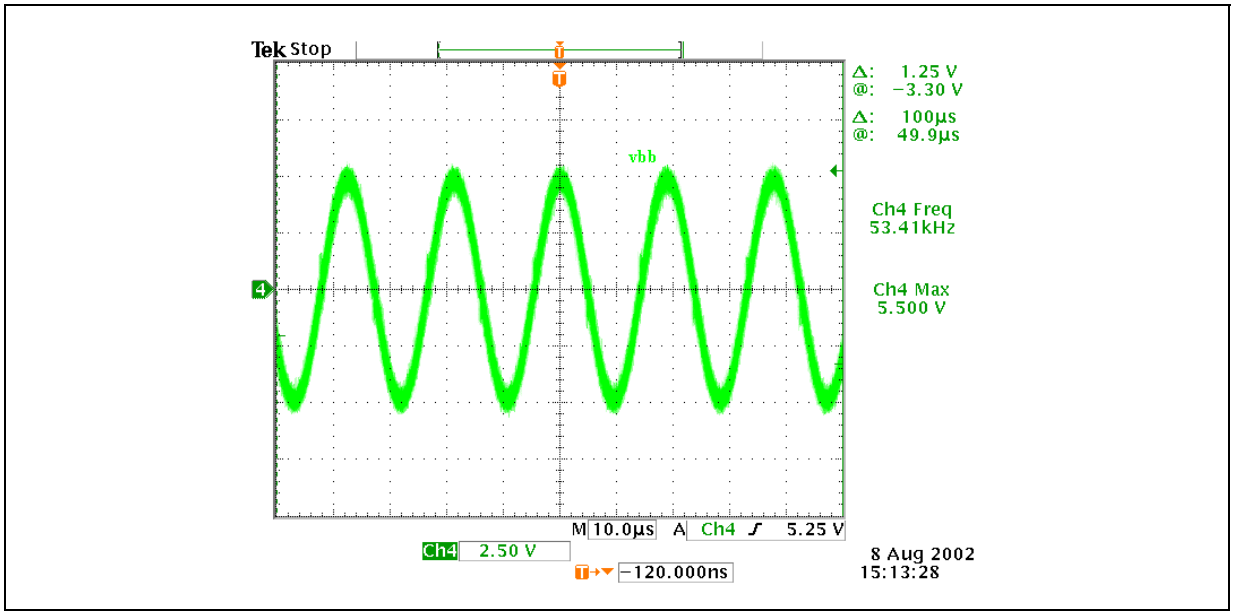

Figure 36: $v_{1/2}$ measured waveforms before striking

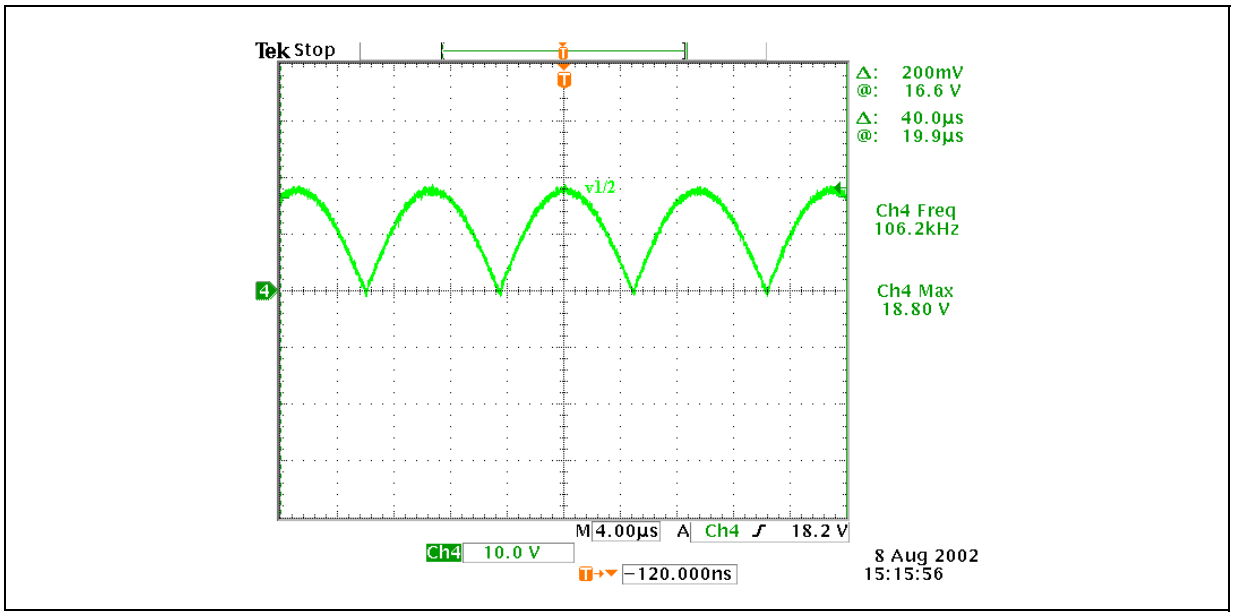

In figure 34 the maximum value of v1 is 37V according to the formulas 10.22:

$$v_{1max} = \pi \cdot V_{dc} = 3{,}14 \cdot 12 \cong 37{,}5V \qquad \textbf{(12.1)}$$

The operation frequency is about 50KHz, in fact, considering the formula 10.1:

$$f = \frac{1}{2 \cdot \pi \sqrt{LTC_9}} = \frac{1}{2 \cdot 3.14 \sqrt{46 \cdot 10^{-6} \cdot 220 \cdot 10^{-9}}} \cong 50Khz \qquad \textbf{(12.2)}$$

The maximum voltage value of $v_{1/2}$ is 18.80V, as stated in formula 9.19:

$$v_{1/2\max} = \frac{\pi}{2} \cdot V_{dc} = \frac{3.14}{2} \cdot 12 \cong 18.8V \qquad \textbf{(12.3)}$$

The voltage $v_{1/2}$ has a frequency twice the v_1 because $v_{1/2}$ has only half positive sin-wave characteristics.

The $\frac{N_2}{N_1/2}, \frac{N_3}{N_1/2}$ ratio are:

$$\frac{N_2}{N_1/2} = \frac{v_{2\max}}{v_{1/2\max}} = \frac{1700}{18.80} \cong 90 \qquad \textbf{(12.4)}$$

$$\frac{N_3}{N_1/2} = \frac{v_{3\max}}{v_{1/2\max}} = \frac{5.5}{18.80} \cong \frac{1}{3} \qquad \textbf{(12.5)}$$

In fig. 37 the waveforms of current and voltage of L_1 are showed.

Figure 37: v_{L1}, i_{L1} and i_{ak} measured waveforms before striking

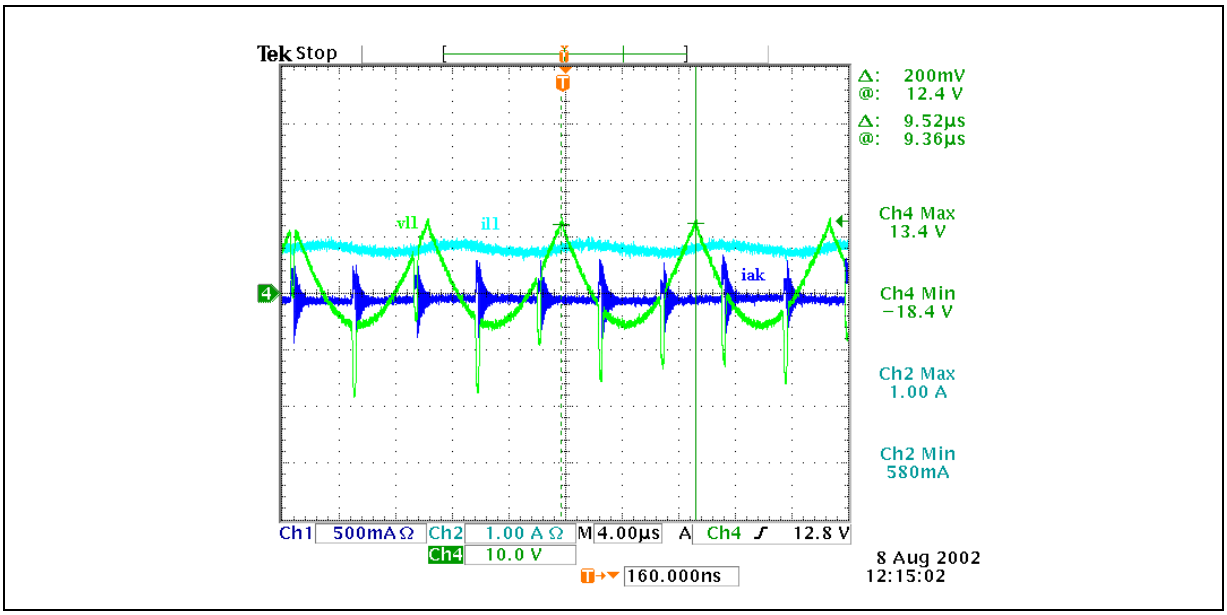

In this condition, the current I_{L1} into the inductor L_1 is 1A. The v_{L1} frequency is the same as the $v_{1/2}$ one, while the maximum v_{L1} voltage is equal to V_{dc}. According to the formula 9.29 the minimum v_{L1} value is:

$$v_{L1min} = V_{dc} - \frac{\pi}{2} V_{dc} = 12 - \frac{3.14}{2} 12 \cong -7V \qquad \textbf{(12.6)}$$

As showed in fig. 37, the minimum v_{L1} value is about -18.5V because during the operation Q_1 switches off, the diode D_1 switches on (in fig. 37 the i_{ak} current is highlighted), and the voltage v_{L1} is $-v_{1/2}$.

The following graph shows current and voltage in D_1 in these conditions.

Figure 38: i_{ak} and v_{ak} measurements before striking

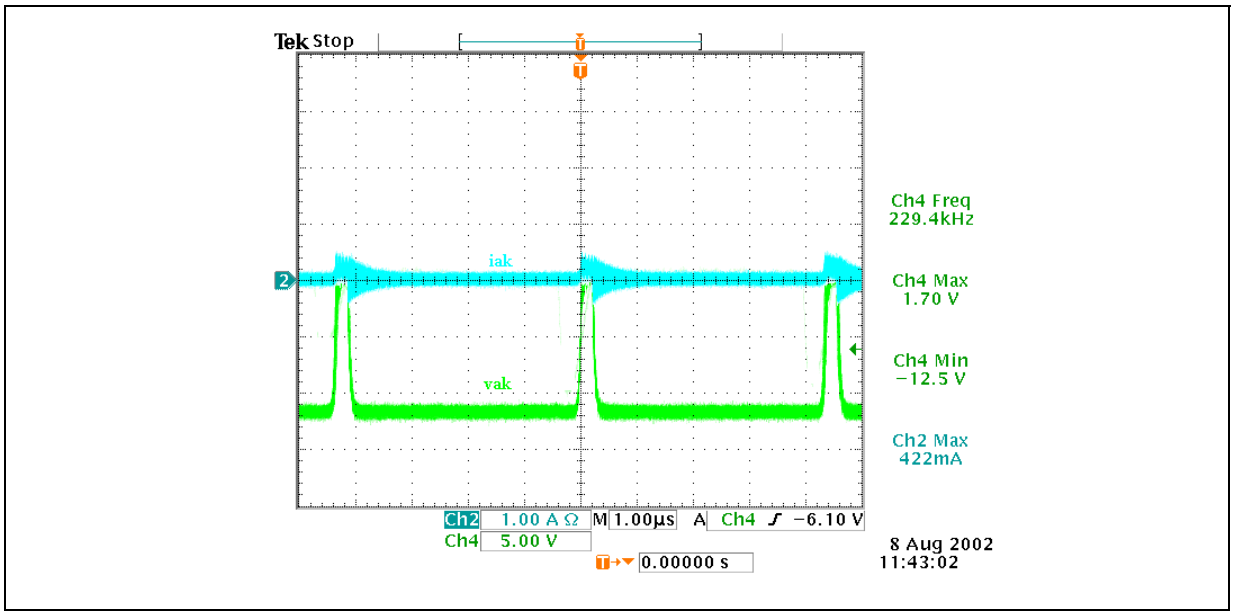

The pictures in the next pages show all voltages and currents when the lamps are connected.

Figure 39: v_2 measurement during the lamps on-state

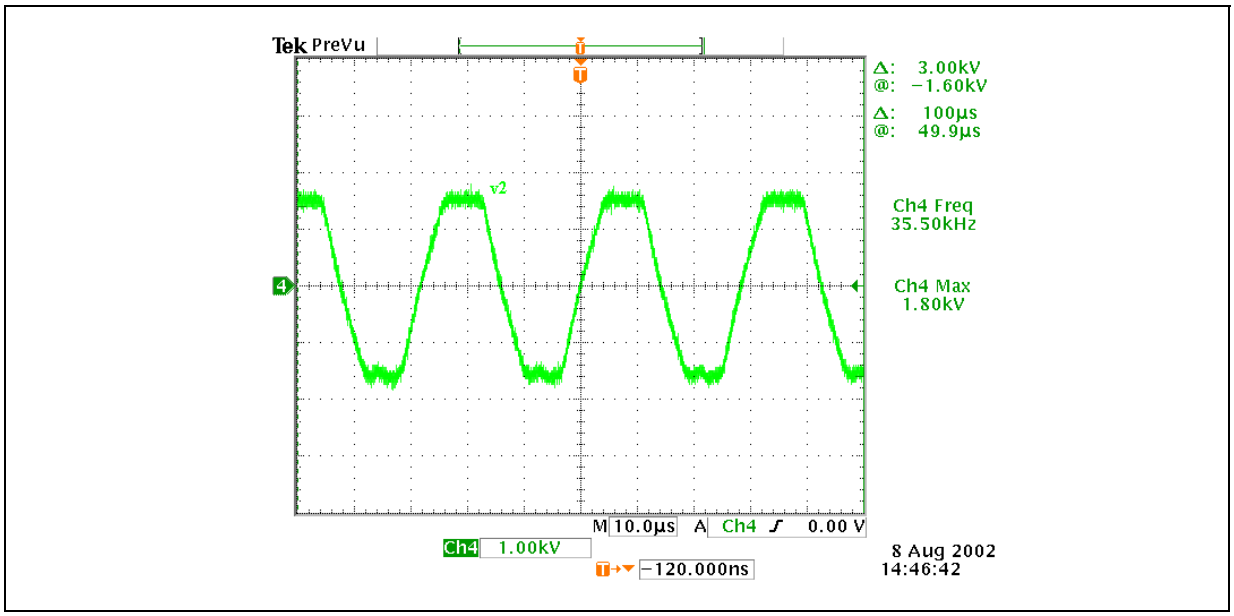

Figure 40: v_1 measurement during the lamps on-state

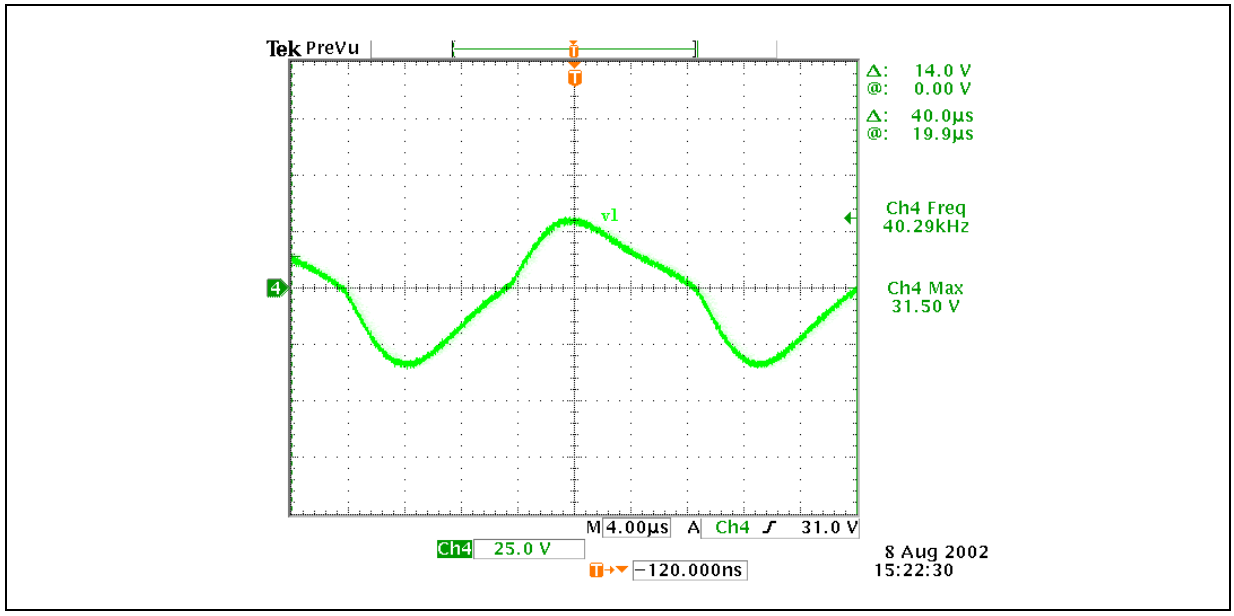

Figure 41: V3 measurement during the lamps on-state

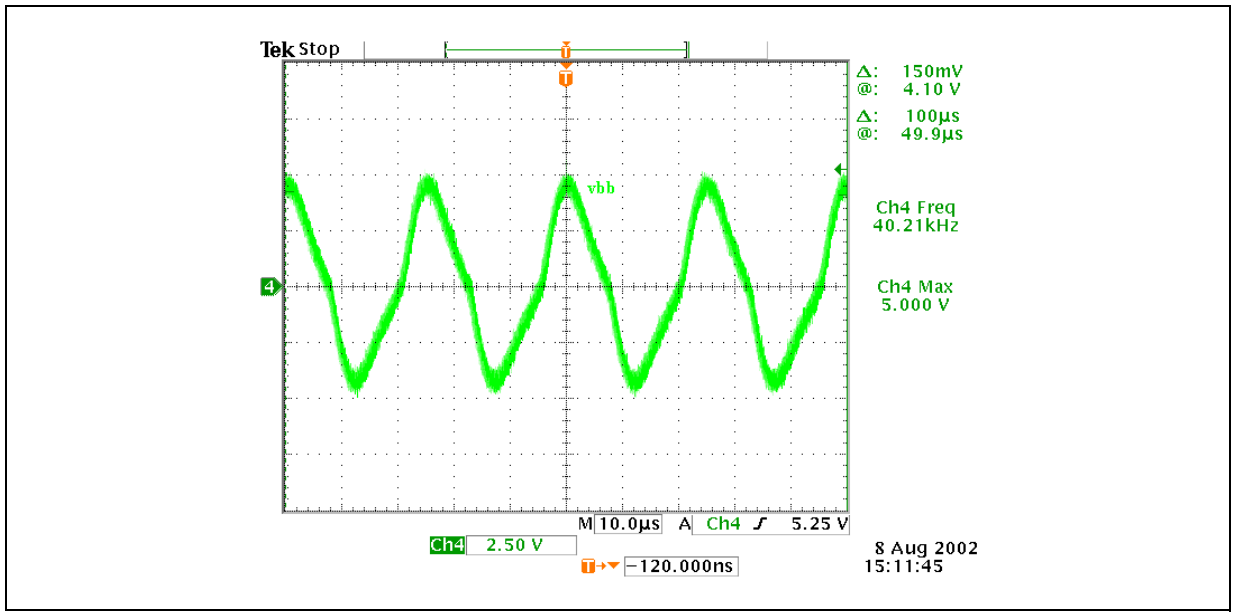

Figure 42: $v_{1/2}$ measurement during the lamps on state

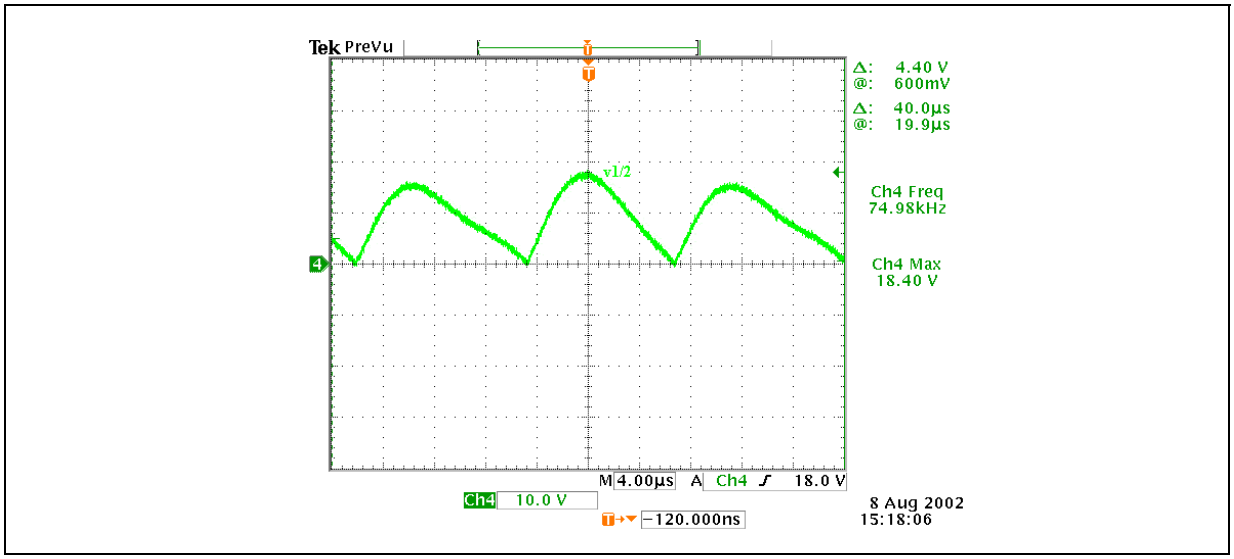

The operation frequency drops from about 50KHz to about 35 KHz, in fact, considering the 10.13:

$$f = \frac{1}{2 \cdot \pi \sqrt{LT(C_9 + 2 \cdot k^2 \cdot C)}} = \qquad \textbf{(12.7)}$$

$$= \frac{1}{2 \cdot 3.14 \sqrt{46 \cdot 10^{-6}(220 \cdot 10^{-9} + 2 \cdot 44 \cdot 90^2 \cdot 10^{-12})}} \cong 32Khz$$

The obtained result theoretically is very much similar to the measured one and the slight difference is mainly due to the simplifications applied in the mathematical model.
Fig.43 shows the current and voltage behavior when lamps are connected.

Figure 43: v_{L1}, i_{L1} and i_{ak} measurements during the lamps on-state

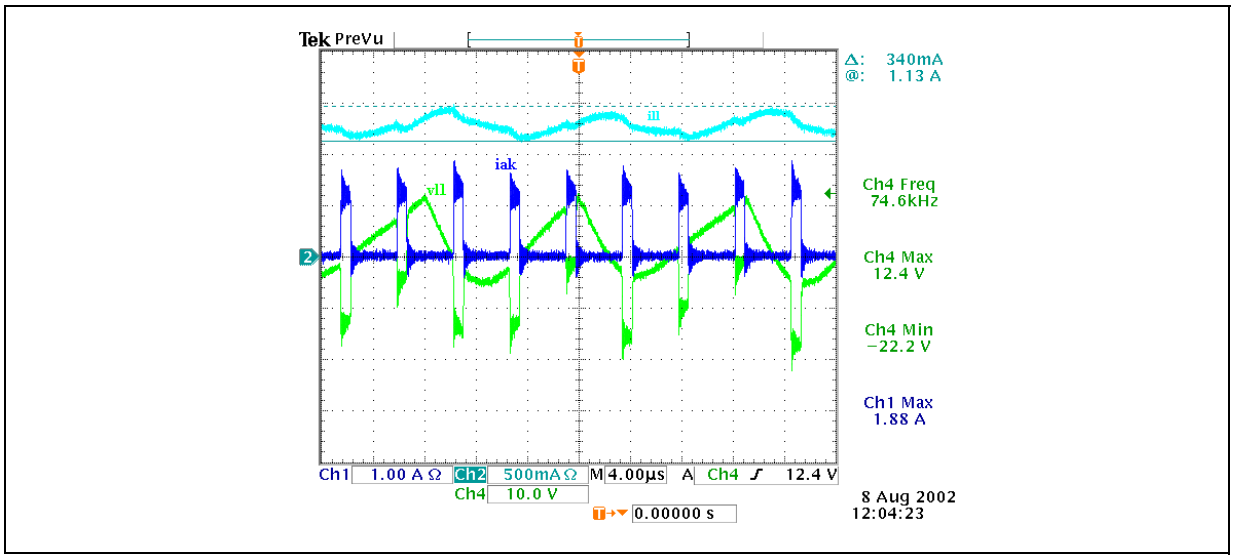

Now, focusing the attention on Q_1, considering the lamps on, the following figures show the power bipolar STN790A and the power MOSFET STS3DPFS30 characteristics (steady state, turn off) considering three different input voltages 12V (standard condition), 10.8V and 13.2V (+-10% of the nominal voltage condition). The tables, following the graphs below, summarize the main electrical parameters. Furthermore, waveforms regarding the free wheeling diode D_1 working under the same above-mentioned conditions are included.

Figure 44: STN790A steady state (V_{dc}=12V)

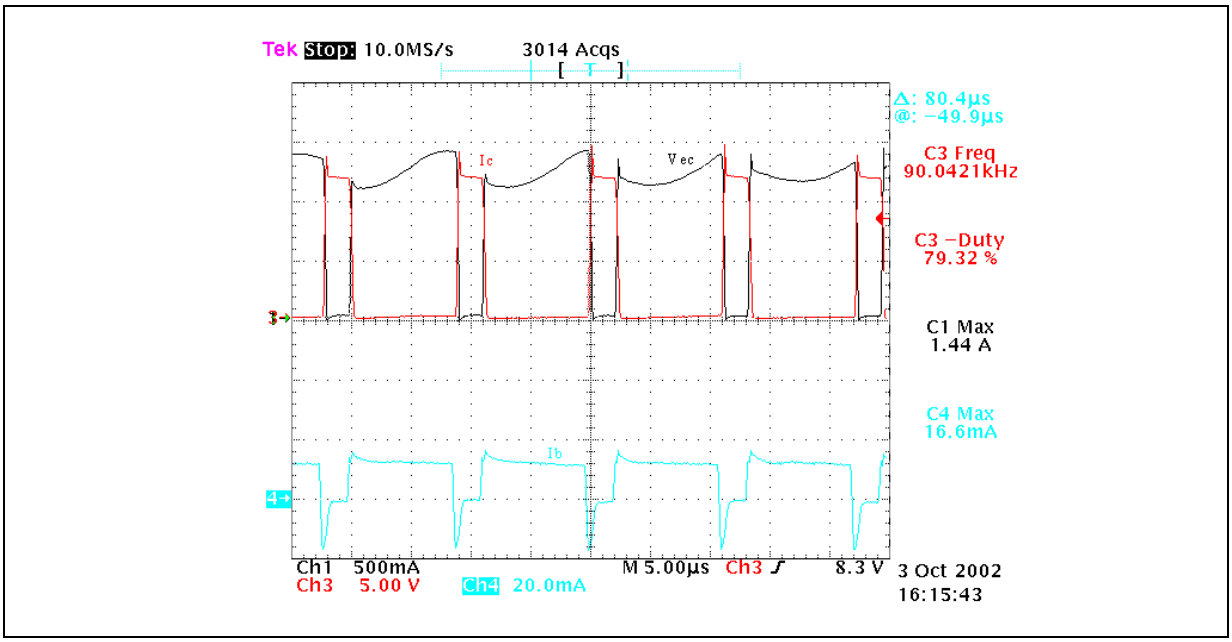

Figure 45: STN790A turn off (V_{dc}=12 V)

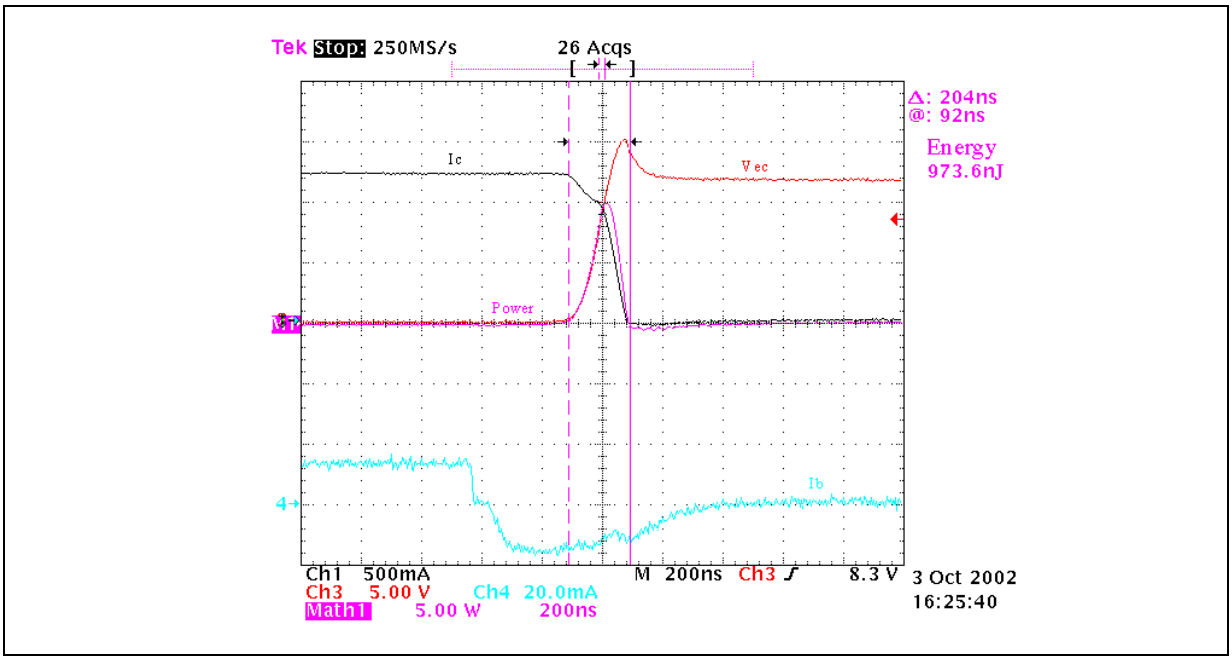

Figure 46: STN790A turn on (V_{dc}=12V)

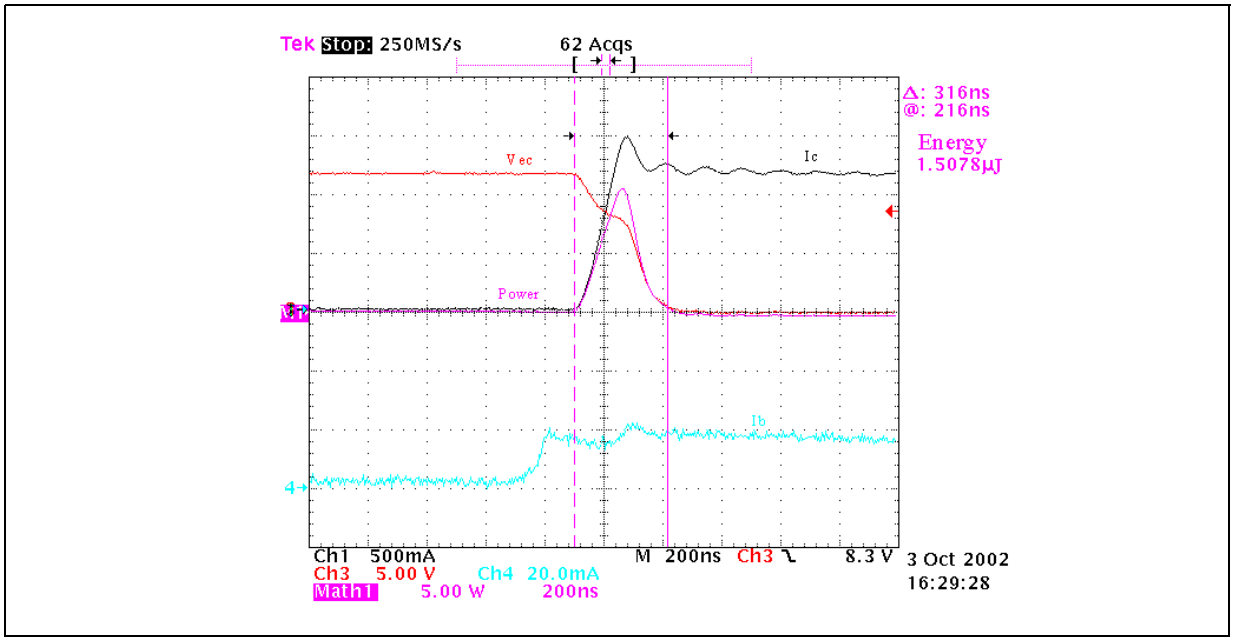

Figure 47: STS3DPFS30 steady state (V_{dc}=12V).

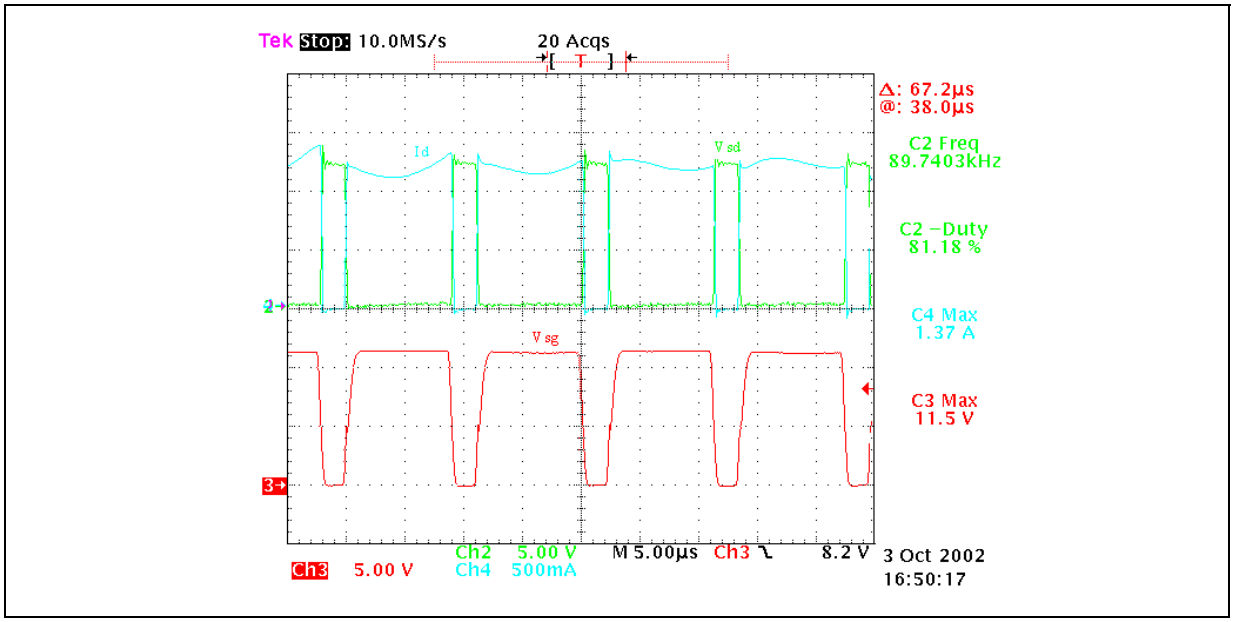

Figure 48: STS3DPFS30 turn off (V_{dc}=12 V)

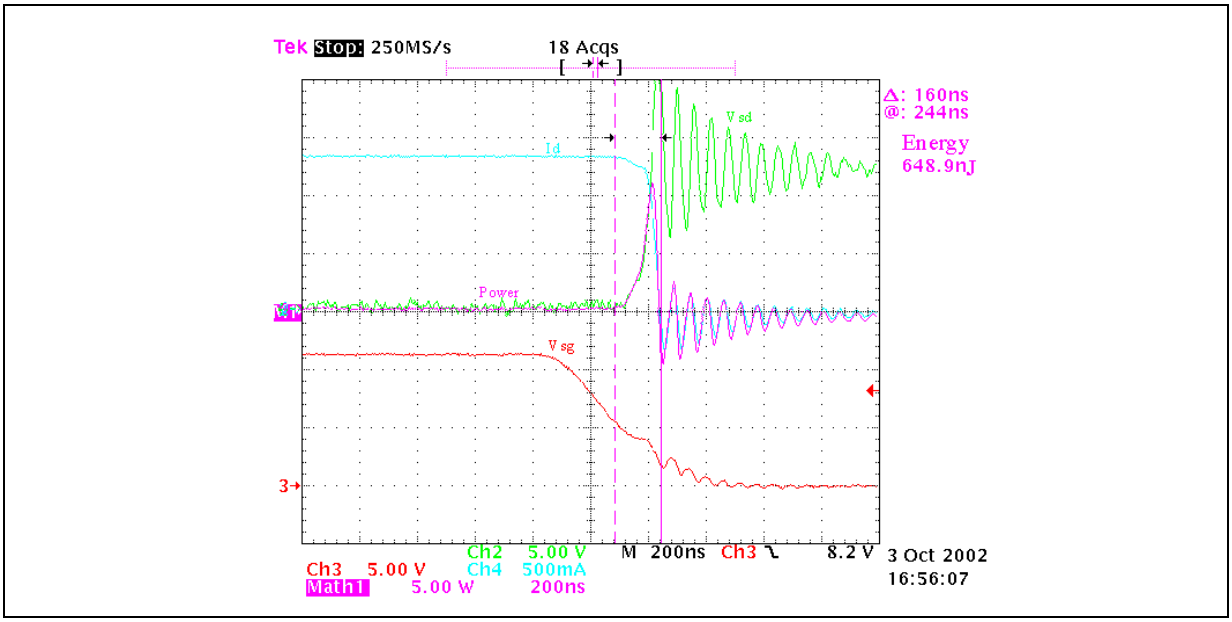

Figure 49: STS3DPFS30 turn on (Vdc=12V).

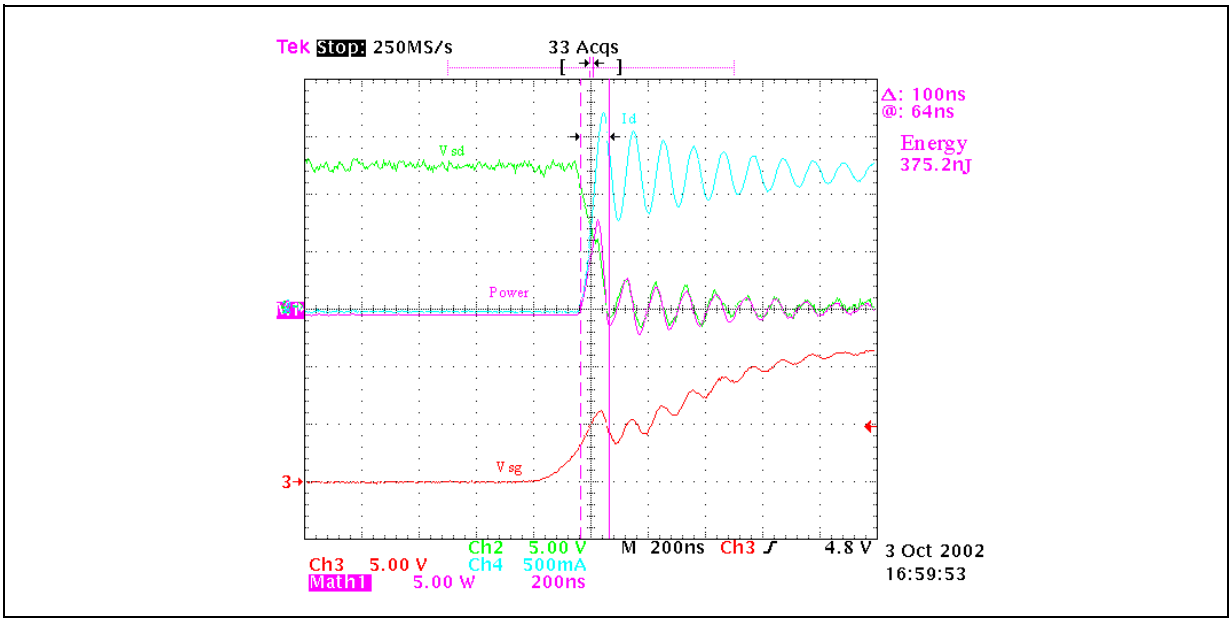

Figure 50: STN790A steady state (V_{dc}=10.8V).

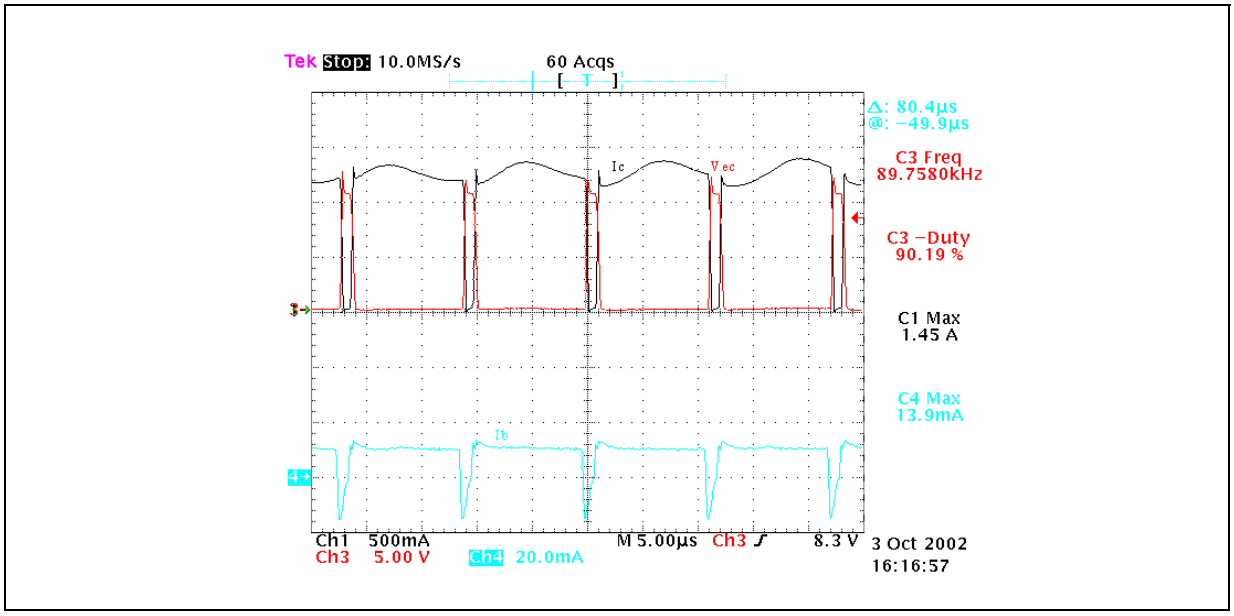

Figure 51: STN790A turn off (Vdc=10.8 V).

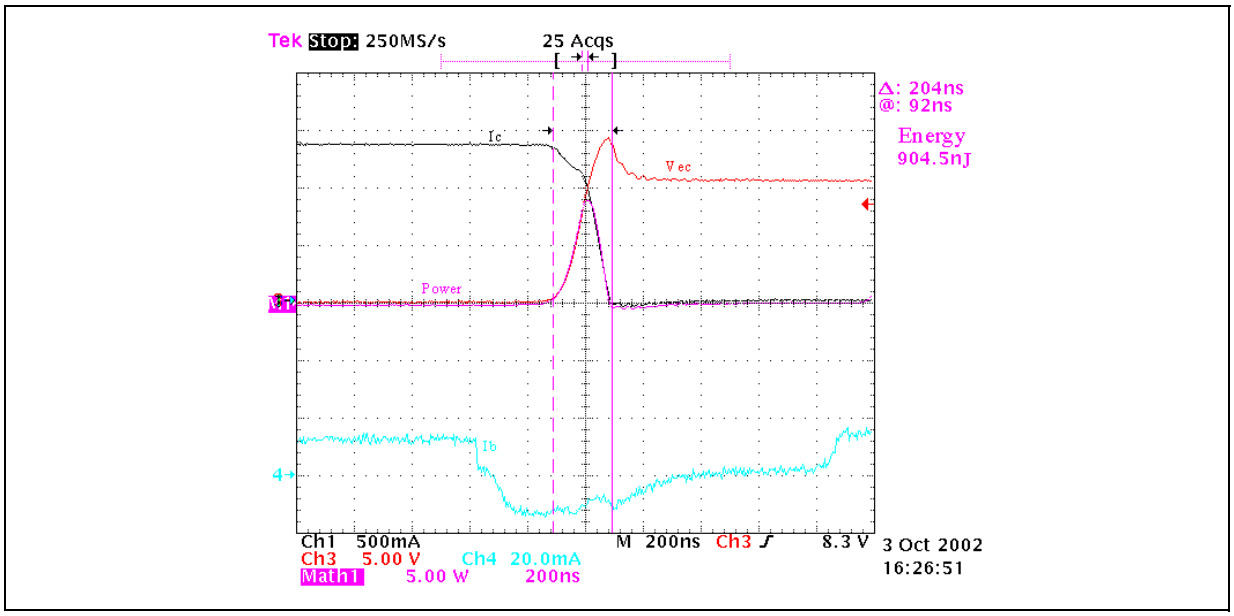

Figure 52: STN790A turn on (V_{dc}=10, 8 V).

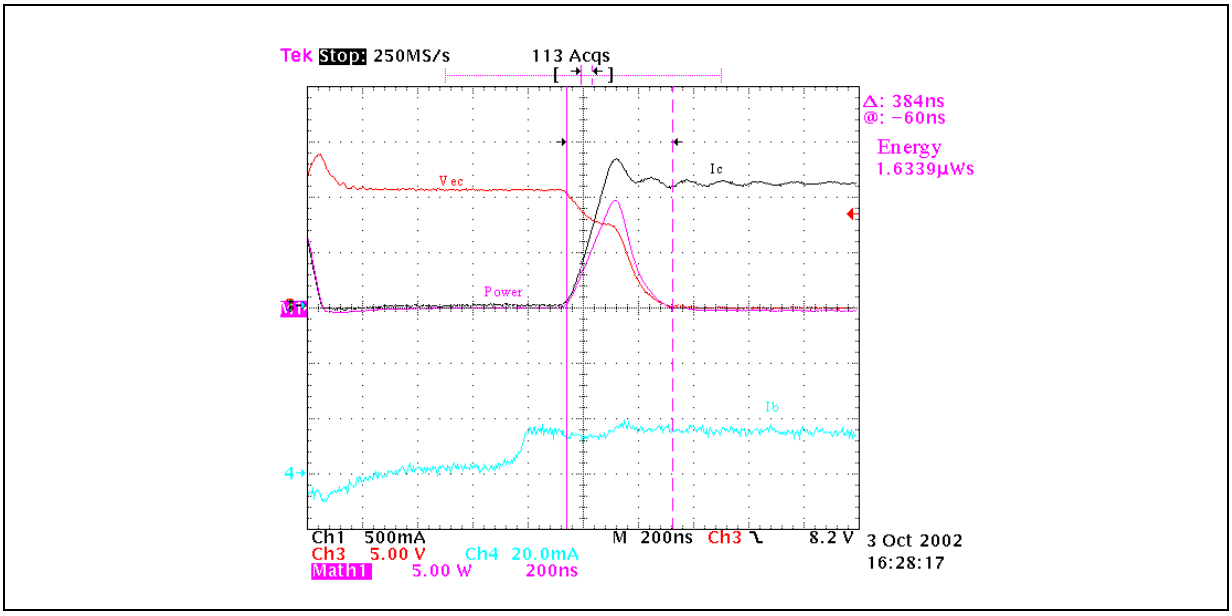

Figure 53: STS3DPFS30 steady state (V_{dc}=10,8 V).

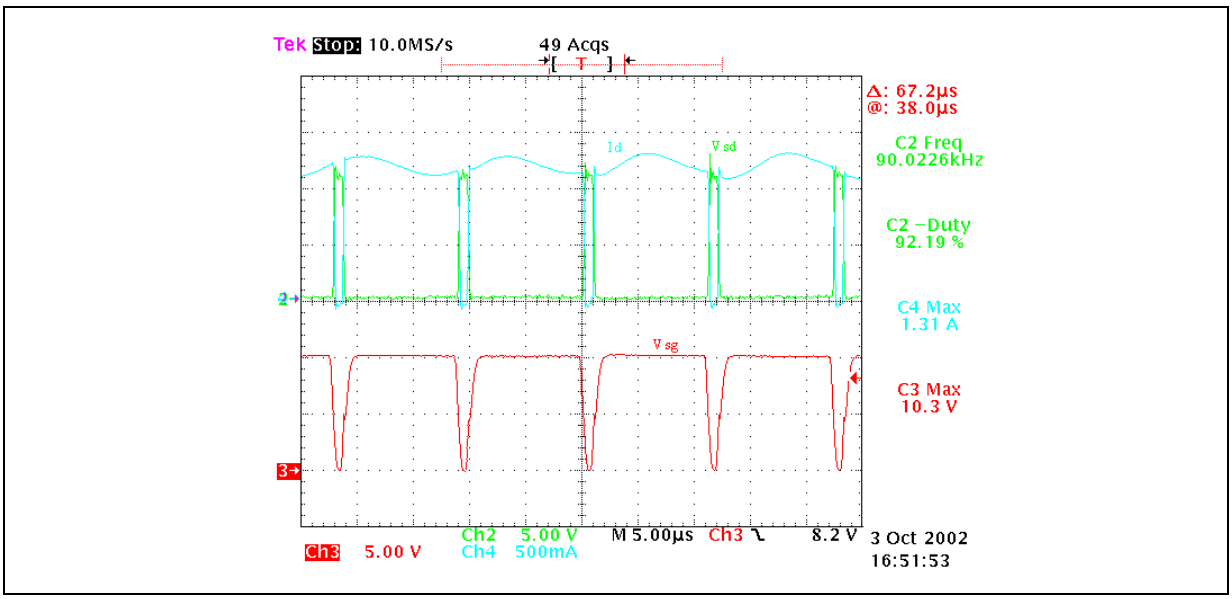

Figure 54: STS3DPFS30 turn off (V_{dc}=10.8 V).

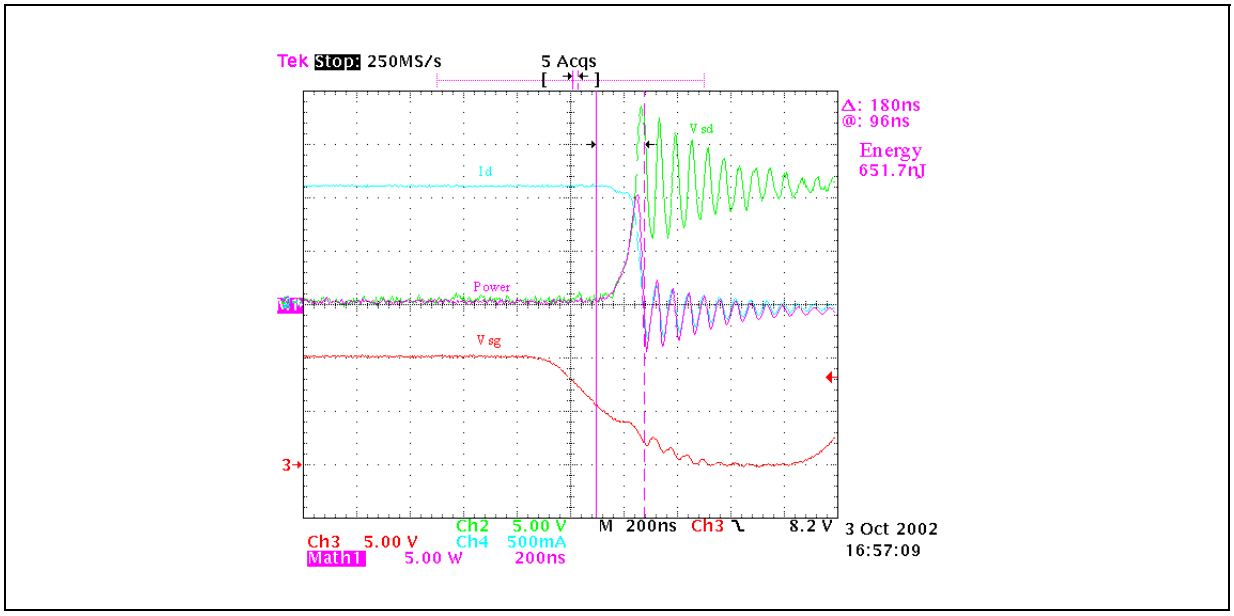

Figure 55: STS3DPFS30 turn on (V_{dc}=10.8 V).

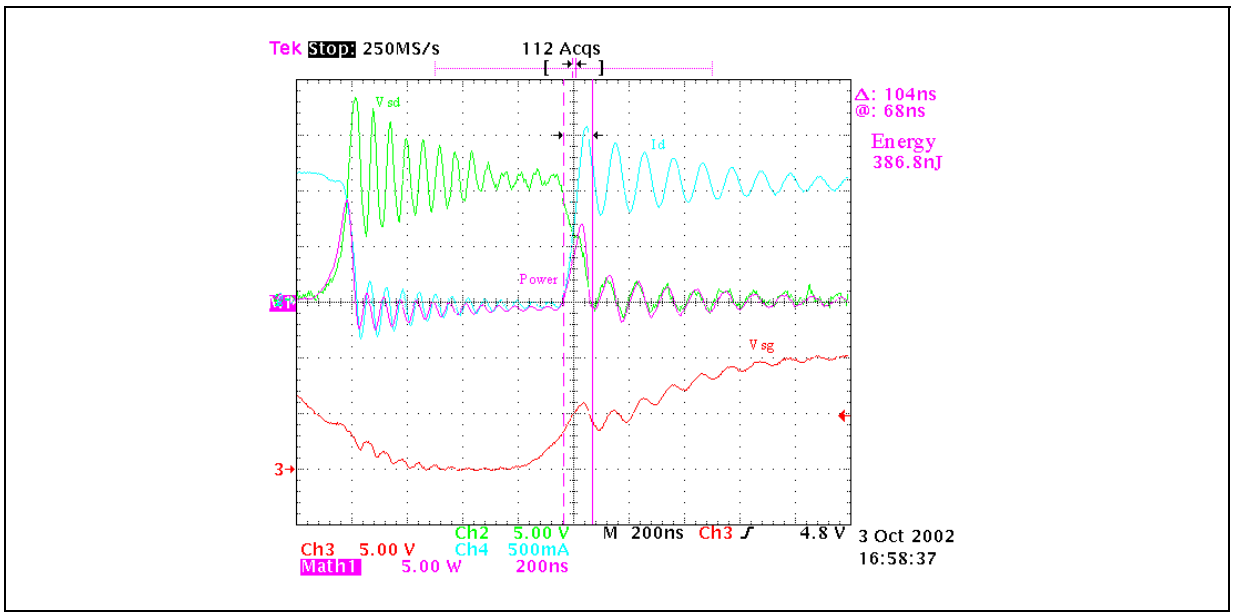

Figure 56: STN790A steady state (V_{dc}=13.2V)

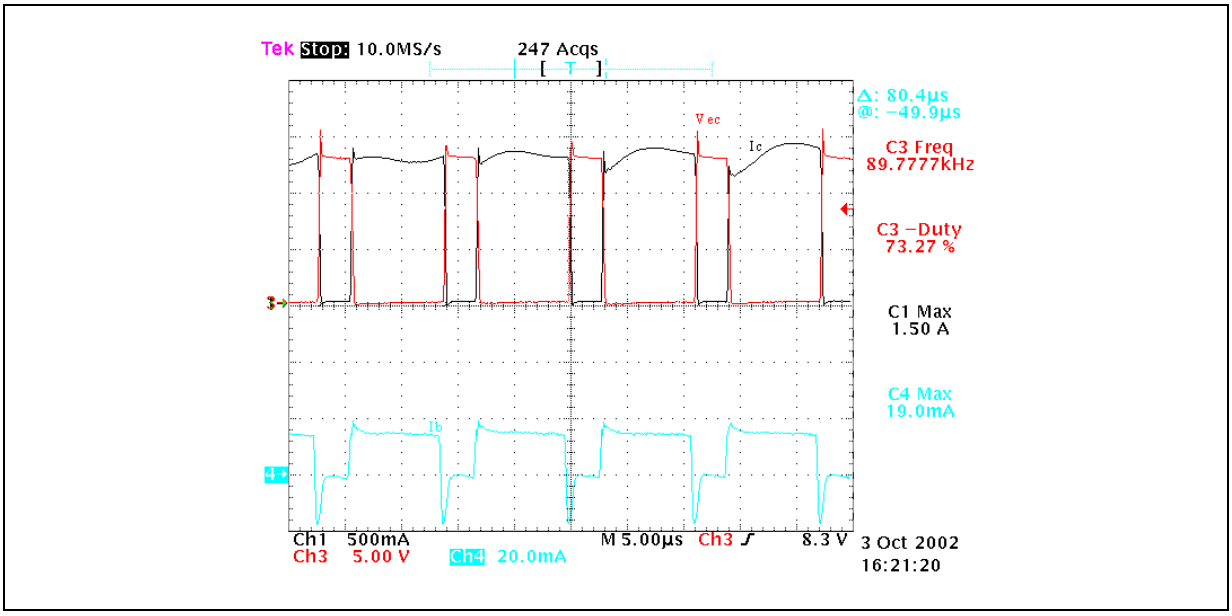

Figure 57: STN790A turn off (V_{dc}=13.2V)

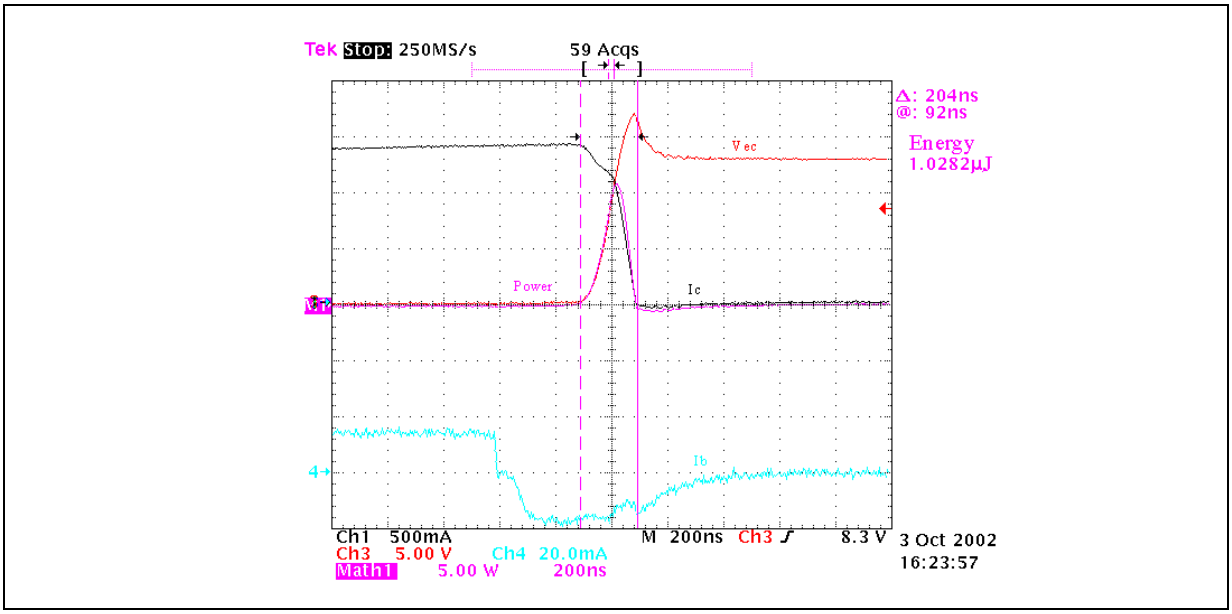

Figure 58: STN790A turn on (V_{dc}=13.2V)

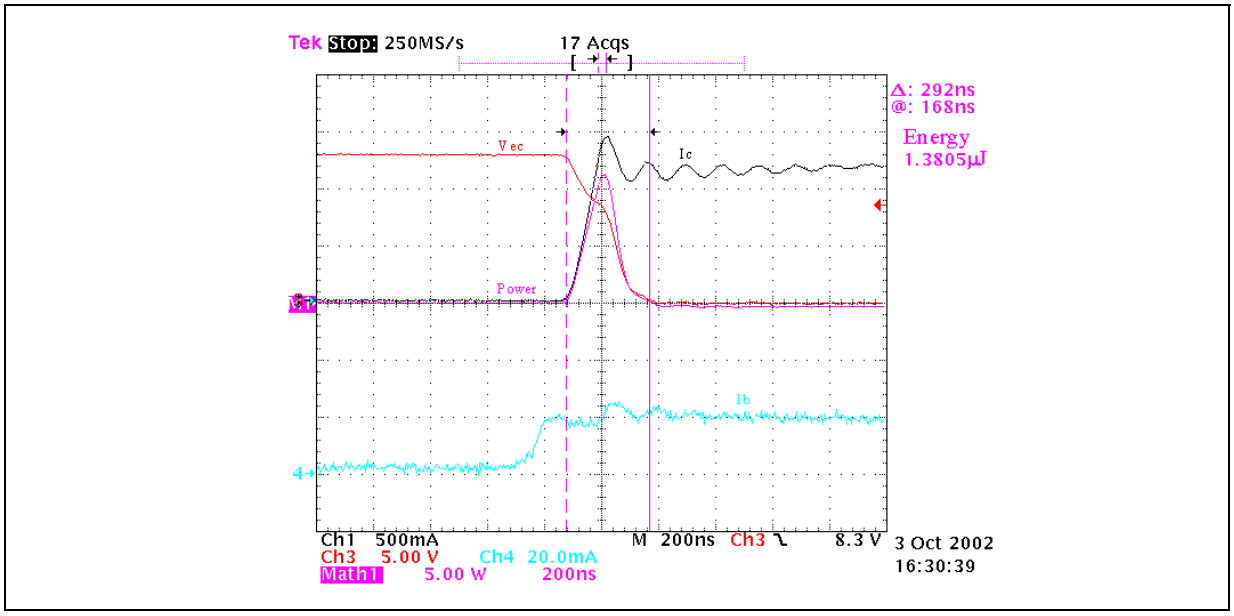

Figure 59: STS3DPFS30 steady state (V_{dc}=13.2V)

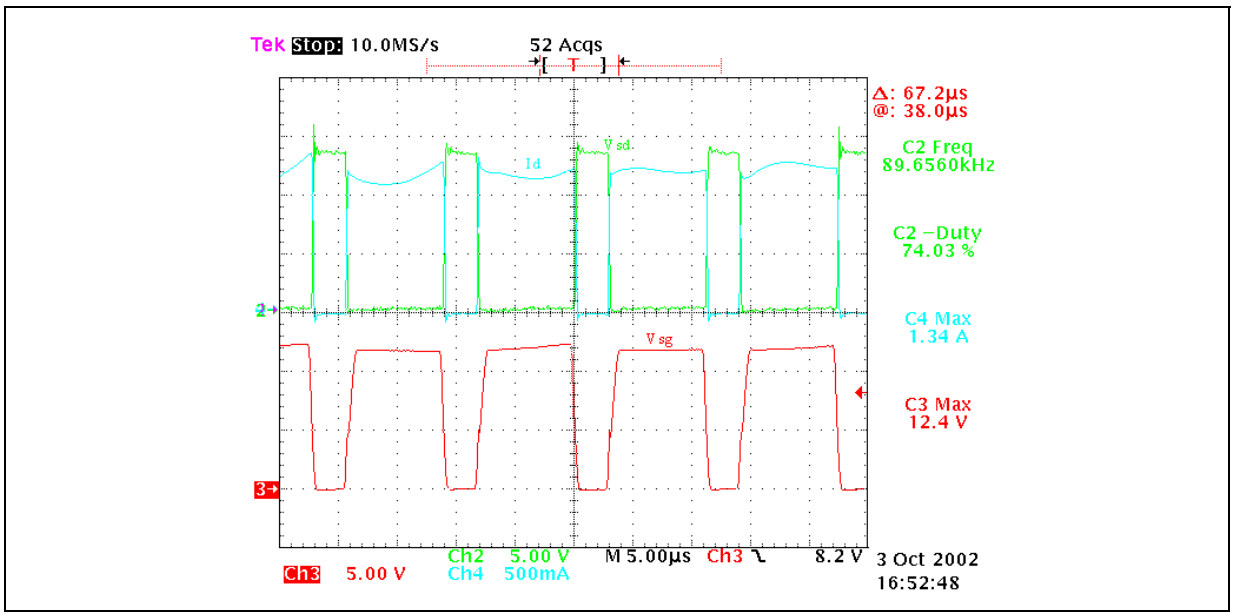

Figure 60: STS3DPFS30 turn off (V_{dc}=13.2V)

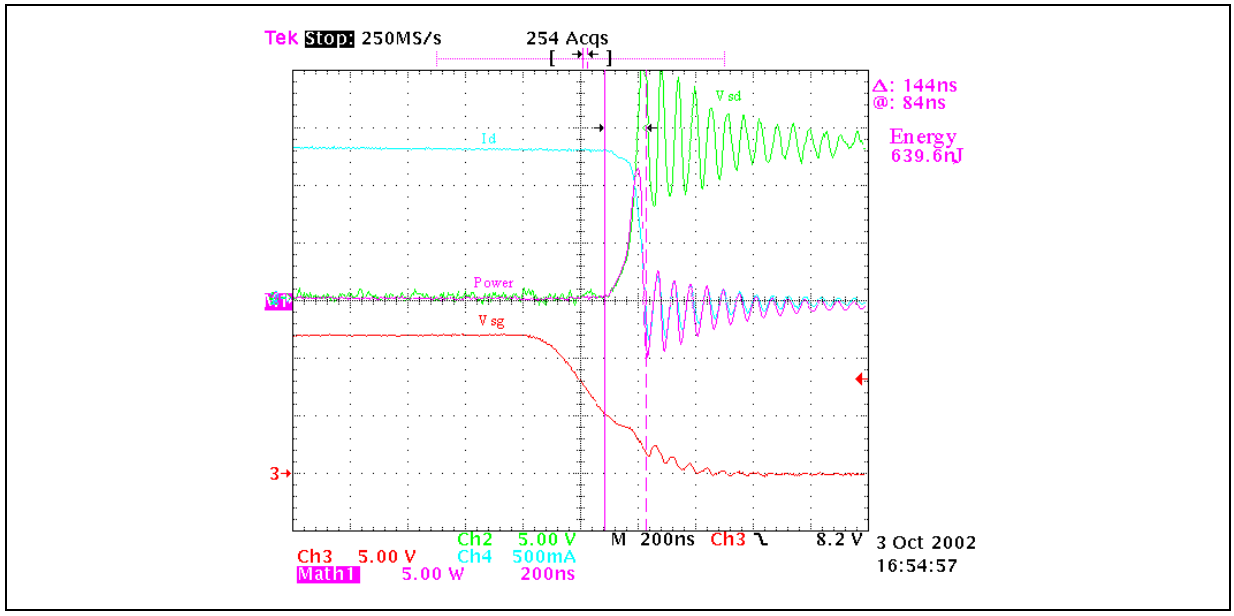

Figure 61: STS3DPFS30 turn on (V_{dc}=13.2V)

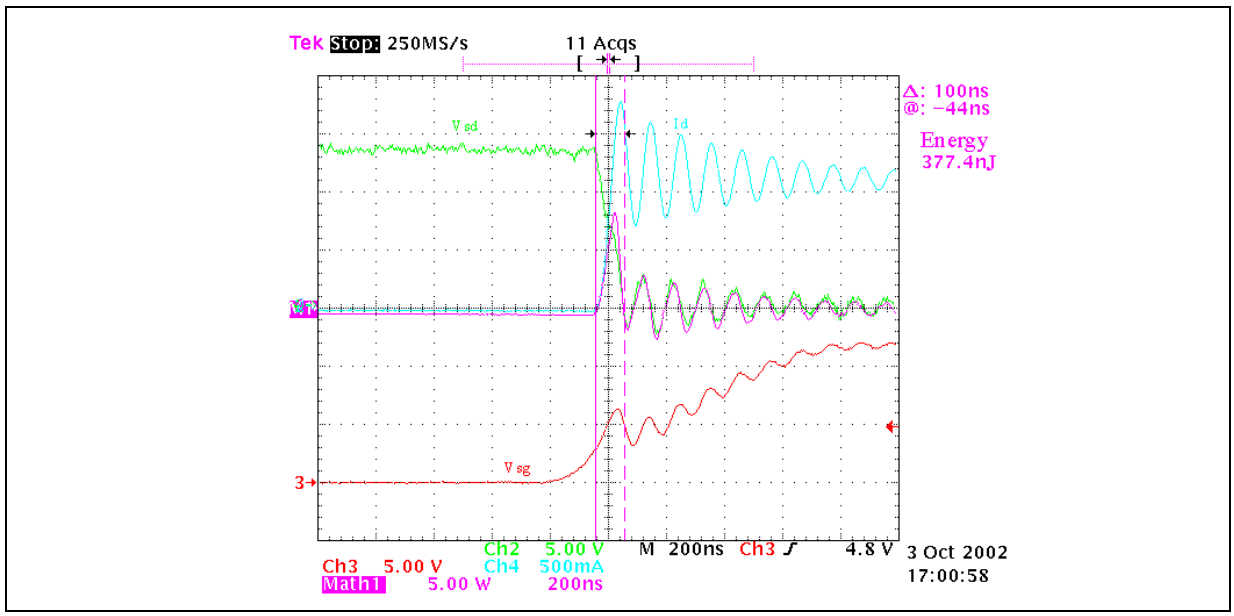

Figure 62: 1N5821 steady state (V_{dc}=12V)

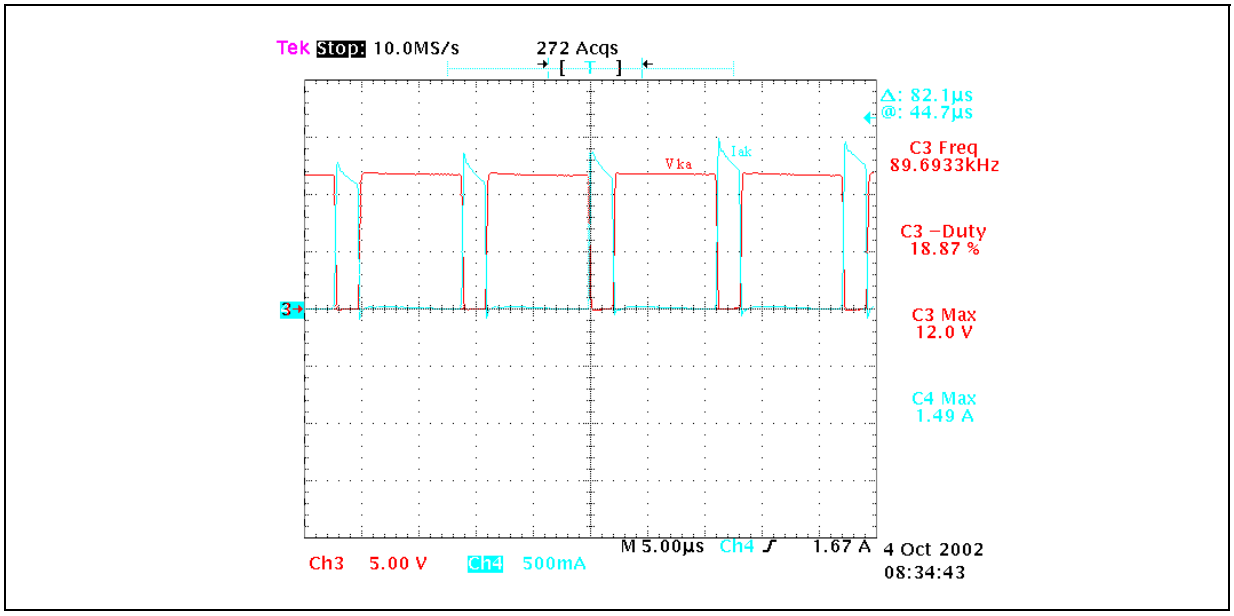

Figure 63: 1N5821 turn off (V_{dc}=12V)

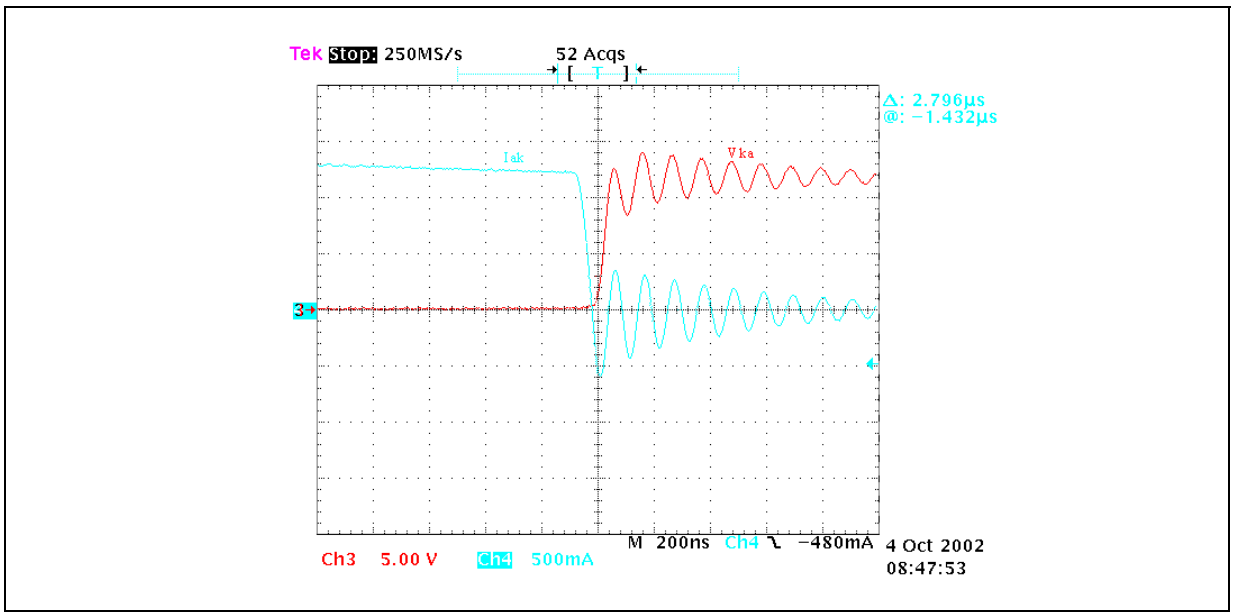

Figure 64: 1N5821 turn on (V_{dc} -12V)

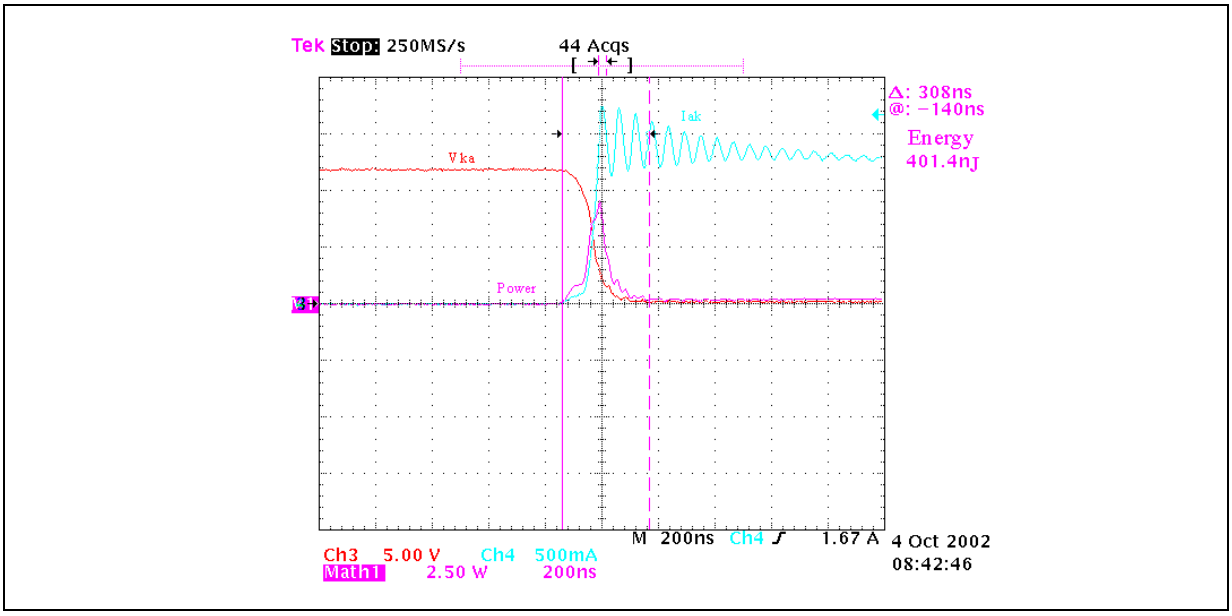

igure 65: 1N5821 steady state (V_{dc} =10.8V)

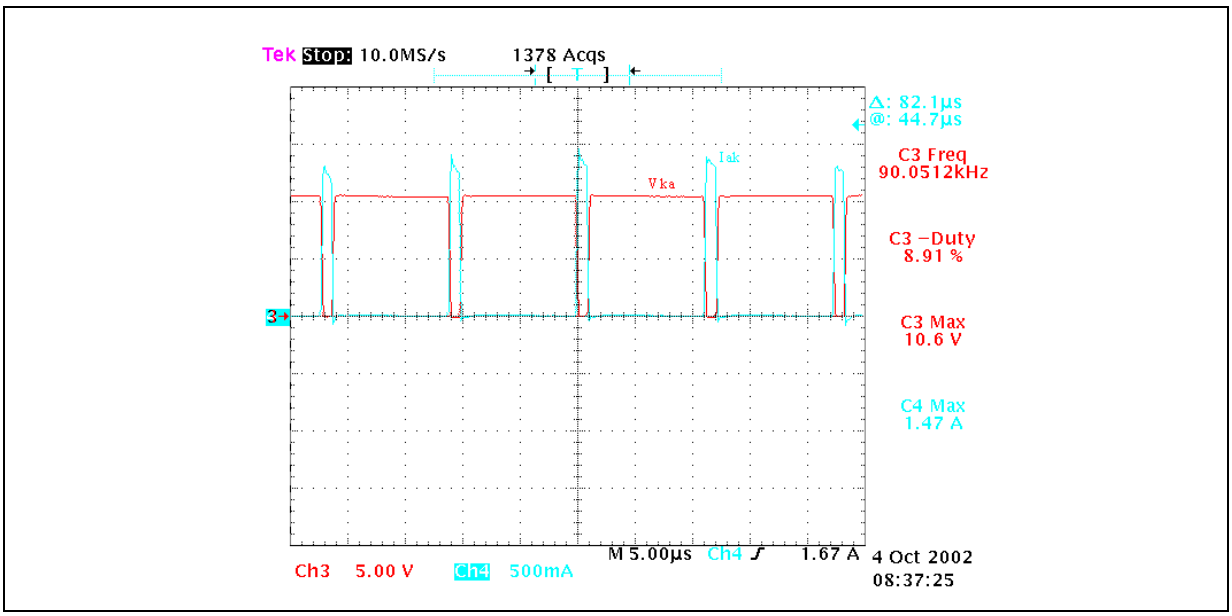

Figure 66: 1N5821 turn off (V_{dc} =10.8V)

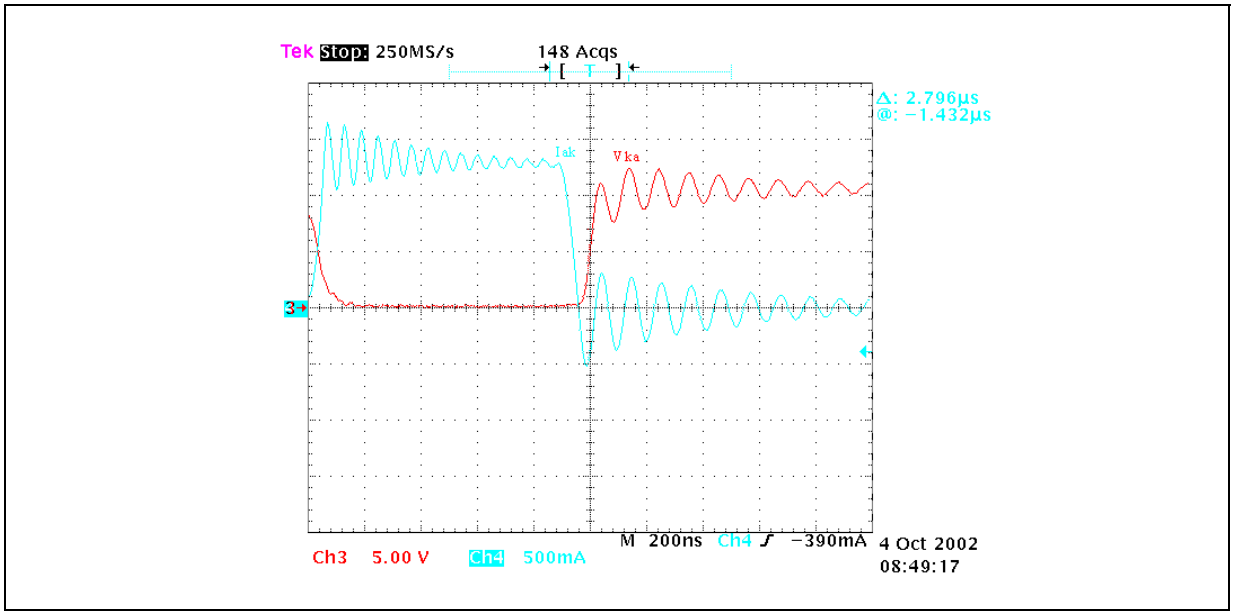

Figure 67: 1N5821 turn on (V_{dc} =10.8V)

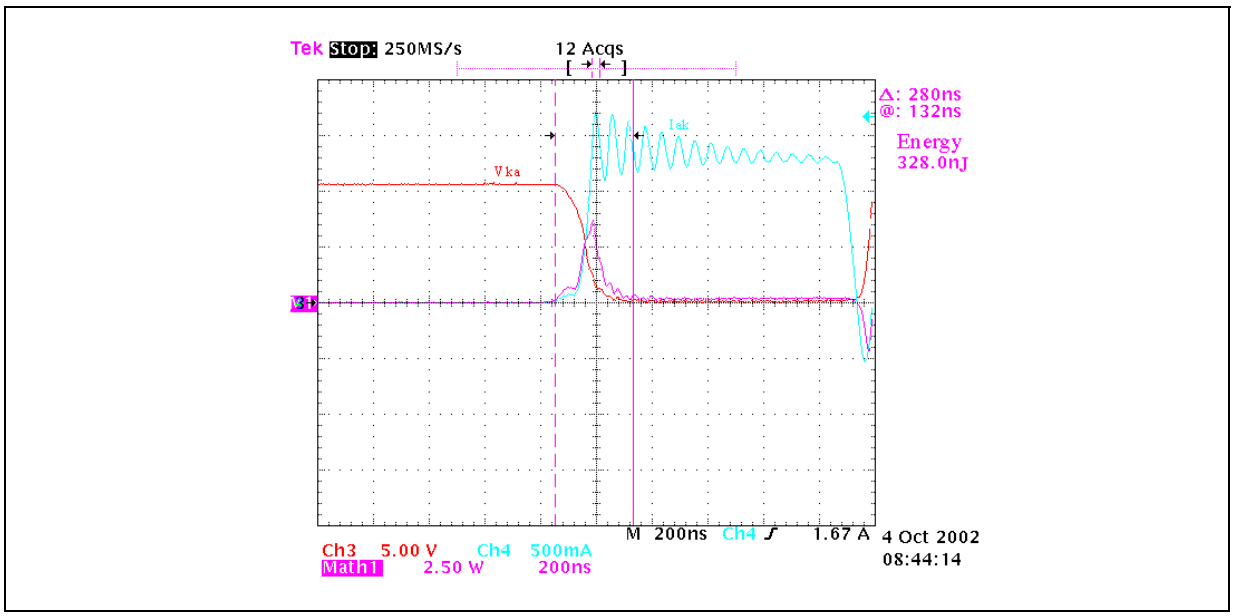

Figure 68: 1N5821 steady state (V_{dc} =13.2V)

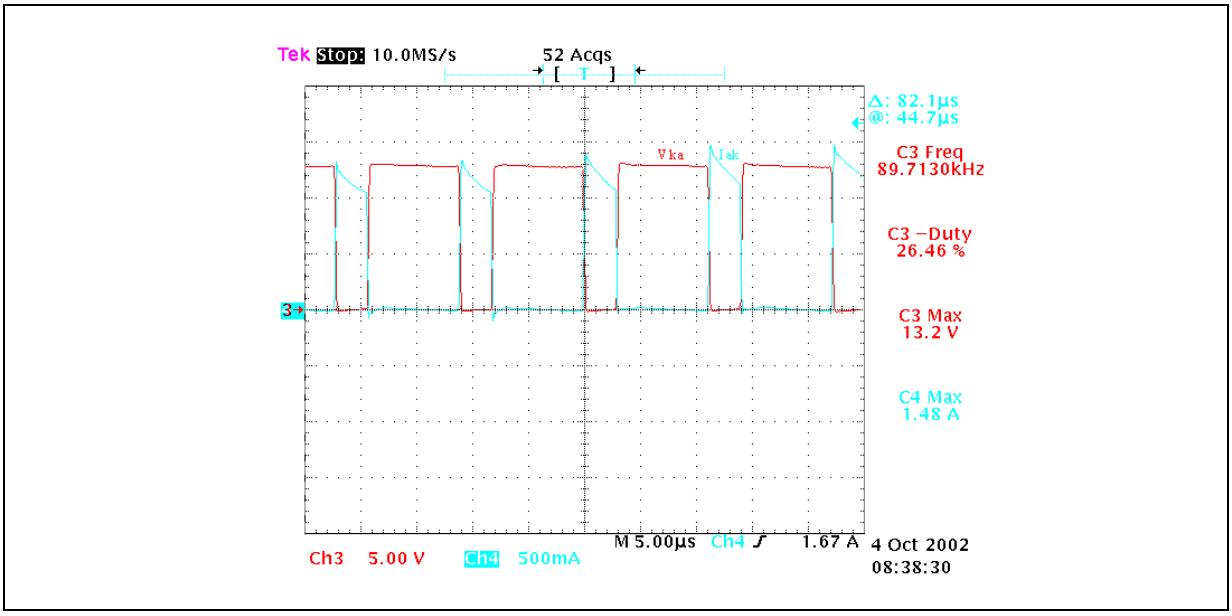

Figure 69: 1N5821 turn off (V_{dc} =13.2V)

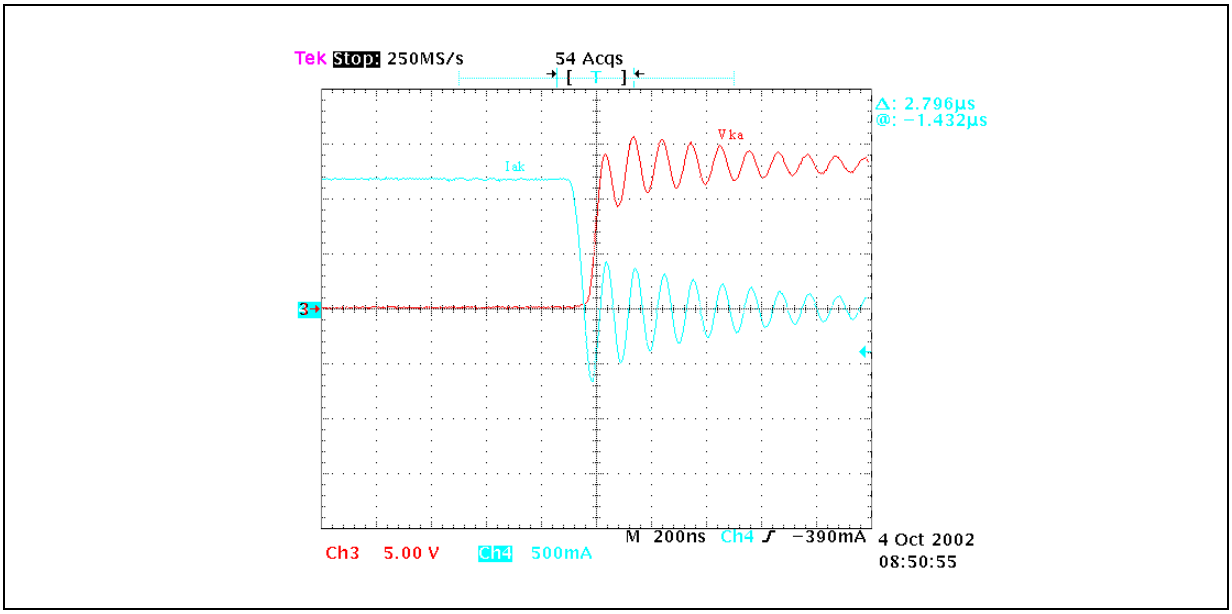

Figure 70: 1N5821 turn on (V_{dc} -13.2V)

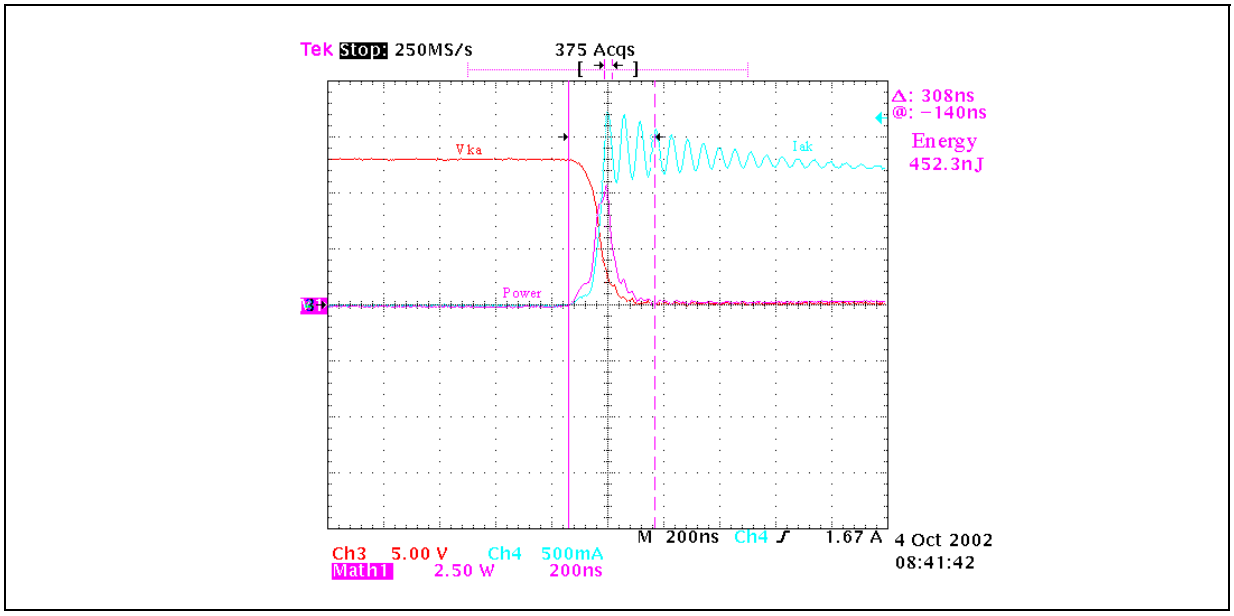

Tab II: Main measured electrical parameters.

	STN790A	STS3DPFS30
Vdc	12 V typ	12 V typ
Idc	1 A	1 A
Vce_sat@Ic=1 A and Ib=15mA	145 mV	-----
Rds(on)@Id=1,15 A and Vsg=9 V	-----	102 mOhm
Hfe @ Ic=1 A and Vec=1 V	169	-----
Frequency	90,0 Khz	89,7 Khz
Tcase	71 °C	49 °C
Turn-off Energy	974 nJ	649 nJ
Turn-on Energy	1508 nJ	375 nJ
Turn-off time	204 ns	160 ns
Turn-on time	316 ns	375 ns
Ic_max	1,44 A	-----
Id_max	-----	1,37 A
Duty cycle	79%	81%
Ibon	12 mA	-----
Vsg	-----	11,5 V
Iboff_max	-16 mA	-----
Vsd_max	-----	13 V
Vec_max	15 V	-----

Tab III: Main measured electrical parameters.

	STN790A	STS3DPFS30
Vdc	10,8 V	10,8 V
Idc	1,12 A	1,12 A
Vce_sat@Ic=1 A and Ib=15mA	145 mV	-----
Rds(on)@Id=1,15 A and Vsg=9 V	-----	102 mOhm
Hfe @ Ic=1 A and Vec=1 V	169	-----
Frequency	89,8 Khz	90,0 Khz
Tcase	72 °C	47 °C
Turn-off Energy	905 nJ	652 nJ
Turn-on Energy	1634 nJ	387 nJ
Turn-off time	204 ns	180 ns
Turn-on time	384 ns	104 ns
Ic_max	1,45 A	-----
Id_max	-----	1,31 A
Duty cycle	90%	90%
Ibon	12,5 mA	-----
Vsg	-----	10,3 V
Iboff_max	-16 mA	-----

Tab IV: Main electrical parameters measured.

	STN790A	STS3DPFS30
Vdc	13,2 V	13,2 V
Idc	0,89 A	0,89 A
Vce_sat@Ic=1 A and Ib=15mA	145 mV	-----
Rds(on)@Id=1,15 A and Vsg=9 V	-----	102 mOhm
Hfe @ Ic=1 A and Vec=1 V	169	-----
Frequency	89,8 Khz	89,7 Khz
Tcase	68 °C	50 °C
Turn-off Energy	1082 nJ	640 nJ
Turn-on Energy	1381 nJ	377 nJ
Turn-off time	204 ns	144 ns
Turn-on time	292 ns	100 ns
Ic_max	1,50 A	-----
Id_max	-----	1,34 A
Duty cycle	73%	74%
Ibon	15 mA	-----
Vsg	-----	12,4 V
Iboff_max	-16 mA	-----
Vsd_max	-----	14 V
Vec_max	16 V	-----

The aim of the table below is to show how stable is the power delivered to the lamps. In fact, the maximum power variation is always below 2% for fluctuations of input voltage of +/-10%.

Table V: Input power variation vs input voltage variation

Vdc	Idc	Pin	Delta_power
12 V	1 A	12 W	-----
10,8 V	1,12 A	12,1 W	0.83%
13,2 V	0,89 A	11,8 W	-1.69%

Furthermore, considering the above graphs and tables it is possible to see that the operation frequency is about 90 KHz, the duty cycle is in the range of 73-81% for all considered input voltages conditions, the max Ic (Id) current is about 1.5A, the max V_{ec} (V_{sd}) voltage is about 14V.

Considering the STN790A device, the I_{bon} (bipolar transistor base current during conductions) is about 13 mA and the I_{boff} (bipolar transistor base current during turn-off) is about -16 mA. Such values are achieved by means of a suitable STN790A polarization net, consisting in the R_2-R_3-R_4-C_1 components. Such net avoids having I_{sink} outside the maximum rating established for TSM108 and, in the meantime, it minimizes the turn off losses of the transistor. In open air, the measured case temperature of STN790A and STS3DPFS30 is about 70 °C and 50 °C respectively. Such difference in temperature between STN790A and STS3DPFS30 is, in particular, due to the higher switching loss of the PNP power bipolar compared to the P channel power MOSFET and, however, it can be considered acceptable.
On the other hand, it is important to highlight that, during the turn on and the turn off, using the P channel power MOSFET, much more noise is observed compared to the PNP power bipolar switching behavior.

In the next graphs all the waveforms regarding STSA1805, mounted in PUSH-PULL converter, are showed considering the three input voltages under analysis.

Figure 71: STSA1805 steady state (V_{dc}=12V)

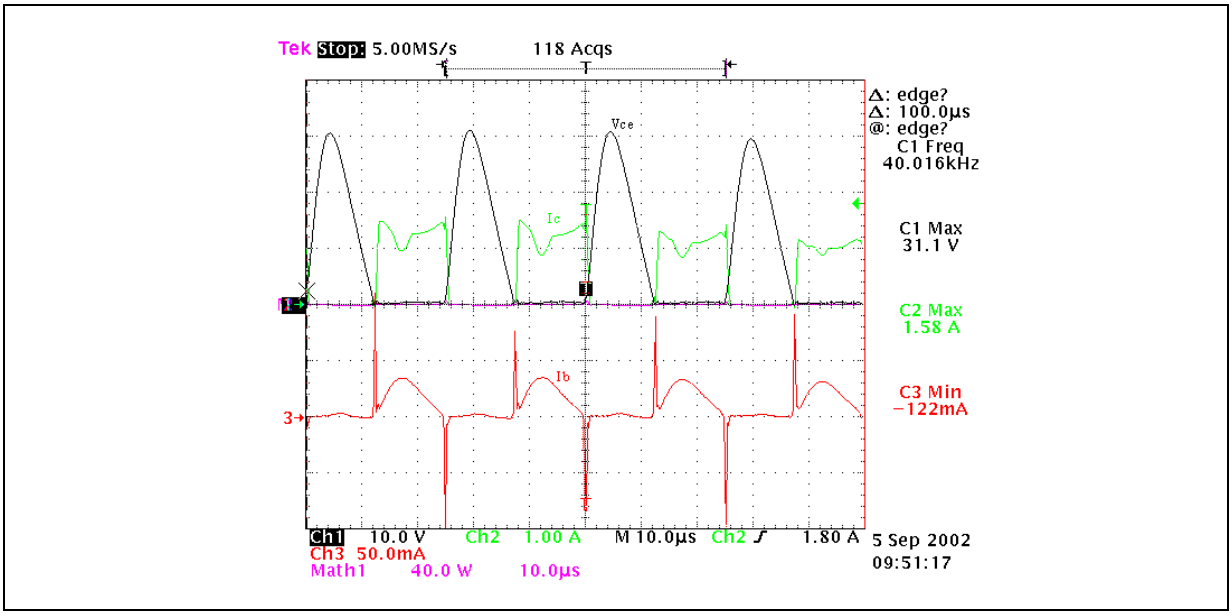

Figure 72: STSA1805 turn off (V_{dc}=12V)

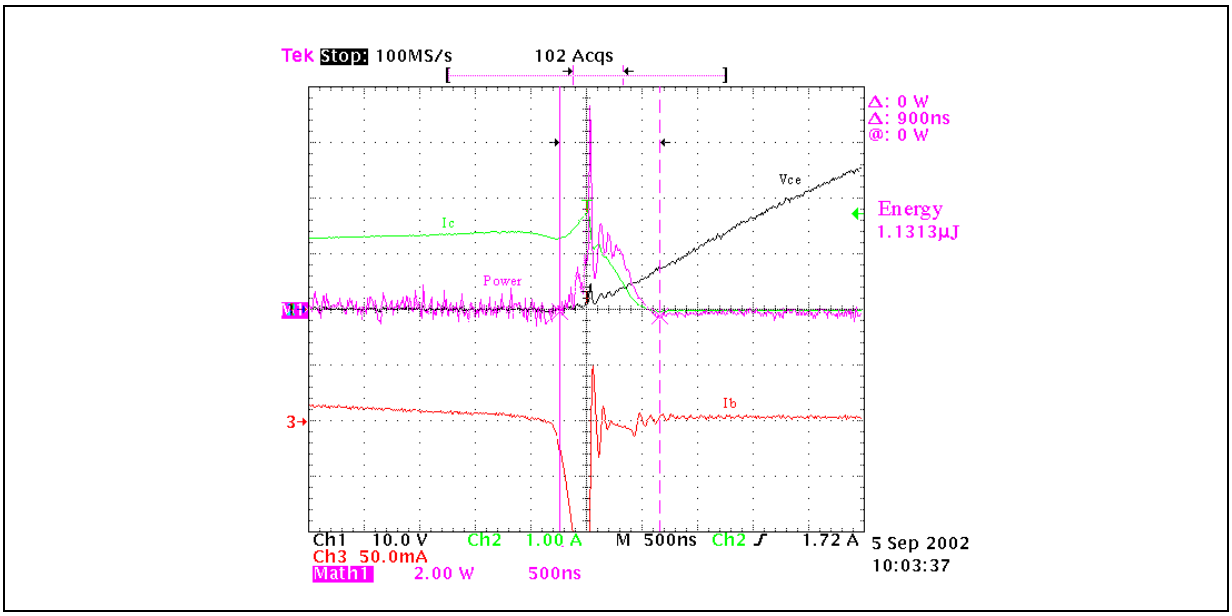

Figure 73: STSA1805 turn on (V_{dc}=12V)

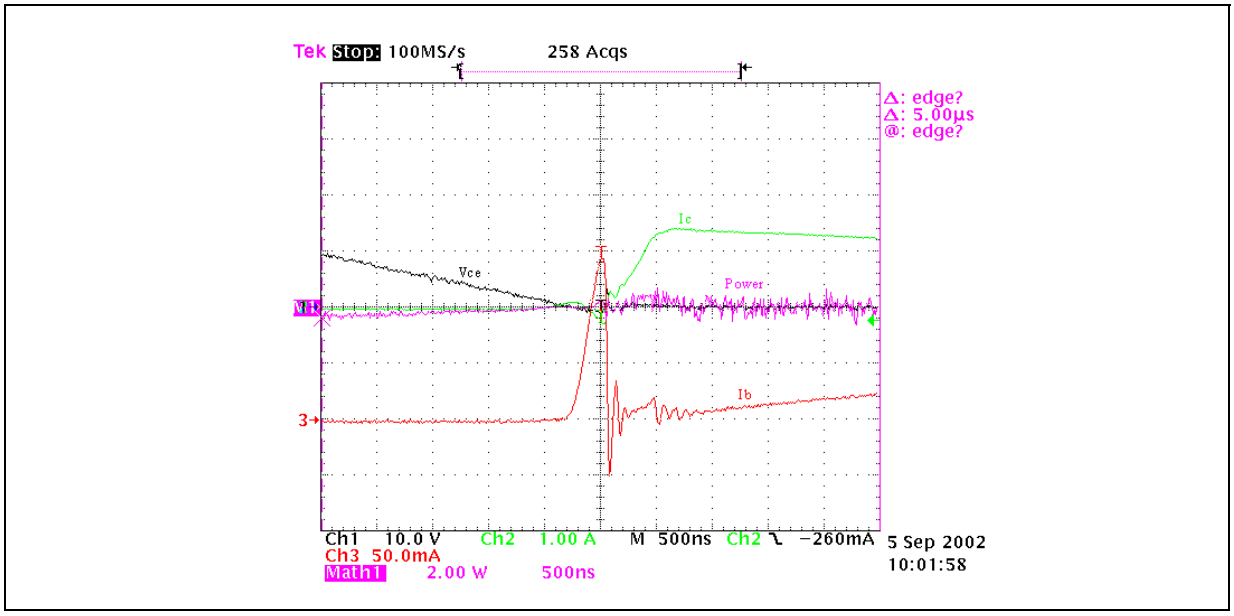

Figure 74: STSA1805 steady state (V_{dc}=10.8V)

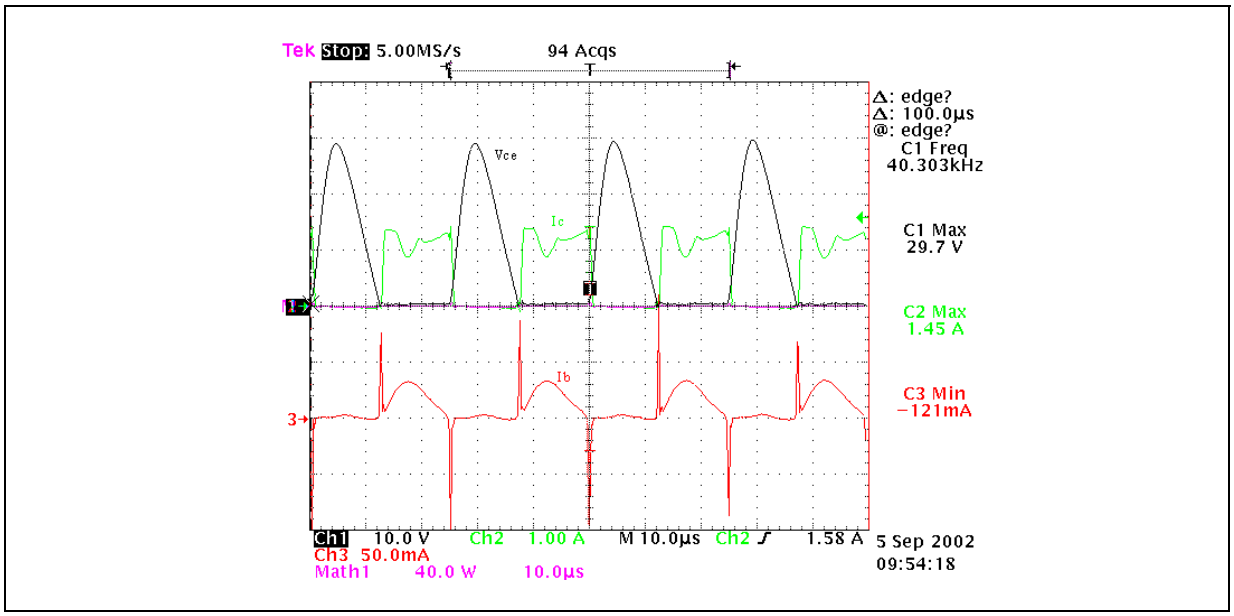

Figure 75: STSA1805 turn off (V_{dc}=10.8V)

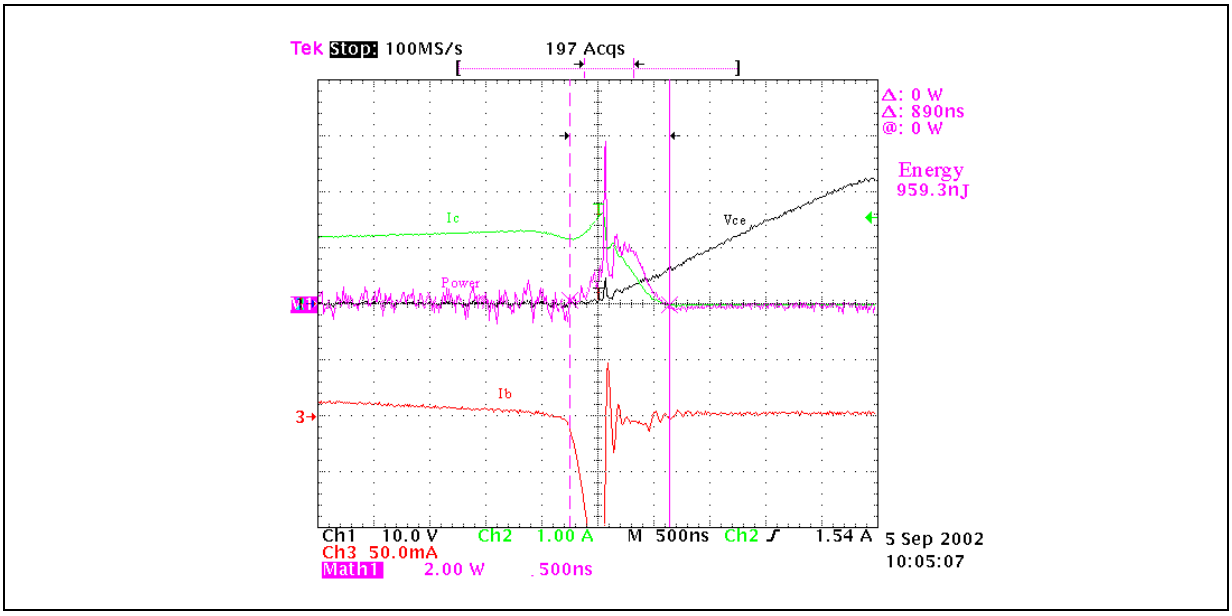

Figure 76: STSA1805 turn on (V_{dc}=10.8V)

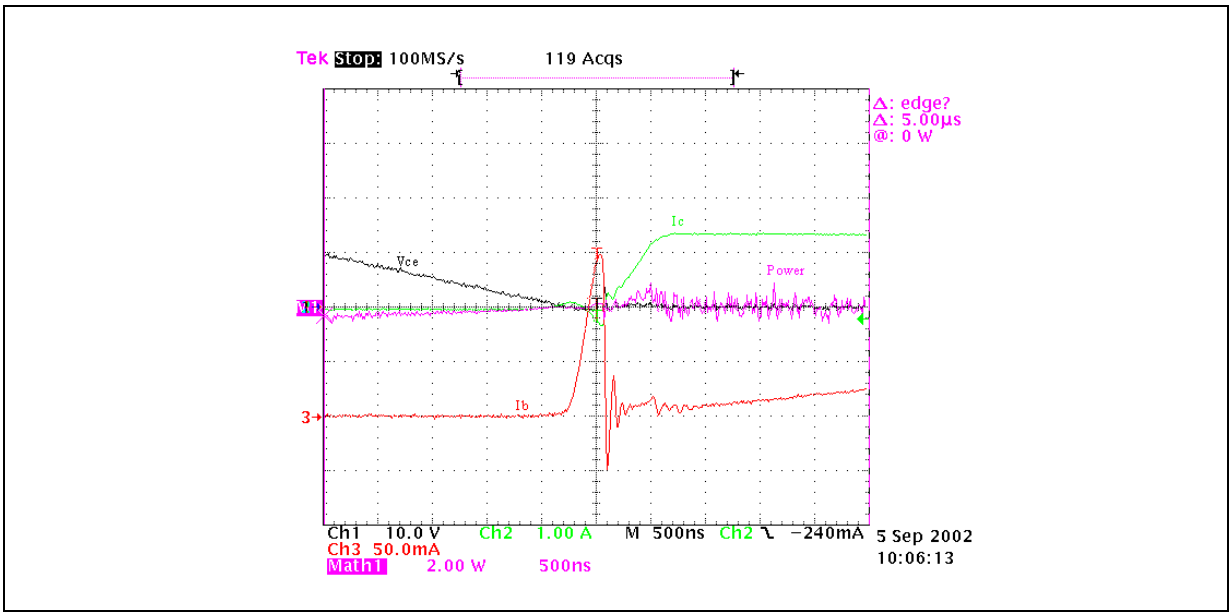

Figure 77: STSA1805 steady state (V_{dc}=13.2V)

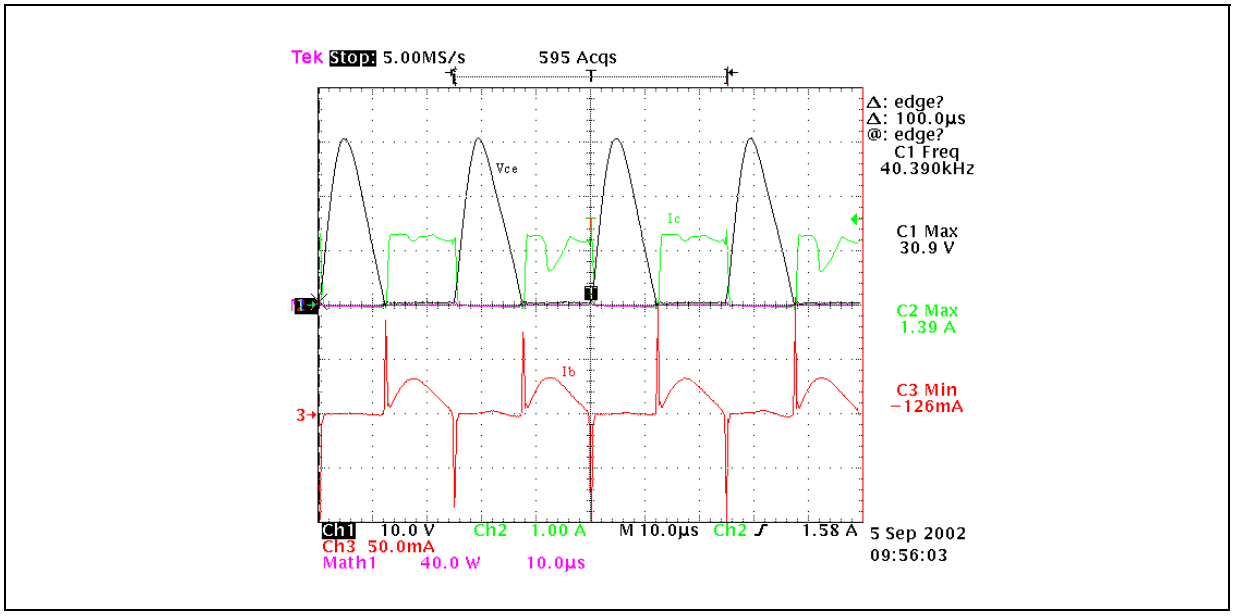

Figure 78: STSA1805 turn off (V_{dc}=13.2V)

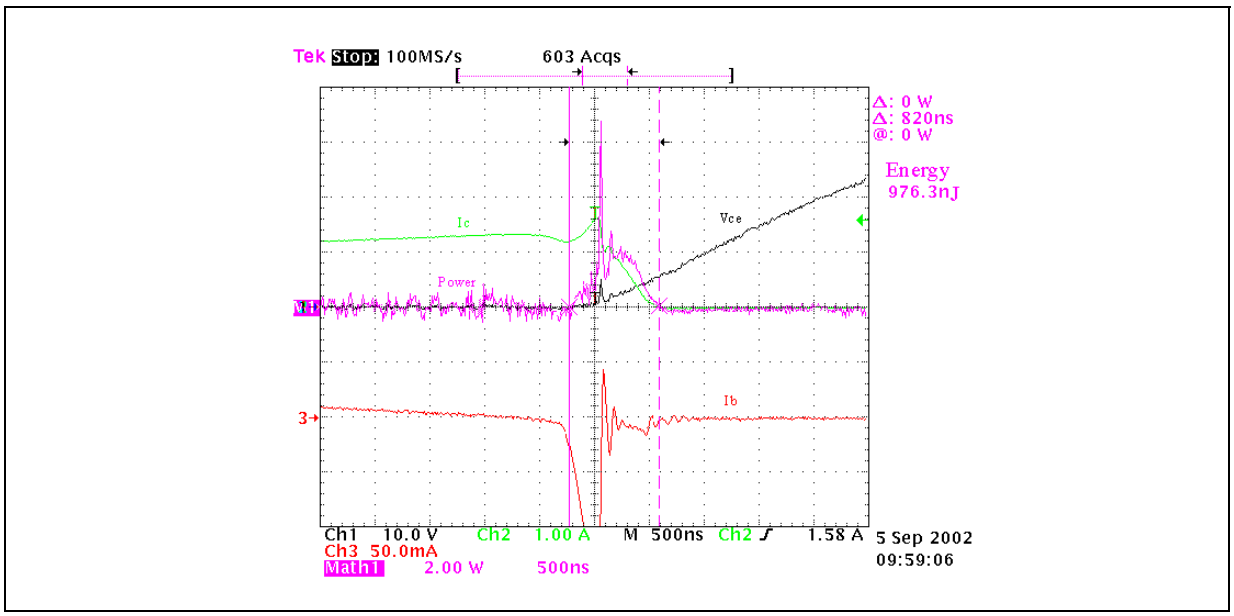

Figure 79: STSA1805 turn on (V_{dc}=13.2V)

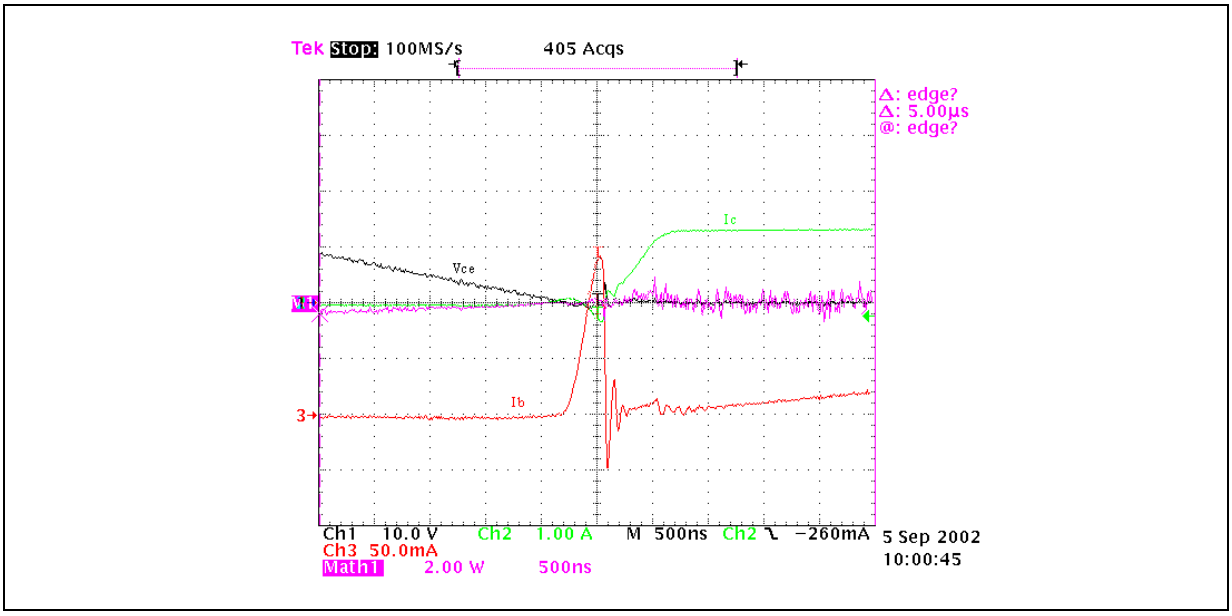

Tab VI: Main electrical parameters measured.

	STSA1805	STSA1805	STSA1805
Vdc	12 V typ	10,8 V	13,2 V
Idc	1 A	1,12 A	0,89 A
Vce_sat@Ic=1 A and Ib=35mA	78 mV	78 mV	78 mV
Hfe @ Ic=1,4 A and Vec=1 V	305	305	305
Frequency	40,0 Khz	40,3 Khz	40,4 Khz
Tcase	41 °C	41 °C	41 °C
Turn-off Energy	1131 nJ	959 nJ	976 nJ
Turn-on Energy	Negligible	Negligible	Negligible
Ic_max	1,58 A	1,45 A	1,39 A
Ibon	35 mA	35 mA	35 mA
Iboff_max	-122 mA	-121 mA	-126 mA
Vce_max	31 V	30 V	31 V

In the above graphs and table it is possible to see that the operation frequency is about 40KHz, the I_{bon} is about 35mA, the max V_{ce} is about 32V and the max I_c is about 1.5A for all the powering conditions. From the thermal measurement, the case temperature for STSA1805 is 41 °C.

The measured case temperature of the TSM108 is 29 °C in all conditions, the ambient temperature is 25°C .

13. CONCLUSIONS

This paper has showed an example on how a CCFL application can be designed and realized using the TSM108, the power bipolar transistors STN790A (or the Power MOSFET STS3DPFS30), STSA1805 and the SCHOTTKY diode 1N5821.
In particular, a detailed theoretical model of the system has been built and the validation of the results has given confirmation of the decided approach. Based on the very good results achieved, this technical paper offers a valid support to whoever is interested in designing such kind of lighting systems.
The application shows a very good operation and it is stable considering the several input voltage conditions. The application uses the 'ROYER' topology and by means of a sensing circuitry it fixes the lamps brightness considering a net fluctuation. In fact, for variations of +/-10% of the nominal powering voltage, the application power variation is always less than 2%. Furthermore, acting on a P trimmer it is possible to regulate the lamps brightness changing the PNP power bipolar duty cycle, or the P channel power MOSFET one.
Such a design considers an output solution with two 6W lamps connected in parallel, but tuning the capacitors and the resistors components any output topology, considering several lamps, can be achieved using the same STMicroelectronics' devices. This design allows, acting on the P trimmer, the output power on the lamps to be fixed between the 2-16W range and the application is enabled when the input voltage is in the range of 8.5-15.5V. The operation frequency of the transistor Q_1, in the BUCK converter part, is fixed at about 90KHz. The application shows a good electrical and thermal behavior considering both the solutions with STN790A (PNP power bipolar) and STS3DPFS30 (P channel power MOSFET). In particular, the measured case temperature of the device STN790A under open air condition, is in the worst case about 70 °C compared to the 50 °C of STS3DPFS30 (such a device has also an integrated SCHOTTKY diode included in the same package). The reason for the difference in the case temperature measured on the two devices is due, in particular, to the higher switching losses of the power bipolar transistor compared to the power MOSFET transistor, and anyway is acceptable for this design. On the other hand, it is important to highlight that, during the turn on and the turn off, of the P channel power MOSFET much more noise was observed compared to the PNP power bipolar. The reason for such a behavior is mainly due to the higher speed of the MOSFET compared to the bipolar transistor. The analysis results achieved in this experiment demonstrate that the TSM108 and the power transistors STN790A, or STS3DPFS30, and the STSA1805 can be used in order to realize the CCFL applications.

Table 6: Revision History

Date	Revision	Description of Changes
28-Apr-2004	1	First Release
18-Jun-2004	2	Some spelling mistakes were corrected